NEUROMODULATOR-MEDIATED CONTROL OF SPATIAL AND NONSPATIAL INFORMATION PROCESSING IN THE HIPPOCAMPUS

Thesis by

Hiroshi Ito

In Partial Fulfillment of the Requirements

for the Degree of

Doctor of Philosophy

California Institute of Technology

Pasadena, California

2010

(Defended July 17, 2009)

Acknowledgements

The work presented in this thesis would not be possible without guidance, support and encouragement from many people.

First, I sincerely thank my advisor, Professor Erin Schuman. My life at the Schuman lab started in the summer of 2001 when I visited Caltech as a summer student. Since then, Erin has been continuously providing guidance for me to become a "scientist." While she gave me much freedom to explore my scientific interests, she was always willing to help to make my interests into a scientific work. I could not imagine being here without her support.

I also thank the professors in my thesis committee, Professors Gilles Laurent, Henry Lester and Thanos Siapas. At each committee meeting, I was always intellectually inspired by their perspectives and philosophy in neuroscience. I am very grateful for many pieces of advice and suggestions from such great scientists.

My collaboration with Professor Paul Patterson's lab was another invaluable experience for me. As I learned medicine in Japan, I have been interested in psychiatric disorders and trying to find some links in my research. I am very thankful to Paul for giving me such a great opportunity and for his guidance and support on this project. I would also like to thank my collaborators, Steve Smith and Elaine Hsiao.

I was really happy to have wonderful colleagues in the Schuman lab. I really enjoyed working, discussing, and chatting with people in the lab. Their advice and encouragement helped me many times, and the lab was always full of fun. I also sincerely thank Alana Rathbun and Ana-Maria Lust for lab administration. The lab would not be such a comfortable workplace without their generous support.

I would like to express my sincere gratitude to Yuki Matsuda for all her warm support and encouragement. It was my great pleasure to meet her at Caltech and walk together on the path toward the PhD.

Finally, I would like to thank my parents, Fumihide and Teruko Ito, for support and understanding of my decision to study abroad. They fostered my curiosities by letting me try many different subjects, including sports, arts, or music. It is no doubt that my scientific curiosity arises from my childhood experiences.

Abstract

How the brain implements learning is a long-standing question in neuroscience research. Many studies have indicated a critical role of the hippocampus in establishing memories of facts and episodes. As episodic memories require the association of many different sensory events in the environment, the hippocampus integrates multimodal information acquired from sensory systems. The brain area that sends major afferent inputs to the hippocampus, the entorhinal cortex, can be further divided into two subareas, the medial and lateral entorhinal cortex, each of which primarily transfers either spatial or nonspatial information to the hippocampus. The proper control of these two information streams is essential for constructing neuronal representations of the environment in hippocampus. To understand this process, my studies have focused primarily on the projection from the entorhinal cortex to area CA1, the temporoammonic pathway. Although this pathway has been relatively unexplored, recent studies have suggested that it plays a unique role in hippocampal function. I investigated how the temporoammonic synapses influence hippocampal function from three different perspectives; in single-neuron studies, local-circuit analyses, and behavioral manipulations. I propose that the temporoammonic pathway gives rise to a unique functional circuit in the hippocampus, which allows for the independent control of spatial and nonspatial information processing. Neuromodulators are a key component to this control as they differentially influence two streams of information from the entorhinal cortex. Finally, I describe my studies on the pathophysiology of schizophrenia-like behaviors at a neuronal circuit level. A mouse model of schizophrenia, generated by maternal immune activation,

displays several behavioral abnormalities relevant to schizophrenia patients. We found that hippocampal slices prepared from these mice exhibit altered synaptic properties in the temporoammonic pathway. The mice also exhibit behavioral abnormality in novel object recognition. Taken together, my studies shed light on two information streams in hippocampal circuits. Anatomical or neuromodulatory-based disturbance of this control may underlie some of the behavioral abnormalities observed in several mental disorders.

Table of Contents

List of Figures

List of Tables

List of Supplementary Figures

List of Abbreviations

4AP	4-aminopyridine (blocker for A-type potassium channels)
AMPA	alpha-amino-3-hydroxy-5-methyl-4-isoxazolepropionic
Bic	bicuculline (blocker for GABAA receptor)
CA1-3	Cornu ammonis fields (subregions of the hippocampus proper)
CGP	CGP55845 (blocker for GABAB receptor)
CR	conditioned response
CS	conditioned stimulus
DA	dopamine
DG	dentate gyrus
EC	entorhinal cortex
EPSC	excitatory postsynaptic current
EPSP	excitatory postsynaptic potential
fEPSP	field excitatory postsynaptic potential
GABA	γ-aminobutyric acid
GluR1	glutamate receptor subtype 1
HFS	high frequency stimulation
IPSC	inhibitory postsynaptic current
IPSP	inhibitory postsynaptic potential
LEC	lateral entorhinal cortex
LTD	long-term depression
LTP	long-term potentiation

MEC	medial entorhinal cortex
mEPSC	miniature excitatory postsynaptic current
mIPSC	miniature inhibitory postsynaptic current
ML	molecular layer
NE	norepinephrine
NMDA	N-methyl-D-aspartic acid
Poly(I:C)	Polyinosinic:polycytidylic acid (a synthetic double-stranded RNA)
PP	perforant pathway
PPF	paired-pulse facilitation
SC	Schaffer-collateral (pathway)
SLM	stratum lacunosum-moleculare
SNc	substantia nigra compacta
SP	stratum pyramidale
SR	stratum radiatum
TA	temporoammonic (pathway)
TEA	tetraethylammonium (blocker for potassium channels)
TTX	tetrodotoxin (blocker for sodium channels)
UR	unconditioned response
US	unconditioned stimulus
VTA	ventral tegmental area

Chapter 1. Introduction

1.1 Animal Learning

Learning is essential for our sociocultural evolution. There are many situations where prefixed responses, such as reflexes, are not sufficient. A certain sound or odor may imply the existence of a predator for animals, but a similar sound or odor may also indicate the existence of prey. Accordingly, animals need to decide whether they approach or avoid target, based on small differences in sensory signals. Considering the thousands of such situations animals experience in a lifetime, it is clearly impossible to master each situation using exclusively innate or reflexive responses. Instead, animals have acquired the capacity for adaptive responses during evolution, so that they can change or update their behaviors to enhance their prospect of survival. As such, animals that adapt better have a selective advantage.

Adaptation through learning is not only important for the survival of individuals, but also for the species or community. Knowledge acquired by individuals can be transmitted to others by communication. For example, honeybees can communicate with conspecifics via a dance to indicate a location of flowers (von Frisch and Seeley, 1993). Monkeys can utilize different alarm calls to indicate the presence of different predators, such as leopards, eagles, or snakes (Cheney and Seyfarth, 1992). Furthermore, some animals can learn a skill from others by observation and imitation (Mazur, 2006). For such communication, animals need to handle abstract information explicitly, such that a

certain sound, visual sign, or behavior indicates a specific event, action, or emotion to other animals.

Finally, if the brain can maintain stored information for a sufficiently long period of time, the knowledge acquired in one generation can be transmitted to the next generation. Such transgenerational transmission has been observed in animals other than humans. For example, Leca et al. (2008) examined multiple troops of monkeys at geologically isolated sites and observed that each troop has a different style of stone-throwing, which has been maintained over a number of years and appears to be transmitted across generations. The transmission of knowledge or skills among community across generation is considered to be a basis of culture.

Thus, for cultural evolution animals, the learning system should be also be adapted to handle and maintain many types of abstract information explicitly. How does our brain implement this process? Which brain structure is necessary for such information processing? As learning is essential for cultural evolution, how the brain implements learning may, in turn, be a fundamental question to be answered by our culture.

1.2 Animal Learning Theory

Behaviorists have proposed many basic rules of learning by observing animal behaviors. I will briefly introduce two fundamental paradigms in learning theory.

1.2.1 Classical Conditioning

Ivan Pavlov first described a learning paradigm about the relation between two stimuli, which is now called classical conditioning (Pavlov, 1903). Two elements of this learning paradigm are the "unconditioned stimulus (US)" and "unconditioned response (UR)." For example, in Pavlov's experiments, the US was the presence of food and the UR was the secretion of saliva. This represents an innate, or unlearned, stimulus–response relation. The third element is the conditioned stimulus (CS). In Pavlov's experiments, the CS was the bell sound. The CS did not evoke any response initially, however as the presentation of the CS (bell) was followed by the US (food) repeatedly, the dog began to salivate as soon as the CS (bell) was presented. This salivation is called conditioned response (CR), which is an acquired response. Thus animals learned the association between the CS and the US, and the presentation of the CS elicits the expectation of US occurrence, which induces the CR.

1.2.2 Operant Conditioning

Animal behaviors are not always elicited by a specific stimulus. Animals perform many voluntary behaviors, the repeat occurrence of which can also be controlled by learning. Thorndike (1898) initially investigated systematically how such voluntary behaviors can be elicited and modified by experiences. In his experiments, animals are housed in a small chamber, called a puzzle box. The animals have to perform appropriate responses to open the door of the puzzle box for food. Thus, animals have to shape their response accordingly for a reward. Thorndike, indeed, found that escape latency of the animals gradually decreased. Based on this results, Thorndike formulated a learning

principle called, the law of effect, where he described "Of several responses made to the same situation, those which are accompanied or closely followed by satisfaction to the animal will, other things being equal, be more firmly connected with the situation…" In other words, the action which leads to the animal's satisfying state (or reinforcer) will be repeated more often.

1.2.3 Issues in Learning Theory

When we attempt to explain our behaviors solely by classical and operant conditioning paradigms, we will soon realize that additional conditions or rules may be required. The following are examples of some additional issues to be considered.

Sensory preconditioning

Sensory preconditioning is a variant form of classical conditioning which demonstrates that animals can learn a relationship between neutral stimuli (Rizley and Rescorla, 1972). In the first phase of sensory preconditioning paradigm, one neutral stimulus (e.g., light; CS1) occurs just before another neutral stimulus (e.g., tone; CS2). After several CS–CS pairings, next phase follows, where CS2 is paired with a US (e.g., food).

First phase: CS1 – CS2

Second phase: CS2 – US

Test phase: CS2 – CR, CS1 – ?

As a classical conditioning paradigm predicts, after multiple CS–US pairings, the CS2 elicits the CR (e.g., salivation). However here, the CS1 also can elicit the CR, even without any direct association with a US. Animals must have acquired an association between the CS1 and CS2 in the first phase of conditioning, even without behaviorally relevant stimuli (US) present. Thus, this paradigm suggests that the brain can acquire associative information about any stimulus pair, even if they are neutral or not directly associated with reward or punishment.

Latent inhibition

A similar issue can be observed in another variant of classical conditioning paradigm called latent inhibition (Reiss and Wagner, 1972). After repeated presentation of the CS (e.g., light) without the US, pairings of the CS (light) and US (food) are performed as in usual classical conditioning paradigm.

First phase: CS alone

Second phase: CS – US

Test phase: CS – ?

In this paradigm, the association between the CS and US is retarded, compared to the situation without a CS pre-presentation in the first phase. This retardation is because animals learned that the CS is not associated with any other stimulus in the first

phase, which makes the CS–US association in the second phase difficult. This learning paradigm suggests that animals can learn something about seemingly neutral sensory stimuli in the absence of association with behaviorally relevant stimuli.

Learning of event sequence

Animals are able to learn a sequence of movements or stimuli (Mazur, 2006). For example, when a human learns to swim, the brain memorizes a sequence of particular movements of joints and muscles during each stroke. Another example of sequence learning is the escape behavior in a maze box (Tolman and Honzik, 1930). Rats can quickly learn how to get out from the maze, but during this process, they cannot tell whether each choice (e.g., left or right turn) is correct or wrong until they finally get out from the maze. Both of these examples indicate that animals have to remember a sequence of actions until they obtain a final outcome.

Context learning

In a classical conditioning paradigm, animals remember not only the stimulus itself, but also the environmental context when the stimulus was applied (Myers and Gluck, 1994). For example, after an electric shock is applied to an animal in a particular home cage, the animal remembers the environmental context when the shock was given, and exhibits a freezing response whenever the animal is placed back in the same cage. Thus, animals process information about the environmental context. A representation of environmental context requires association of multimodal information, such as color,

sound, odor, location, time, or objects around them. How does the brain handle such multimodal abstract information?

Many studies have indicated that the hippocampus may play a key role in solving the issues described above. For example, animals with hippocampal lesions display deficits in sensory preconditioning (Port and Patterson, 1984), latent inhibition (Kaye and Pearce, 1987), sequence learning (Fortin et al., 2002) and contextual learning (Myers and Gluck, 1994). The hippocampus, indeed, is considered to be important for storing information about stimuli even without direct outcome association (Gluck and Myers, 2001) or for handling multimodal abstract information (Rudy and Sutherland, 1995; Quiroga et al., 2005; Bird and Burgess, 2008).

Below I describe a brief history of the hippocampus and how understanding hippocampal function has become a major emphasis of modern neuroscience research.

1.3 The Hippocampus

1.3.1 Behavioral Significance

The hippocampus has attracted attention since the beginning of brain investigations, because of its unique shape and highly condensed single layers (Golgi, 1886). Among the many hypotheses on hippocampal function, a major hypothesis in early 20th century was proposed by Papez. He considered the hippocampus as a structure which links subcortical and cortical structures and is involved in emotion (Papez, 1937).

One of the major breakthroughs in the hippocampal research occurred by clinical studies of brain-damaged patients. Scoville and Milner studied patients who underwent a surgical resection of a part of medial temporal lobe for relief of epileptic or other neurological symptoms. The most famous of these patients is H. M. (Scoville and Milner, 1957). After the surgery, he exhibited severe memory deficits. A more detailed examination revealed that he could not form any new long-term memories, although he had no problem in short-term memory. He also showed retrograde amnesia, which extended up to 11 years before surgery (Sagar et al., 1985).

The initial studies on H. M. inspired research on the hippocampus and memory. Early studies on hippocampal-lesioned animals, however, did not reveal a consistent role of the hippocampus in memory formation. For example, animals with hippocampal lesions still learned the delayed response task, where animals have to repeat the same response after some delay (Correl and Scoville, 1967), and also were able to learn some operant conditioning tasks. Around 1970, scientists realized that there are many types of memory and the hippocampus may be involved in some types of memories, rather than all memories. Tulving (1972) described a distinction between memories for episodes and those for semantic items such as facts. Another distinction was made between declarative and procedural memories (Winograd 1975; Cohen and Squire, 1980). Studies based on these memory classifications revealed a specific role of the hippocampus for declarative memory, which includes both semantic and episodic memory (Squire et al., 2004). Another important development in the analysis of hippocampal function was the ability to record single-neuron activity *in vivo* in the hippocampus of awake animals. O'Keefe and

Dostrovsky (1971) described a strong correlation between the activities of hippocampal neurons and an animal's location in the environment. Inspired by these observations, more optimal behavioral tests became available to examine hippocampal function such as the Olton radial arm maze (Walker and Olton, 1979) or the Morris water maze (Morris, 1984).

1.3.2 Anatomy

The hippocampal formation comprises three cytoarchitectually distinct regions: the dentate gyrus; the hippocampus proper, which is subdivided into three fields (CA3, CA2, CA1); and the subiculum (Witter and Amaral, 2004). The entorhinal cortex, which provides major afferent inputs to the hippocampal formation, is included in the parahippocampal region. The parahippocampal region also includes presubiculum, parasubiculum, perirhinal and postrhinal cortices (Witter and Amaral, 2004).

The hippocampal formation is categorized as an archicortex, and has several important differences from the neocortex. For example, the principal neurons of the hippocampus are located in a single layer, rather than multiple layers as in the neocortex. Another difference is the direction of the axon fibers, which run parallel to the layer of principal neurons or orthogonal to the apical dendrites, whereas the cortical axons run radially, parallel to the apical dendrites.

Microscopic anatomical studies using Golgi methods (1886) and silver degeneration techniques (Nauta, 1950) revealed another interesting feature of the hippocampus. Each area of the hippocampus projects to the neighboring region, but

generally does not receive a return pathway from the target (Hjorth-Simonsen, 1973). This anatomical study was also supported by *in vivo* electrophysiology (Andersen et al., 1966). Following the stimulation of the perforant pathway (the projection from the entorhinal cortex to the dentate gyrus), activation of CA3 followed by CA1 was observed. When CA3–CA1 fibers were removed, activation of area CA1 and the subiculum was abolished. These findings together provide evidence for the major functional circuit in the hippocampus, trisynaptic circuit (Andersen et al., 1966), i.e., EC – DG – CA3 – CA1.

As initially described by Ramon Cajal, the entorhinal cortex is the first step of the hippocampal circuit, because most neocortical inputs to the hippocampus are relayed through the entorhinal cortex (Cajal, 1911). The entorhinal cortex provides major afferent inputs to the DG, through the perforant pathway. The principal cells of the DG, the granule cells, projects to CA3 pyramidal neurons via mossy fibers. Likewise, pyramidal neurons in area CA3 send their projections to CA1 pyramidal neurons through the Schaffer-collateral pathway. Although the volume of the hippocampus is about 10 times larger in macaque monkeys and 100 times larger in human than in rats, the basic hippocampal architecture described above is common to all species (Amaral and Lavenex, 2007).

Another feature of the hippocampal circuit is the proposed existence of independent functional circuits along a longitudinal axis of the hippocampus. When some fibers in the hippocampus were stimulated, activation was observed largely along the strip oriented transverse to the longitudinal axis of the hippocampus. This arrangement of fibers is called lamellar organization (Andersen et al., 1969).

The estimated number of principal neurons in the hippocampus in rat is as follows: layer II in the EC: 2×10^5, DG: 1×10^6, CA3: 3.3×10^5, CA1: 4.2×10^5, subiculum: 1.28×10^5 (Amaral et al., 1990). The estimated number of neurons in human is DG: 11.2×10^6, CA3: 2.3×10^6, CA1: 6.14×10^6 (Harding et al., 1998).

The size of somata of pyramidal neurons in areas CA3 and CA2 is about 20 μm in diameter, whereas that in area CA1 is about 15 μm. The distinction between area CA3 and CA2 can be made by existence of mossy fiber inputs, since CA2 pyramidal neurons do not receive mossy fiber projections. Although both CA3 and CA2 pyramidal neurons give rise to highly divergent associational connections to both ipsilateral and contralateral hippocampus, this massive association network is largely missing in area CA1 (Amaral and Lavenex, 2007).

Fiber architecture of afferent inputs in the hippocampus

The entorhinal cortex projects its fibers through the angular bundle, which travel through the pre- and para-subiculum to reach the hippocampus and subiculum at all septotemporal levels. The perforant pathway traverses, or perforates, the subiculum on the way to the dentate gyrus. Entorhinal fibers also reach the hippocampus via the alveus. In the entorhinal cortical projection to area CA1, most of the entorhinal fibers reach area CA1 after perforating the subiculum, at the temporal level of the hippocampus. However, at more septal levels, more fibers take the alvear pathway to reach area CA1 (Deller et al., 1996). These alvear fibers make sharp turns in the alveus, perforating the pyramidal cell layer to terminate in the stratum-lacunosum-moleculare.

The fimbria-fornix pathway provides the major circuit for subcortical afferent and efferent connections (Daitz and Powell, 1954). Many subcortical inputs including neuromodulator releasing areas, such as the septal nucleus, the locus coeruleus or the raphe nuclei, travel through this pathway to reach the hippocampus.

EC to DG: perforant pathway

The DG receives its major input from the entorhinal cortex. The projection arises mainly from neurons located in layer II of the entorhinal cortex. Each layer II entorhinal cell is estimated to have 17,710 synapses in the molecular layer of the dentate gyrus (Amaral et al., 1990), implying that each layer II cell would form synapses with about 2% of the total granule cell population. The perforant projection to the DG also arises from layer V and VI cells in the entorhinal cortex (Steward and Scoville, 1976; Koganezawa et al., 2008). Because input from the entorhinal cortex is dispersed onto an extensive layer of sparsely firing granule cells, each granule cell can carry only a small and distinct fraction of information in the EC. As such, this circuit architecture is considered to be important for distinguishing a slight difference in inputs, suggesting a role for pattern separation (Leutgeb et al., 2007)

In the dentate gyrus, the outer third of molecular layer receives a projection from the lateral entorhinal cortex, whereas the middle third receives inputs from the medial entorhinal cortex. The most abundant cell type in layer II in the MEC is the stellate cell, however in layer II in the LEC, stellate cells are less common and replaced by fan cells (Canto et al., 2008). The synaptic terminals of the lateral and medial perforant pathway

exhibit a number of distinct features. For example, the medial perforant pathway fibers are immunoreactive for the metabotropic glutamate receptor mGluR2/3, whereas the lateral fibers are not (Shigemoto et al., 1997). On the other hand, the lateral perforant pathway showed enkephalin immunoreactivity but the medial pathway does not (Fredens et al., 1984).

DG to CA3: Mossy fibers

Each granule cell communicates with only about 15 pyramidal neurons in area CA3. Considering that each CA3 pyramidal neuron receives approximately 3,500 perforant path and 10,000 recurrent path projections, the mossy fiber projections are, by comparison, very limited in convergence (~50 mossy projections per pyramidal cell) and divergence (~15 pyramidal cells per single mossy fiber) (Morris, 2001; Henze et al., 2002). Because of intensive recurrent connections in area CA3, the patterns which have been stored in this network can be restored even with a slightly different input, suggesting a role in pattern completion (Marr, 1971; Nakazawa et al., 2002). Mossy fibers contain large amounts of zinc and opioid peptides which are coreleased with the main glutamate transmitter (Stengaard-Pedersen et al., 1981; Howell et al., 1984; Aniksztejn et al., 1987).

CA3 to CA1: Schaffer-collateral pathway

It has been estimated that the axon of each CA3 pyramidal neuron makes synapses with 30,000 – 60,000 neurons (Li et al., 1994). This projection shows extensive

spatial distribution throughout the both ipsilateral and contralateral hippocampus (Amaral and Lavenex, 2007). Most of these CA3 projections are received by CA1 pyramidal neuron via the Schaffer-collateral pathway. Each CA1 pyramidal neuron, in turn, receives approximately 30,000 excitatory inputs (Megias et al., 2001), which is primarily due to the convergence of thousands of CA3 pyramidal neurons (Sorra and Harris, 1993). This huge divergence-convergence architecture is one of major features of Schaffer-collateral pathway.

EC to CA1

The entorhinal cortex not only sends projections to the dentate gyrus, but also projects to area CA1; this input is called the temporoammonic (TA) pathway. Although layer II cells in the entorhinal cortex give rise to the perforant pathway, the temporoammonic pathway originates from layer III cells. The TA pathway terminates in the stratum lacunosum-moleculare of area CA1.

The TA pathway includes two components of projections from the MEC and LEC, which are topographically organized along the transverse axis of area CA1, such that the projections from MEC make synapses at proximal CA1 (close to CA3), but those from the LEC projects to distal CA1 (close to subiculum) (Witter and Amaral, 2004). Thus, the topographic projection allows neurons in area CA1 to receive primarily one set of inputs either from the MEC or LEC. This contrasts with the laminar organization of the perforant pathway projection, from the entorhinal cortex to the dentate gyrus or area CA3, where each neuron receives both LEC and MEC inputs in either distal or proximal

regions of dendrites (Witter and Amaral, 2004). The efferents from area CA1 are also topographically organized such that neurons in proximal CA1 send projections back to the MEC, while neurons in distal CA1 project back to the LEC (Tamamaki and Nojyo, 1995). Thus, two independent circuit loops exist between the entorhinal cortex and area CA1 (Amaral and Lavenex, 2007).

Layer III pyramidal cells in the MEC and LEC have comparable morphological as well as electrophysiological characteristics (Canto et al., 2008). The majority of entorhinal terminals, irrespective of their origin in the LEC or MEC, make asymmetric synaptic contacts (>96%) with both dendritic spines (93%) and dendritic shafts (7%) (Witter and Amaral, 2004). Because the TA projection is focally distributed (Naber et al., 1999) and also strongly innervates inhibitory basket and chandelier cells (Kiss et al., 1996), the existence of a bona fide excitatory input has been strongly debated (Naber et al., 1999) and the TA pathway was relatively unexplored until recently.

Extrinsic inputs to the EC

The cortical projections to the LEC are heavier than to the MEC and differ in origins. The LEC is primarily innervated by the perirhinal, insular, piriform, and postrhinal cortices, whereas the MEC is primarily innervated by the piriform and postrhinal cortices, but also receives minor projections from retrosplenial, posterior parietal and visual association areas (Burwell and Amaral, 1998). The cortical afferents that reach the deep layers of the entorhinal cortex terminate diffusely, but those terminating in the superficial layer have a more restricted distribution. The projections to

superficial layers of the EC originate from olfactory stuructures, perirhinal and postrhinal cortices (Burwell and Amaral, 1998), whereas cortical afferents to the deep layer of the EC include projections from the agranular insular cortex and the medial prefrontal region (Insausti et al., 1997). Recent *in vivo* recording studies indicate that MEC neurons exhibit strong spatial modulation (Fyhn et al., 2004), but LEC neurons appear to be involved in nonspatial information processing about specific objects or cues in the environment (Hargreaves et al., 2005; Knierim et al., 2006).

1.3.3 Novelty Detection

Although the hippocampus play a key role in declarative memory formation (Squire et al., 2004), recent studies indicate that the hippocampus may also have important roles outside of declarative memory, such as short-term (Hartley et al., 2007) or implicit memory (Greene, 2007), or imagination (Hassabis et al., 2007) or perception (Lee et al., 2005). What would be a unified role of the hippocampus to explain these studies? One prominent feature of hippocampal neurons is their differential activation depending on stimulus novelty (Stern et al., 1996; Knight, 1996; Dolan and Fletcher, 1997; Vinogradova, 2001; Rutichauser et al., 2006), suggesting that the hippocampus may act as a novelty detector (Parkin, 1997; Kumaran and Maguire, 2009). The novelty-dependent activation of hippocampal neurons is likely to be a critical feature for learning, allowing circuit modifications that optimize stimulus prediction. Furthermore, in learning stimulus sequences, the hippocampus is strongly activated when mismatches in associative sequences occur, although no significant activation is observed when mere

presence of novel sequence per se (Kumaran and Maguire, 2006). Thus, the hippocampus may not be a simple novelty-detector, but rather a comparator, that generates mismatch signals when predictions derived from previous experience are violated by current sensory inputs (Vinogradova, 2001).

The comparator function of the hippocampus may be crucial for the controlling, saving or loading of information in hippocampal circuits. Many lines of evidence indicate that the hippocampus is critical for both memory encoding and the retrieval process (Riedel et al., 1999). Memory encoding requires circuit modifications to represent the new associative information of applied stimuli, whereas during memory retrieval, a circuit modification will be unfavorable, because it may disrupt previously acquired information. Many models have been suggested to implement both memory encoding and retrieval in same circuit architecture (Paulsen and Moser, 1998). Here, mismatch signals in the hippocampus may play a key role because the hippocampus can modify synaptic connections only when mismatch or prediction-error occurs. How such mismatch signals can be generated to control hippocampal circuits is still unclear, but a number of studies have indicated a critical role of neuromodulators (Hasselmo and Schnell, 1994; Ranganath and Rainer, 2003; Lisman and Grace, 2005).

1.3.4 Neuromodulators in the Hippocampus

The hippocampus receives many neuromodulatory inputs (Storm-Mathisen, 1978; Straughan, 1975, Swanson, 1982). Among them, two major classes of monoaminergic neurons, dopaminergic and noradrenergic, change their firing rate

depending on stimulus novelty (Vankov et al., 1995; Schultz, 1998; Matsumoto and Hikosaka, 2009). The noradrenergic neurons in the locus coeruleus send massive projections to the DG (Swanson, 1987) but also to area CA1 (Castle et al., 2005). Although neurons in both the ventral tegmental area (VTA) and substantia nigra compacta (SNc) distribute their axons along a septotemporal axis of the hippocampus, only about 15% of these neurons appear to be dopaminergic (Gasbarri et at., 1997). Most projections from the VTA and SNc terminate in area CA1 and the subiculum (Gasbarri et al., 1994a). Dopaminergic neurons in the VTA project predominantly to the ventral hippocampus rather than the dorsal hippocampus, whereas those in the SNc only send their projections to the ventral hippocampus. Supporting these anatomical connections, Ihalainen et al. (1999) observed the release of both dopamine and norepinephrine in the hippocampus by microdialysis after animals were exposed to novel environment.

Behavioral studies have revealed important roles for either dopamine or norepinephrine in hippocampal function. For example, intrahippocampal injections of the dopamine receptor agonist, apomorphine, increase spontaneous and exploratory locomotor activities (Smialowski, 1976). Either lesions of the hippocampus or functional manipulations of dopamine system influence the magnitude of latent inhibition (Gray et al., 1997; Buhusi et al., 1998). Furthermore, animals with selective lesions of the dopaminergic projection to the hippocampus exhibit deficits in spatial learning in Morris water maze (Gasbarri et al., 1996b). Thus the reciprocal interaction between the dopamine system and the hippocampus is likely to be crucial for hippocampal-dependent learning (Lisman and Grace, 2005). In contrast, norepinephrine appears to play a

selective role in retrieval of contextual and spatial memory (Murchison et al., 2004).

Chapter 2. Distance-Dependent Homeostatic Synaptic Scaling Mediated by A-type Potassium Channels

2.1 SUMMARY

Many lines of evidence suggest that the efficacy of synapses on CA1 pyramidal neuron dendrites increases as a function of distance from the cell body. The efficacy of an individual synapse is also dynamically modulated by activity-dependent synaptic plasticity, which poses the question as to how a neuron can reconcile individual synaptic changes while maintaining the proximal to distal gradient of synaptic efficacy along the dendrites. As the density of A-type potassium channels exhibits a similar gradient from proximal (low) to distal (high) dendrites, the A-current may play a role in coordinating local synaptic changes with the global synaptic efficacy gradient. Here we describe a form of homeostatic plasticity elicited by conventional activity blockade (with TTX) coupled with a block of the A-type potassium channel. Following A-type potassium channel blockade for 12 hrs, recordings from CA1 somata revealed a significantly higher miniature excitatory postsynaptic current (mEPSC) frequency, whereas in dendritic recordings, there was no change in mEPSC frequency, suggesting a differential influence along the dendrites. Consistent with mEPSC recordings, we observed a significant increase in relative AMPA receptor density at stratum pyramidale by immunohistochemistry. This synaptic scaling was independent of calcium signaling but prevented by transcription or translation inhibitors. We propose that the differential

distribution of A-type potassium channels along the apical dendrites creates a proximal-to-distal membrane potential gradient. This gradient may regulate AMPA receptor distribution along the same axis. Taken together, our results indicate that A-type potassium channels play an important role in controlling synaptic efficacy along the dendrites, which may help to maintain the computational capacity of the neuron.

2.2 INTRODUCTION

CA1 pyramidal neurons in the hippocampus receive approximately 30,000 excitatory inputs along their dendrites (Megias et al., 2001). Due to voltage attenuation by cable filtering, distal synapses must be stronger than proximal synapses to provide the same amplitude of voltage change at the soma (London and Segev, 2001). Recent studies, indeed, observed that the synapses located at distal dendrites of CA1 pyramidal neurons have higher synaptic efficacy than those in proximal synapses (Magee and Cook, 2000; Smith et al., 2003; Nicholson et al., 2006). As such, neurons appear to adjust synaptic efficacy so that synapses at different dendritic locations can have a comparable impact on the soma. These findings suggest that neurons possess mechanisms to control AMPA receptor distribution along the dendrites.

A number of recent studies have emphasized the importance of homeostatic control of the synaptic strength. After a long-term neuronal inactivation with a sodium channel blocker, tetrodotoxin (TTX), synaptic strength becomes larger, whereas after a chronic enhancement of activities with a $GABA_A$ receptor blocker, bicuculline, the synaptic strength becomes smaller (Turrigiano et al., 1998, Burrone et al., 2002;

Stellwagen and Malenka, 2006). As such, neurons manage to keep their firing frequency within an appropriate range and neuronal networks remain stable (Turrigiano, 2008). This scaling, elicited by neuronal activity, is often called global scaling because the synaptic strength is increased multiplicatively or decreased divisively throughout synapses in neurons (Rabinowitch and Segev, 2008).

Synaptic strength can also be controlled locally by spontaneously released synaptic vesicles (i.e., miniature synaptic transmission) (Sutton et al., 2006; Sutton and Schuman, 2006). This mechanism does not require action potentials, but instead, each synapse monitors and adjusts synaptic strength according to the levels of miniature synaptic transmission. The calcium-mediated signal evoked by miniature synaptic transmission controls dendritic protein synthesis and synaptic efficacy appropriately. This scaling occurs locally, allowing for neurons to control individual synapses independently.

Although homeostatic scaling mechanisms can work either globally or locally, it remains unexplored how neurons maintain the distance-dependent synaptic efficacy along the proximal-distal axis in dendrites in the face of scaling. Previous studies have provided several clues to potential mechanisms. For example, the distance-dependent distribution of AMPA receptors is abolished in animals lacking either GluR1 or Kv4.2 channel, a molecular component of A-type-mediated potassium current (Andrasfalvy et al., 2003; Andrasfalvy et al., 2008). This implies that both GluR1 and A-type channels may contribute to distance-dependent AMPA receptor distribution. Interestingly, similar to AMPA receptors, A-type potassium channels are also differentially distributed, exhibiting higher channel density in distal, compared to proximal regions of apical CA1 dendrites

(Hoffman et al., 1997). The distribution pattern of A-type channels may be crucial for the proximal to distal gradient of synaptic efficiacy because layer V pyramidal neurons in the neocortex exhibit uniform A-type channel density along the dendrites (Bekkers, 2000; Korngreen and Sakmann, 2002) and do not exhibit the distance-dependent increase in synaptic efficacy (Williams and Stuart, 2002). Here, we asked whether A-type channels can directly influence the distance-dependent differences in synaptic efficacy observed in the dendrites of hippocampal neurons.

2.3 RESULTS

2.3.1 Chronic blockade of A-type potassium channels enhanced mEPSC frequency in the region near the soma of CA1 pyramidal neurons

The observation that slices prepared from Kv4.2 knockout animals do not exhibit a distance-dependent increase in synaptic efficacy (Andrasfalvy et al., 2008), suggests that A-type potassium channel activity may participate in the differential distribution of ion channels along the dendritic axis. To initially test this idea, we asked whether chronic blockade of A-type potassium channels (by the antagonist 4-aminopyridine, 4AP; Thompson, 1982) can also change the synaptic efficacy. To avoid the influence of seizure-like activities induced by 4AP we included tetrodotoxin (TTX) in our experiments.

Using acute hippocampal slices to preserve the channel or receptor distribution found *in vivo*, we examined miniature excitatory synaptic transmission by recording from

the soma of CA1 pyramidal neurons after treatment with either TTX alone or TTX + 4AP for 12 hrs. We found that mEPSC frequency was significantly enhanced in 4AP-treated slices, relative to slices treated with TTX alone (TTX: 3.12 ± 0.32 Hz, TTX + 4AP: 6.88 ± 0.41 Hz) (Figure 2-1A). Treatment with 4-AP did not elicit a significant difference in mEPSC amplitude (TTX: 12.24 ± 0.76 pA, TTX + 4AP: 13.24 ± 0.76 pA). Our analysis indicates that this scaling is, at least in part, mediated by a postsynaptic mechanism (Figure 2-2). A similar treatment with a blocker for a different class of potassium channels, (tetraethylammonium; TEA) did not influence synaptic scaling (mEPSC amplitude: TTX 12.15 ± 0.61 pA, TTX + TEA 10.96 ± 0.29 pA; mEPSC frequency: TTX 2.49 ± 0.25 Hz, TTX + TEA 2.14 ± 0.16 Hz) (Figure 2-1C), thus this scaling is specifically mediated by A-type potassium channels.

Next we examined miniature synaptic transmission in dendrites, because A-type channel blockade may differentially influence synaptic efficacy along the apical dendrites. We recorded from dendrites of CA1 pyramidal neuron by targeting the middle of stratum radiatum (approximately 200 to 250 μm from the stratum pyramidale). We found that 4AP had a significantly smaller influence on mEPSC frequency in dendrites (mEPSC amplitude: TTX 12.60 ± 0.55 pA, TTX + 4AP 13.04 ± 0.54 pA; mEPSC frequency: TTX 1.91 ± 0.34 Hz, TTX + 4AP 2.61 ± 0.33 Hz) (Figure 2-1B). Thus, A-type potassium channel blockade enhanced mEPSC frequency primarily in the region near soma, which indicates that 4AP disrupted the balance of synaptic efficacy along dendrites.

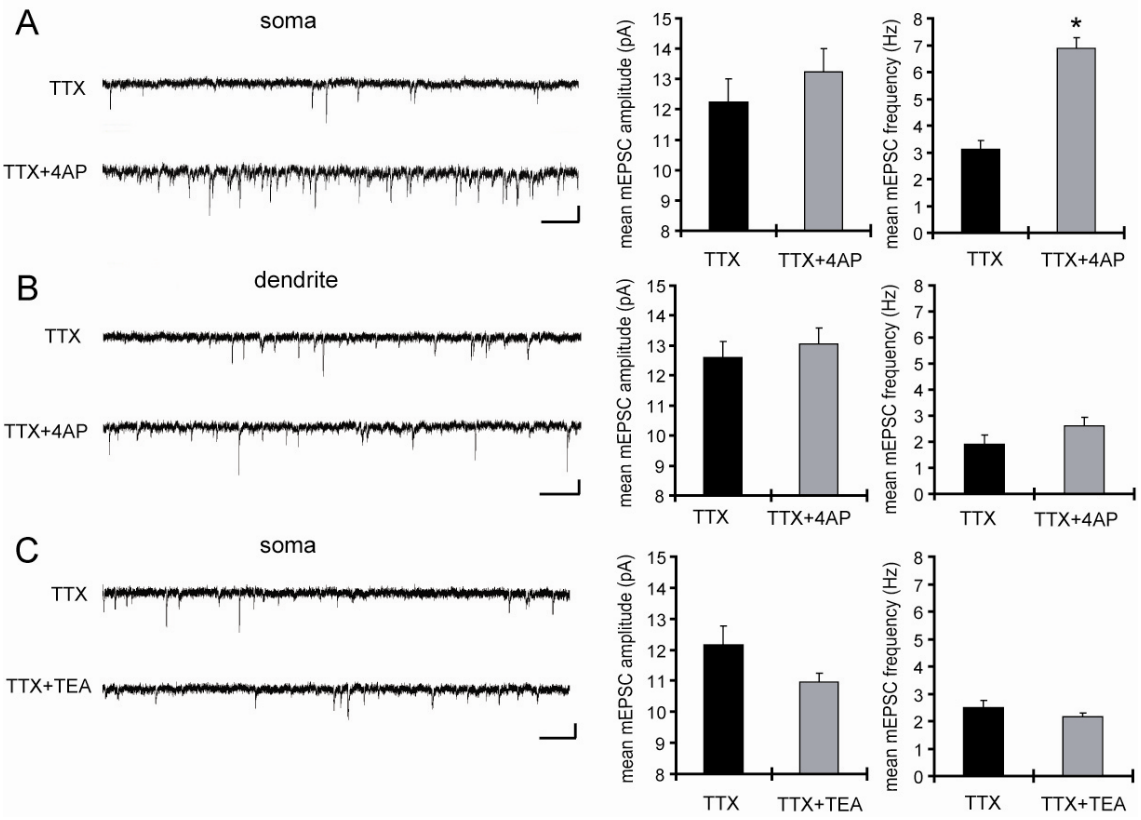

Figure 2-1: A-type potassium channel blockade enhances the frequency of mEPSCs recorded in the soma, but not the dendrites, of CA1 pyramidal neurons

(A) Representative mEPSCs recorded from the somata of CA1 pyramidal neurons. Hippocampal slices were treated with either TTX alone or TTX + 4AP (5 mM) for 12 hrs. The slices treated with 4AP showed enhanced mEPSC frequency (TTX: n = 8, TTX + 4AP: n = 9) (scale bar = 10 pA, 500 ms) (*$p < 0.05$). **(B)** Representative mEPSCs recorded from the dendrites of CA1 pyramidal neurons. The recorded sites were in the middle of the stratum radiatum, which is approximately 200 – 250 μm away from the soma. The slices treated with 4AP did not exhibit a significant enhancement of mEPSC frequency in dendrites (n = 10 for each group) (scale bar = 10 pA, 500 ms). **(C)**

Representative mEPSCs recorded from the somata of CA1 pyramidal neurons. The hippocampal slices were treated with either TTX alone or TTX + TEA (10 mM) for 12 hrs. TEA-treated slices did not exhibit enhanced mEPSC frequency (n = 8 for each group) (scale bar = 10 pA, 500 ms) (*$p < 0.05$).

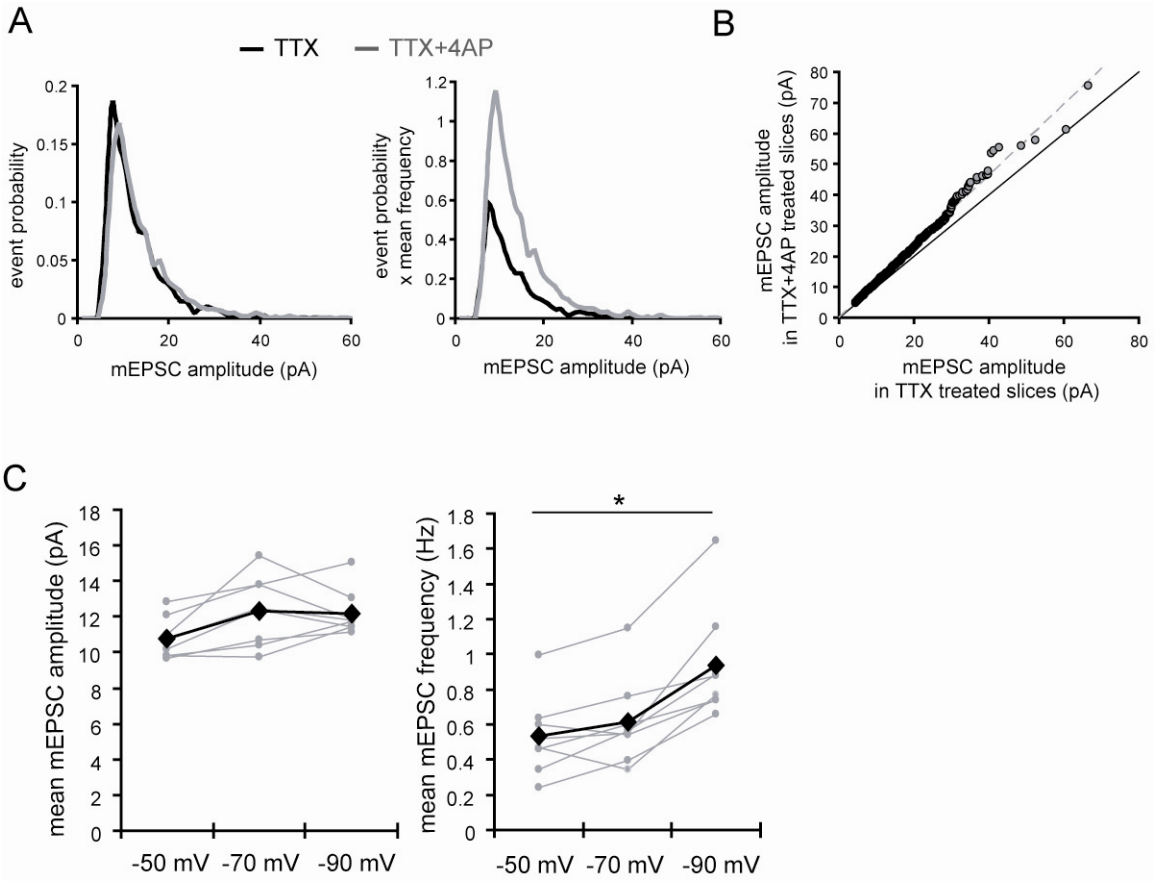

Figure 2-2: A postsynaptic mechanism contributes to the enhancement of mEPSC frequency by chronic A-type channel blockade

(A) Analysis of mEPSC amplitude recorded from the soma in either TTX or TTX + 4AP treated slices. The left figure shows the event probability of mEPSC amplitude. In the right figure, the mean mEPSC frequency was multiplied by the event probability, thus the resulting traces are equivalent to the event histogram. Note that most events are of small amplitude, indicating that the detection threshold for mEPSC analysis can have an influence on the recorded frequency of events (n = 2,080 mEPSCs chosen randomly from recording data used in figure 2-1A). **(B)** Ranked mEPSC amplitudes from TTX-treated

slices were plotted against ranked mEPSC amplitudes from TTX + 4AP treated slices. Data were subjected to a linear fit (gray dotted line; $y = ax$). The estimated line slope is 1.155 (between 1.153 and 1.156 with 95% confidence), which is significantly larger than a slope of 1 (black solid line), suggesting postsynaptic scaling. **(C)** An example showing the effect of postsynaptic membrane potential on mEPSC frequency. The mEPSC was recorded at different holding potential (-50, -60 or -70 mV) from the same neuron. An ANOVA revealed a significant influence of the holding potential on mEPSC frequency, suggesting that postsynaptic membrane potential can influence the detection of mEPSCs ($n = 8$) ($*p < 0.05$).

2.3.2 A-type channel blockade enhances mEPSC frequency by a protein synthesis dependent mechanism

Miniature synaptic transmission influences synaptic scaling by controlling dendritic protein synthesis and enhancing the synaptic insertion of GluR2-lacking AMPA receptors, an effect mediated by NMDA receptor activity (Sutton et al., 2006). Thus, we examined whether a NMDA receptor blocker, APV, influences synaptic scaling by A-type channel blockade. We did not find a significant influence of concurrent APV treatment on 4AP-induced synaptic scaling (mEPSC amplitude: TTX + 4AP 11.39 ± 1.04 Hz, TTX + 4AP + APV 12.06 ± 0.73 Hz, mEPSC frequency: TTX + 4AP 8.17 ± 1.41 Hz, TTX + 4AP + APV 8.79 ± 1.26 Hz) (Figure 2-3A). In addition, a specific blocker for GluR2-lacking AMPA receptors, Naspm, had no influence on 4AP-treated slices (mEPSC amplitude: before 12.87 ± 0.40 pA, after Naspm 12.68 ± 0.57 pA, mEPSC frequency: before 5.93 ± 0.59 Hz, after Naspm 5.89 ± 0.56 Hz) (Figure 2-3B), suggesting a different mechanism is involved in 4AP-induced scaling. Furthermore, even when slices were treated in a nominally zero calcium solution during the 12 hr incubation, we still observed the enhancement of mEPSC frequency by A-type channel blockade (mEPSC amplitude: TTX 9.33 ± 0.40 pA, TTX + 4AP 9.76 ± 0.45 pA, mEPSC frequency: TTX 2.25 ± 0.32 Hz, TTX + 4AP 5.06 ± 0.58 Hz) (Figure 2-3C), suggesting that this scaling is mediated by a calcium-independent mechanism.

We then asked whether 4AP-mediated scaling is protein-synthesis dependent. When slices were co-treated with a protein synthesis inhibitor, anisomycin, we did not observe significant influence of 4AP (mEPSC amplitude: TTX + Aniso 13.18 ± 0.66 pA,

TTX + 4AP + Aniso 12.1 ± 0.55 pA, mEPSC frequency: TTX + Aniso 2.09 ± 0.53 Hz, TTX + 4AP + Aniso 2.57 ± 0.51 Hz) (Figure 2-3D), suggesting that 4AP-mediated scaling is protein-synthesis dependent.

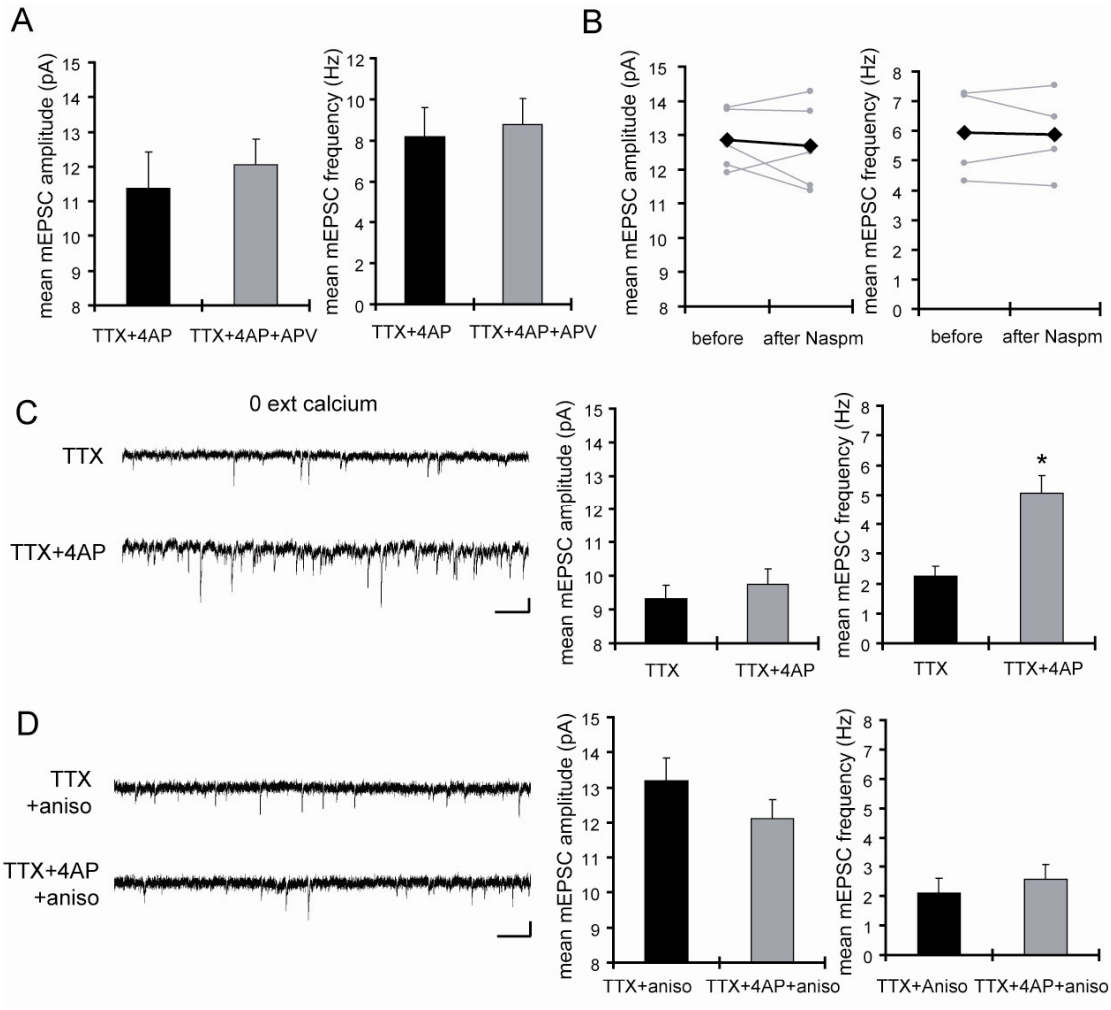

Figure 2-3: Synaptic scaling induced by A-type channel blockade is protein synthesis dependent, but calcium-signaling independent

(A) The NMDA receptor antagonist, APV, did not influence synaptic scaling by A-type channel blockade (n = 7 for each). **(B)** The synaptic scaling by A-type channel blockade was not mediated by GluR2-lacking receptors. After 12 hr treatment with TTX + 4AP, mEPSCs were recorded and the acute influence of Naspm (10 μM) application was examined (n = 5 for each). **(C)** Extracellular calcium did not influence 4AP-induced synaptic scaling. The slices were treated in ACSF, which contains zero calcium; the

divalent cation concentration was adjusted with magnesium (TTX: n = 5, TTX + 4AP: n = 7) (*$p < 0.05$). **(D)** 4AP-induced synaptic scaling was protein-synthesis dependent. The slices were treated with either TTX alone or TTX + 4AP, together with anisomycin (50 μM) for 12 hrs (n = 9 for each).

2.3.3 A-type channel blockade enhanced GluR1 density in stratum pyramidale, but not in stratum radiatum, of area CA1

Because synaptic scaling can be detected in recordings from the soma, but is largely absent in dendritic recordings, we examined whether there are any differences in synaptic protein expression after A-type channel blockade. We performed immunohistochemistry on slices after either TTX alone or TTX + 4AP treatment, examining the distribution patterns of synaptic proteins along the somatic-dendritic axis. Although we did not find any 4AP-induced differences in presynaptic protein distribution in area CA1 (signal ratio of s. pyramidale to s. radiatum; synaptophysin: TTX 0.46 ± 0.03, TTX + 4AP 0.43 ± 0.04, bassoon: TTX 0.08 ± 0.02, TTX + 4AP 0.12 ± 0.01) (Figure 2-4B), we observed a significant enhancement of GluR1 distribution in the soma, relative to the dendrites, following 4AP treatment (TTX: 1.10 ± 0.09, TTX + 4AP: 1.59 ± 0.13) (Figure 2-4B). The selective enhancement of GluR1 density in soma is consistent with mEPSC recording results, where the enhancement was observed only in regions near the soma (Figure 2-1). A similar change in distribution was also observed in other subunits of AMPA receptor, GluR2/3 (TTX: 0.83 ± 0.04, TTX + 4AP: 1.31 ± 0.06).

We next addressed potential cellular mechanisms for the 4AP-induced change in GluR distribution. The change in GluR1 distribution was observed either under AMPA receptor blockade, GABA receptor blockade, zero extracellular calcium condition, or disruption of microtubules or microfilament (Table 2-1). However, protein synthesis inhibitors (anisomycin and cycloheximide) or a transcription inhibitor (actinomycin D) completely blocked GluR1 redistribution by 4AP (Table 2-1). Thus, our results suggest

that A-type channels influence the synaptic efficacy by calcium-independent, but protein synthesis and/or transcription-dependent mechanism.

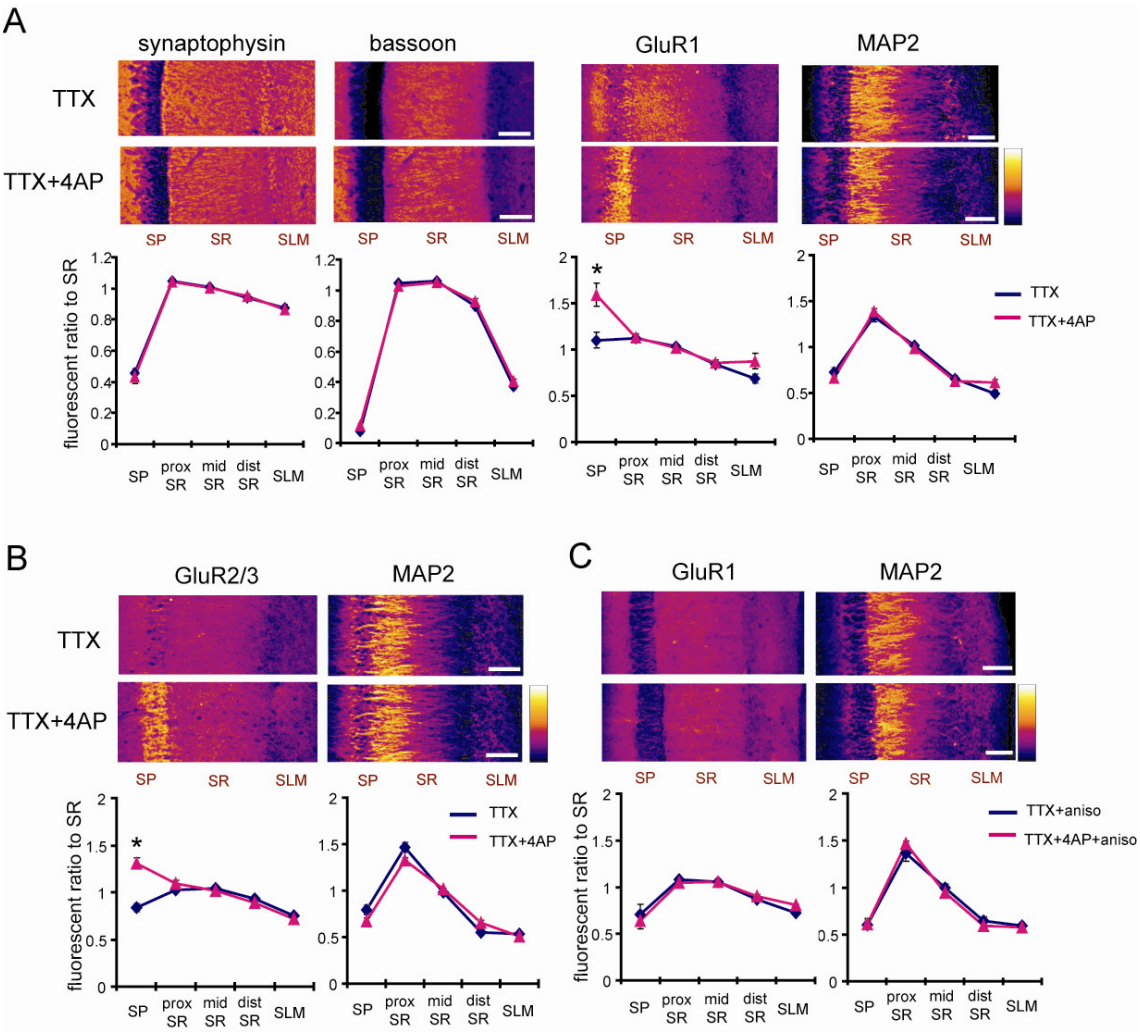

Figure 2-4: A-type channel blockade enhanced the relative density of GluR1 in stratum pyramidale

(A) Immunohistochemistry of hippocampal slices after 12 hr treatment with either TTX alone or TTX + 4AP. The hippocampal slices were stained with antibodies raised against a pair of presynaptic proteins (synaptophysin and bassoon), or a pair of postsynaptic proteins (GluR1 and MAP2) (scale bar = 200 μm). **(B)** A quantitative analysis of protein distribution along the dendrites in area CA1. The fluorescent signal was measured along

the apical dendrites from the stratum pyramidale to the stratum lacunosum-moleculare. The stratum radiatum was equally divided into three parts; proximal, middle and distal. The fluorescent signal was normalized to the mean signal in the stratum radiatum. The somatic signal ratio of GluR1 was significantly enhanced after A-type channel blockade (presynaptic protein staining: n = 8 for each, postsynaptic protein staining: TTX n = 8, TTX + 4AP n = 7) (scale bar = 100 μm) (*$p < 0.05$). **(C)** The enhancement of somatic GluR2/3 signal ratio after A-type channel blockade (n = 8 for each group) (scale bar = 100 μm) (*$p < 0.05$). **(D)** A protein synthesis inhibitor, anisomycin, blocked the somatic GluR1 signal enhancement produced by chronic A-type channel blockade (n = 4 for each) (scale bar = 100 μm).

	TTX mean ± SE	TTX + 4AP (5 mM) mean ± SE	TTX + TEA (10 mM) mean ± SE	
control (+APV)	1.10 ± 0.09 (n = 8)	1.59 ± 0.12 (n = 7)*	1.20 ± 0.03 (n = 4)	
bicuculline (20 μM) + CGP55845 (1 μM)	1.16 ± 0.06 (n = 6)	2.29 ± 0.41 (n = 6)*		* $GABA_A$ and $GABA_B$ receptor blockers
cytochalasin D (5 μM)	0.82 ± 0.03 (n = 6)	1.60 ± 0.12 (n = 6)*		* disruptor of actin filament
colchicin (10 μM)	0.80 ± 0.05 (n = 8)	1.30 ± 0.05 (n = 8)*		* depolymerizor of microtubules
0 extracellular calcium	0.55 ± 0.11 (n = 7)	1.05 ± 0.09 (n = 7)*		
NBQX (20 μM)	0.76 ± 0.08 (n = 11)	1.38 ± 0.12 (n = 11)*		* AMPA receptor blocker
anisomycin (50 μM)	0.71 ± 0.11(n = 4)	0.64 ± 0.09 (n = 4)		* protein synthesis inhibitor
cycloheximide (50 μg/ml)	0.74 ± 0.03 (n = 6)	0.73 ± 0.11 (n = 6)		* protein synthesis inhibitor
actinomycin D (25 μM)	1.06 ± 0.09 (n = 7)	1.04 ± 0.06 (n = 5)		* transcription inhibitor
SQ22536 (100 μM)	0.91 ± 0.02 (n = 4)	1.75 ± 0.04 (n = 4)*		* adenylate cyclase inhibitor
LY294002 (50 μM)	0.96 ± 0.04 (n = 4)	1.33 ± 0.04 (n = 4)*		* PI3K inhibitor
SB203580 (1 μM)	0.97 ± 0.05 (n = 5)	1.72 ± 0.07 (n = 5)*		* p38 MAPK inhibitor
SP600125 (10 μM)	1.00 ± 0.05 (n = 5)	1.46 ± 0.06 (n = 5)*		* JNK inhibitor
K93 (5 μM)	1.29 ± 0.07 (n = 5)	1.85 ± 0.09 (n = 5)*		* CaMK inhibitor
U0126 (5 μM)	0.86 ± 0.04 (n = 5)	1.52 ± 0.06 (n = 5)*		* MEK 1,2 inhibitor
rapamycin (1 μM)	1.00 ± 0.09 (n = 6)	1.38 ± 0.08 (n = 6)*		* mTOR inhibitor
JSH-23 (20 μM)	0.83 ± 0.02 (n = 3)	1.23 ± 0.03 (n = 4)*		* NF-κB inhibitor
U73122 (5 μM)	0.93 ± 0.03 (n = 5)	1.16 ± 0.05 (n = 5)*		* PLC inhibitor
Go6976 (0.5 μM)	0.84 ± 0.04 (n = 4)	1.33 ± 0.06 (n = 4)*		* PKC inhibitor

Table 2-1: The signal ratio of GluR1 in the stratum pyramidale: stratum radiatum after 12 hr incubation in the indicated conditions

*$p < 0.05$ relative to slices treated with TTX alone

2.3.4 Chronic external electric field application to slices mimicked the effect of A-type potassium channel blockade

How can A-type potassium channels influence synaptic efficacy by calcium-independent mechanism? Because A-type channels can be activated near the resting membrane potential of neurons (Hoffman et al., 1997), the distance-dependent distribution of A-type channels may differentially influence the resting membrane potential along the dendrites. To examine this idea, we directly measured the resting membrane potential either from soma or dendrites in CA1 pyramidal neurons, using whole-cell recordings. In recordings conducted in control medium (ACSF + TTX), the resting membrane potential was significantly different between soma and dendrites (soma: -72.7 ± 0.44 mV, dendrites: -75.7 ± 0.65 mV; Figure 2-5A). However, when 4AP was applied to the slices, the observed difference in resting membrane potential was abolished (soma: -73.3 ± 0.62 mV, dendrites: -73.6 ± 0.55 mV; Figure 2-5A). Thus, A-type potassium channels appear to create the voltage gradient along the dendrites, which may contribute to synaptic efficacy and GluR1 distribution.

If the dendritic electric field, generated by voltage gradient along the dendrites, plays a key role in controlling GluR1 distribution, then an externally applied electric field might be able to similarly alter GluR1 distribution. We tested this hypothesis by applying a chronic electric field, parallel to the main apical dendritic axis, to the hippocampal slices (Figure 2-5B; see methods for detail). The field was applied for 4 hrs, with the somatic region representing either the positive or negative pole. Following chronic field stimulation, we found that GluR1 distribution was significantly influenced in a direction

sensitive manner (signal ratio of s. pyramidale to s. radiatum: soma positive: 0.76 ± 0.06, soma negative: 1.05 ± 0.08; Figure 2-5C). Furthermore, this differential electric-field induced change in GluR1 distribution was completely abolished by the addition of a protein synthesis inhibitor, anisomycin (soma positive: 0.82 ± 0.07, soma negative: 0.78 ± 0.06; Figure 2-5C). These results suggest the possibility that A-type potassium channel blockade might influence scaling by changing the electric field along the dendrites.

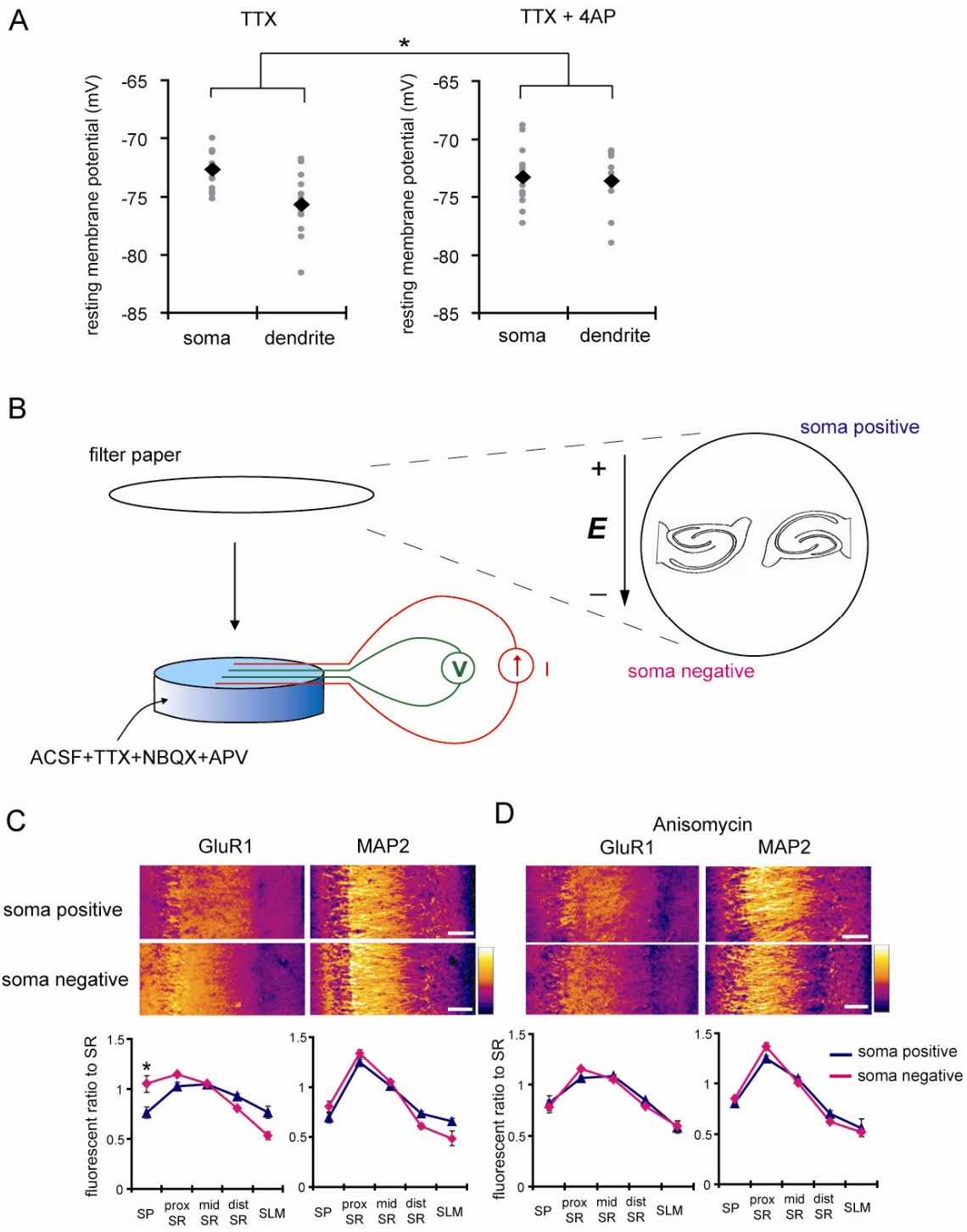

Figure 2-5: A chronically applied external electric field influenced GluR1 distribution

(A) The resting membrane potentials measured from soma and dendrites of CA1 pyramidal neurons. The recording sites in dendrites were in the distal half of the stratum radiatum (approximately 300 - 350 μm away from soma). The application of 4AP abolished the voltage difference between soma and dendrites (n = 15 for each group) (*p < 0.05). **(B)** Scheme of apparatus used for the electric field application to slices. The external electric field was applied to slices with a current source. The current amplitude was appropriately adjusted by monitoring the voltage difference between the two electrodes using a voltameter. The slices were treated with TTX + NBQX + APV to block neuronal activities. A chronic DC electric field (10 mV/mm) was applied to slices for 4 hrs. **(C)** The influence of the externally applied electric field on the GluR1 distribution. The relative somatic GluR1 signal was significantly higher when the electric field was applied in a direction such that somatic side was negative relative to apical dendrites (n = 8 for each group) (*p < 0.05). **(D)** A protein synthesis inhibitor, anisomycin (50 μM), abolished the GluR1 redistribution by differentially applied chronic electric field (n = 7 for each group).

2.4 DISCUSSION

The computational power of a single neuron arises from the large number of synaptic inputs distributed in its complex dendritic structure. These synaptic inputs are integrated in the dendrites and soma, shaping the neuron's final output as action potentials. The strength of each synaptic input is dynamically modulated by activity-dependent synaptic plasticity, such as LTP or LTD, which will change the integrative pattern of the synaptic inputs. As such, the dynamics of synaptic plasticity at individual synapse allows for neurons to have an enormous number of synaptic integration patterns, giving rise to different types of computation.

It has been suggested, however, that activity-dependent synaptic plasticity poses a problem for neuronal stability (Miller and MacKay, 1994; Miller, 1996; Abbott and Nelson, 2000). During LTP induction, strongly activated synapses achieve higher synaptic efficacy, resulting in a positive-feedback system. As strongly activated synapses continue to potentiate, synaptic strength will be eventually saturated and the output of a given neuron will be dominated by just a few strong synapses, sacrificing the computational power of the cell. Homeostatic synaptic plasticity can solve this issue, because it endows neurons with the ability to adjust their firing frequency in an appropriate range (Turrigiano et al., 1998; Turrigiano, 2008). The homeostatic mechanisms proposed thus far, however, do not address the synaptic balance problem. How is a distance-dependent increase in synaptic efficacy (i.e. proximal synapses are weaker than distal synapses) maintained during epochs of activity-dependent plasticity? The data presented here suggest that A-type potassium channels may be a key mediator of

the distance-dependent scaling. Our results suggest that A-type potassium channels influence AMPA receptor distribution via controlling the voltage gradient along the dendrites.

A number of studies have examined the influence of an externally applied electric field on different neuronal functions, including neurite elongation (Patel and Poo, 1982), receptor clustering (Poo et al., 1978, Orida and Poo, 1978), or spike initiation (Gluckman et al., 1996, Jefferys et al., 2003, Francis et al., 2003). In addition, the distribution of several molecules can be directly influenced by electric fields. For example, the acetylcholine receptor (Young and Poo, 1982) and epidermal growth factor receptor (Zhao et al., 2002), are accumulated to the cathodal side of electric fields. McLaughlin and Poo (1981) suggested that charged macromolecules on the cell surface generate electro-osmotic fluxes during electric field application to redistribute surface proteins. Externally applied electric fields can also influence distributions of intracellular signaling molecules, including phosphoinositide 3-kinases (Zhao et al., 2006), cAMP (Sebestikova et al., 2005) and guanylyl cyclases (Sato et al., 2009). Thus, if A-type potassium channels create a voltage gradient via their differential distribution along the dendritic axis, it is possible that some signaling molecules or surface receptors are influenced by this self-generating electric field.

In our studies, the application of a weak electric field (10 mV/mm) changed the GluR1 distribution along the dendrites. This effect was not due to a direct influence of the electric field on GluR1 diffusion (Supplementary Figure 2-2). Electric fields may influence the transcription of GluR1 as several transcription factors, such as β-catenin or

NF-κB, exist in synaptic regions (Abe and Takeichi, 2007; Meffert et al., 2003). Electric fields may influence the translocation of these transcription factors from synaptic regions to the nucleus. Another possibility is that electric fields may influence the expression or distribution of proteins essential for GluR1 trafficking from the soma to the dendrites. As the dendritic transport of GluR1 requires its phosphorylation or interactions with a GluR1-interacting protein, stargazin (Kessels et al., 2009), electric fields may influence these interactions to control GluR1 transport along the dendrites.

We demonstrated that A-type potassium channels play a key role in the distance-dependent scaling of AMPA receptors along the dendrites. Our results suggest a novel homeostatic scaling mechanism, which is mediated by a dendritic voltage gradient generated by differentially distributed A-type potassium channels. Neurons require a long-distance mechanism to control neurotransmitter receptor and ion channel density along the proximal to distal gradient of dendrites. The varied distribution of receptors and channels along this gradient may exceed the capacity of molecular diffusion. An electric field-mediated mechanism has the potential advantage to effect and enduring and long-range influence along the dendrites.

2.5 MATERIALS AND METHODS

2.5.1 Hippocampal slice preparation

Slices were prepared from 21 – 32 day old Sprague-Dawley rats (Charles River). In brief, a vibrating microtome (Leica VT1000S) or a tissue chopper (Stoelting) was used to cut hippocampal slices (500 μm thickness) in ice-cold oxygenated artificial cerebrospinal fluid (ACSF) containing (in mM) 119 NaCl, 2.5 KCl, 1.3 $MgSO_4$, 2.5 CaCl, 1.0 NaH_2PO_4, 26.2 $NaHCO_3$, 11.0 glucose. After a 2 hr recovery at room temperature, slices were treated for 12 hr at 32 °C with pharmacological inhibitors (as indicated) and nutritional supplements (1/10 concentration of GlutaMax, MEM vitamin and MEM amino acids, purchased from Invitrogen).

For electric field application, a pair of Ag/AgCl pellets (WPI) were positioned parallel to one another for current application from the current source (Axon Instruments). Between current injecting electrodes, a pairs of Ag/AgCl wires was positioned to measure the voltage difference between the electrodes using a voltmeter. The amplitude of current injection was appropriately adjusted by monitoring the voltmeter. Since we observed a ~2 mV difference in resting membrane potential along the 300 μm length of dendrites, we estimate the strength of dendritic electric field to be approximately 6 - 7 mV/mm, which is comparable to the strength of externally applied electric field (10 mV/mm).

2.5.2 Electrophysiology

Whole-cell voltage-clamp recordings from CA1 pyramidal neuron somata or

dendrites were made (without visualization) with an Axopatch 200B (Axon Instruments). Internal solution of patch pipettes was as follows: for the mEPSC recordings (in mM) 115 cesium gluconate, 20 cesium chloride, 10 sodium phosphocreatine, 10 HEPES, 2 MgATP, 0.3 NaGTP (pH 7.3); for the measurement of the resting membrane potential (in mM) 115 potassium gluconate, 20 potassium chloride, 10 sodium phosphocreatine, 10 HEPES, 2 MgATP, 0.3 NaGTP (pH 7.3). After recovery or the pharmacological treatment, slices were transferred to a submerged recording chamber perfused with ACSF at 24.5 - 25.5 °C or 32 - 34 °C (for resting membrane potential recording). The mEPSC recordings were done under TTX (1 μM) and bicuculline (20 μM). Membrane voltage was clamped at -70 mV (without liquid junction potential correction) for mEPSC recordings. For the resting membrane potential measurement, potentials were corrected for liquid junction potentials, which were approximately -11 mV for TTX alone and -9 mV for TTX + 4AP (10 mM). Recordings were discarded when the series resistance was over 20 MΩ or either series or membrane resistance changed more than 20% during data acquisition. Data were collected by DigiData 1200 and pClamp 9 (Axon Instruments). All numerical values listed represent mean ± s.e.m. Student's t-test was performed for all statistical analysis.

2.5.3 Immunohistochemistry

Slices (500 μm thickness) were prepared using the same procedure as for electrophysiology recordings. After the 12 hr incubation in pharmacological inhibitors (as indicated), slices were quickly fixed in 4% paraformaldehyde in phosphate-buffered saline (PBS) for at least 2 days. An NMDA receptor antagonist, APV, was always applied

during the incubation for the immunohistochemistry to avoid the influence of dendritic protein synthesis (Sutton et al., 2006). Thin (50 μm) sections were cut with a vibrating microtome (Leica VT1000S). The sections were incubated overnight with either of 1:1000 of anti-Synaptophysin I (Millipore), 1:1000 of anti-Bassoon (Stressgen), 1:1000 of anti-GluR1 (Millipore), 1:100 of GluR2/3 (Millipore), 1:250 of anti-p65 (Millipore), 1:1000 of rabbit anti-MAP2 (Millipore), or 1:1000 of mouse anti-MAP2 (Sigma) antibodies. The incubation was carried out at room temperature in Tris-buffered saline containing 0.2% Triton X-100, BSA 2%, NGS 4 %, followed by 4 hrs of secondary-antibody incubation with 1:1000 of Alexa 488-conjugated anti-rabbit and 1:1000 of Alexa 543-conjugated anti-mouse antibodies (Invitrogen). For the analysis of immunohistochemistry experiments, images were obtained with a Zeiss LSM 510 laser scanning confocal microscope using a Plan-Neofluor 10×/0.3 air objective. Alexa 488 and 546 were visualized by excitation with the 488 line of an argon ion laser and the 543 nm line of a HeNe laser, respectively. The optical section was 20 μm and fluorescent signals were acquired and summed throughout the slice thickness (50 μm). Student's t-test was performed for statistical analysis.

2.6 SUPPLEMENTARY FIGURES

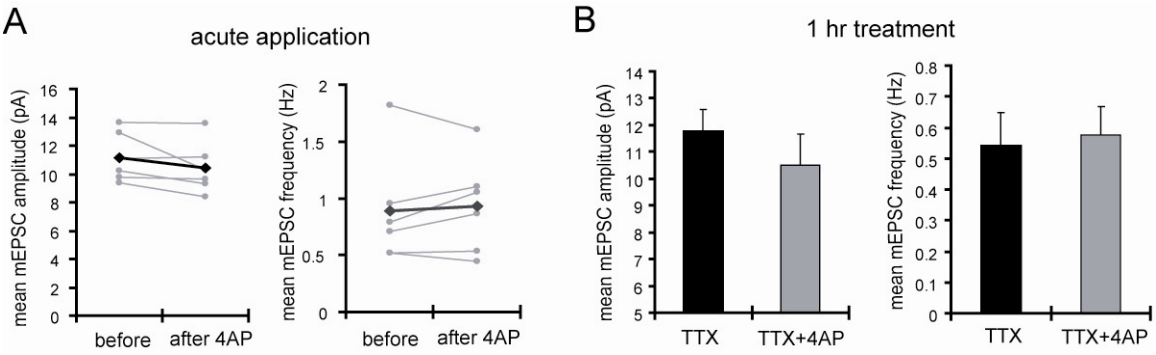

Supplementary Figure 2-1: Acute application of 4AP had no influence on either amplitude or frequency of mEPSC

(A) 4AP was applied during mEPSC recording from the soma (n = 6 for each). **(B)** mEPSCs were recorded from the soma after 1 hr, rather than 12 hr, incubation with either TTX alone or TTX + 4AP (n= 5 for each group).

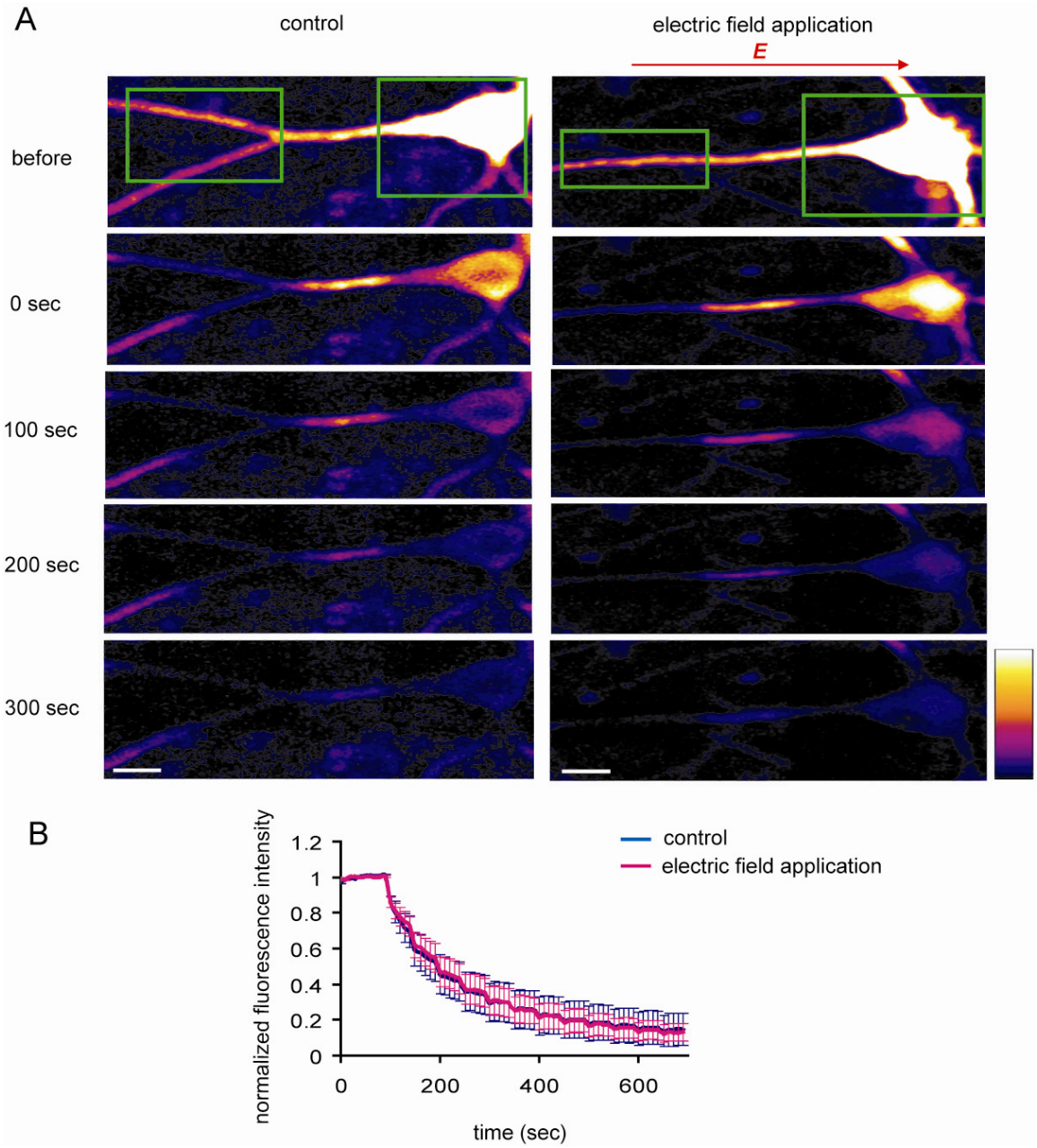

Supplementary Figure 2-2: An externally applied electric field does not influence the diffusion of GluR1-GFP

(A) GluR1-GFP was expressed in hippocampal dissociated culture neurons by a Sindbis virus expression system. The photobleaching was applied to both the soma and the distal

dendrites (green boxes), leaving a 25 μm length segment in proximal dendrite. The external electric field (20 mV/mm) was applied along the dendrites during photobleaching (scale bar = 25 μm). **(B)** Analysis of fluorescence decay in a 25 μm segment in proximal dendrite. No difference was observed in fluorescence decay, suggesting that the electric field did not influence GluR1-GFP diffusion (n = 5).

	TTX		TTX + 4AP	
	capacitance (pF)	resistance (MΩ)	capacitance (pF)	resistance (MΩ)
soma	309 ± 66	99 ± 37	304 ± 52	106 ± 31
dendrites	345 ± 89	135 ± 37	336 ± 83	168 ± 104
soma (0 extracellular calcium)	349 ± 81	183 ± 54	347 ± 49	200 ± 29
soma (anisomycin)	364 ± 50	164 ± 62	344 ± 72	181 ± 48

	TTX		TTX + TEA	
	capacitance (pF)	resistance (MΩ)	capacitance (pF)	resistance (MΩ)
soma	309 ± 58	161 ± 39	272 ± 42	171 ± 43

	TTX+4AP		TTX + 4AP+APV	
	capacitance (pF)	resistance (MΩ)	capacitance (pF)	resistance (MΩ)
soma	274 ± 69	138 ± 60	311 ± 67	140 ± 73

Supplementary Figure 2-3: No significant differences exist in the membrane properties of neurons used for mEPSC analysis

All numerical values listed represent mean ± SD.

Chapter 3. Frequency-Dependent Synaptic Transmission and Plasticity by Dopamine

3.1 SUMMARY

The neurotransmitter dopamine (DA) plays an important role in learning by enhancing the saliency of behaviorally relevant stimuli. How this stimulus selection is achieved on the cellular level, however, is not known. Here, in recordings from hippocampal slices, we show that DA acts specifically at the direct cortical input to hippocampal area CA1 (the temporoammonic pathway) to filter the excitatory drive onto pyramidal neurons based on the input frequency. During low-frequency patterns of stimulation, DA depressed excitatory temporoammonic (TA) inputs to both CA1 pyramidal neurons and local inhibitory GABAergic interneurons via presynaptic inhibition. In contrast, during high-frequency patterns of stimulation, DA potently facilitated the TA excitatory drive onto CA1 pyramidal neurons, owing to diminished feed-forward inhibition. Analysis of DA's effects over a broad range of stimulus frequencies indicates that it acts as a high-pass filter, augmenting the response to high-frequency inputs while diminishing the impact of low-frequency inputs. These modulatory effects of DA exert a profound influence on activity-dependent forms of synaptic plasticity at both TA-CA1 and Schaffer-collateral-CA1 synapses. Taken together, our data demonstrate that DA acts as a gate on the direct cortical input to the hippocampus, modulating information flow and synaptic plasticity in a frequency-dependent manner.

3.2 INTRODUCTION

Midbrain dopaminergic neurons increase their firing activity when animals receive unexpected rewards or experience a novel environment – both the hedonic value and familiarity of stimuli are important determinants in learning (Horvitz, 2000; Schultz and Dickinson, 2000). The learning-related activities of dopaminergic neurons may induce modifications of the neural networks that underlie behavioral plasticity (McClure et al., 2003; Montague et al., 2004).

One of the targets of dopaminergic neurons is the hippocampus, a brain structure crucial for some types of learning and memory (Swanson, 1982; Gasbarri et al., 1994a; Gasbarri et al., 1994b; Gasbarri et al., 1996a; Scoville and Milner, 1957; Zola-Morgan and Squire, 1986; Squire et al., 2004). Dopamine (DA) is released in the hippocampus when animals are exposed to novel environments (Ihalainen et al., 1999), influencing hippocampal-dependent learning (Gasbarri et al., 1996b).

In the hippocampus, the primary targets of dopaminergic neurons are the subiculum and area CA1 (Gasbarri et al., 1997). CA1 pyramidal neurons receive two distinct excitatory synaptic inputs: one from area CA3 (the Schaffer-collateral pathway), and the other from the entorhinal cortex (the temporoammonic pathway) (Cajal, 1911). Each pathway appears to have a distinct function in learning (Brun et al., 2002; Steffenach et al., 2002; Remondes and Schuman, 2004) and may be differentially modulated depending on the familiarity of the environment (Hasselmo and Schnell, 1994; Otmakhova and Lisman, 1999; Otmakhova et al., 2005). This differential pathway

modulation may contribute to the distinct informational representation between area CA1 and CA3, as observed in *in vivo* animals (Leutgeb et al., 2004; Lee et al., 2004; Vazdarjanova and Guzowski, 2004). Indeed, independent modulation of the two pathways has been hypothesized to play a significant role in learning (Hasselmo et al., 1996; Lisman and Otmakhova, 2001; Guzowski et al., 2004; Knierim et al., 2006). Here we explored how DA modulates the signal integration of these two hippocampal pathways with the goal of understanding how DA might regulate information selection during learning.

3.3 RESULTS

3.3.1 DA selectively depresses excitatory synaptic transmission at TA-CA1 pyramidal neuron synapses

To examine the differential influence of DA on the two excitatory inputs to area CA1, we made extracellular field recordings from both the Schaffer-collateral (SC) pathway and the temporoammonic (TA) pathway in hippocampal slices (Figure 3-1A). As previously described (Otmakhova and Lisman, 1999), when DA (20 μM) was applied to the bathing solution, the field EPSP (fEPSP) evoked by the TA pathway stimulation was depressed, whereas the fEPSP by the SC pathway stimulation was not significantly altered (Figure 3-1B; DA: 49.2 ± 8.8%, SC: 93.6 ± 15.8%, mean percentage of baseline 20 – 30 min after DA application). To identify the synaptic locus of DA's effect, we conducted whole-cell voltage-clamp recordings from CA1 pyramidal neurons. DA also depressed the EPSC evoked by the TA pathway stimulation (Figure 3-1C; 56.8 ± 2.3%,

average of 15 – 20 min after DA application), indicating a decrease in excitatory neurotransmission. We also analyzed paired-pulse facilitation [inversely correlated with vesicle release probability (Katz and Miledi, 1968; Zucker, 1973; Dobrunz and Stevens, 1997)], before and after DA application. After DA application, paired-pulse facilitation was significantly enhanced (Figure 3-1D), suggesting that DA acts, at least in part, via an inhibition of neurotransmitter release. The DA-induced depression was reversible (Figure 3-1E) and blocked by dopamine receptor antagonists (Figure 3-1F).

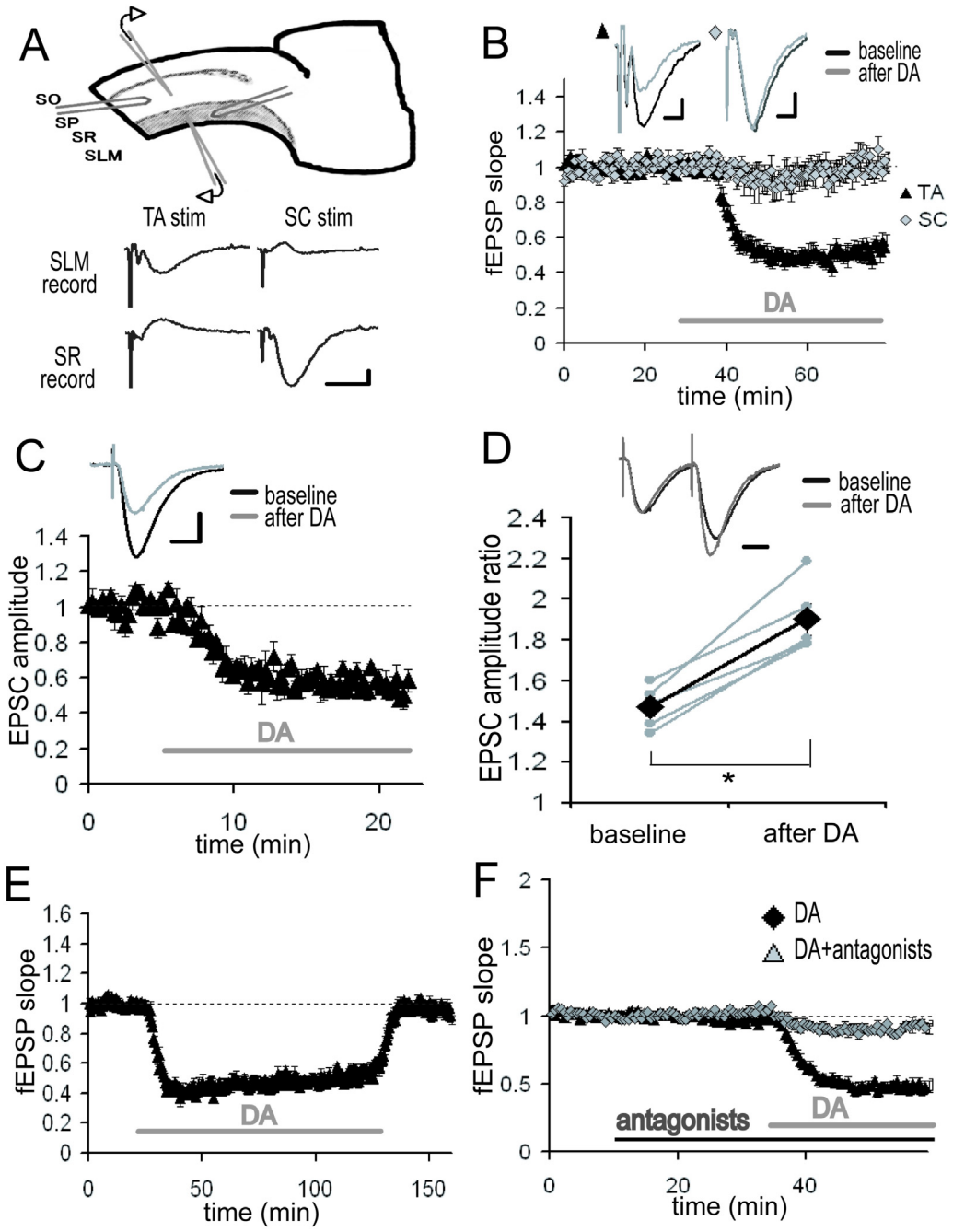

Figure 3-1: Inhibition of TA-CA1 pyramidal excitatory synaptic transmission by DA

(A) Simultaneous extracellular field recording from SC-CA1 and TA-CA1 synapses. Extracellular recording and stimulating electrodes are placed in stratum lacunosum

moleculare (SLM) or stratum radiatum (SR), respectively. (SO: stratum oriens, SP: stratum pyramidale). Shown are representative fEPSP recorded in SLM or SR as a result of TA or SC stimulation (scale bar = 0.1 mV, 10 msec). **(B)** Application of DA (20 μM; indicated by bar) significantly depressed the fEPSP slope of TA-CA1 synapses, but did not affect SC-CA1 synapses (n = 6) (scale bar = 0.1 mV, 5 msec). **(C)** Whole-cell patch-clamp recording from CA1 pyramidal neurons in the presence of the $GABA_{A\text{ and }B}$ receptor antagonists, bicuculline (10 μM) and CGP 55845A (1 μM). After DA application, the EPSC evoked by TA pathway stimulation was significantly depressed (n = 4) (scale bar = 50 pA, 20 msec) (*$p < 0.01$). **(D)** Paired pulse facilitation analysis using the same condition described in **C**. Pulse interval was 50 msec. Data from individual experiments are represented by small gray circles; large diamonds represent the mean. After DA application, paired pulse facilitation of the TA-CA1 EPSC was significantly enhanced (n = 5) (scale bar = 20 msec) (*$p < 0.01$). **(E)** Recovery from long-term application of DA (n = 4). **(F)** Blockade of DA-induced depression at TA-CA1 synapses by dopamine receptor antagonists, SKF 83566 (1 μM) and Sulpiride (10 μM) (DA: n = 8, DA antagonists: n = 5).

3.3.2 DA depresses excitatory synaptic transmission at TA-interneuronal synapses

In addition to excitatory connections with CA1 pyramidal neuron dendrites, the axons of the TA pathway also make synapses with interneurons in area CA1 (Freund and Buzsaki, 1996). Among the various classes of interneurons present, the interneurons located at the border between stratum radiatum and stratum lacunosum-moleculare receive excitatory synapses from the TA pathway. (Lacaille and Schwartzkroin, 1988; Dvorak-Carbone and Schuman, 1999b). We obtained intracellular recordings from those interneurons and examined the effects of DA on the TA-interneuron excitatory synapse. We found that DA also depressed the TA-pathway evoked EPSP in interneurons (Figure 3-2B; 57.7 ± 4.2% in EPSP amplitude, 44.0 ± 12.5% in EPSP slope after DA application). Thus, DA depressed the excitatory synaptic inputs at both TA-pyramidal and TA-interneuron synapses. Although we did not examine connections between TA axons and other type of interneurons in area CA1, considering the presynaptic action of DA (Figure 3-1D), it is possible that other TA-interneuron synapses will be similarly depressed.

Previous studies have reported that relatively strong inhibitory responses can be observed in CA1 pyramidal neurons following TA pathway stimulation (Empson and Heinemann, 1995). Since the TA-CA1 synapses are primarily excitatory (Desmond et al., 1994), the inhibition of pyramidal neurons is caused by interneurons which receive excitatory inputs from the TA pathway and, in turn, make inhibitory connections with pyramidal neurons (Lacaille and Schwartzkroin, 1988). We thus examined the inhibitory

responses in CA1 pyramidal neurons evoked by TA pathway stimulation. Whole-cell monosynaptic IPSCs were recorded from CA1 pyramidal neurons at a holding potential of 0 mV in the presence of glutamate receptor antagonists (CNQX + APV). The monosynaptic IPSC (Figure 3-2D) was not modulated by DA (Figure 3-2E), suggesting that DA does not influence inhibitory synaptic transmission.

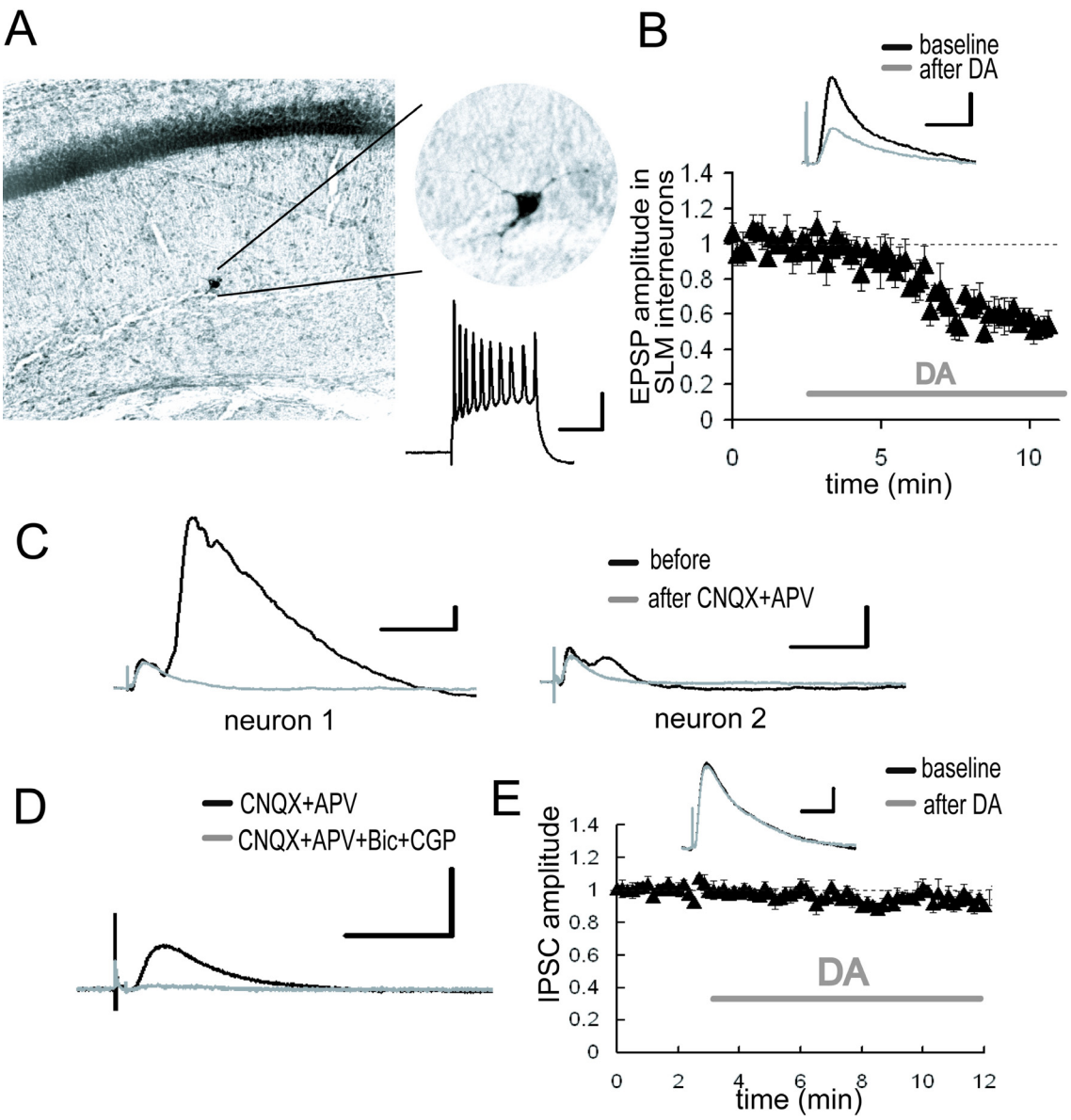

Figure 3-2: DA-induced depression of excitatory inputs to SLM interneurons

(A) Intracellular recording from SLM interneurons. Biocytin-filled electrodes were used for the staining of SLM interneurons. The inset shows representative spike activities following current injection (scale bar = 50 msec, 20 mV). **(B)** After DA application, the EPSP evoked by the TA pathway stimulation was significantly depressed (scale bar = 1

mV, 20 msec) (*$p < 0.01$). **(C)** Whole-cell voltage clamp recordings from CA1 pyramidal neurons at a holding potential of 0 mV. The late component of the IPSC disappeared after excitatory blockade with CNQX (10 μM) and APV (25 μM). The size of late IPSC showed large variability among recorded neurons (scale bar = 50 pA, 100 msec). **(D)** The monosynaptic IPSC was blocked by GABA receptor antagonists, bicuculline (10 μM) and CGP 55845A (1 μM) (scale bar = 50 pA, 100 msec). **(E)** DA did not influence monosynaptic IPSC (scale bar = 20 pA, 50 msec).

3.3.3 DA-induced presynaptic inhibition enhances synaptic transmission at TA-CA1 synapses during HFS

The above indicate that DA appears to selectively inhibit the excitatory TA connections with both local interneurons and CA1 pyramidal neurons (Figure 3-3A). The DA-induced depression of excitatory inputs to interneurons is predicted to reduce the impact of inhibitory transmission on CA1 pyramidal neurons (disinhibition). Because this inhibitory transmission is disynaptic, the inhibition of pyramidal neurons is delayed relative to excitation. This raises the possibility that DA's ability to modulate the output of the TA-CA1 circuit may be modulated by stimulation frequency. In particular, we predicted that appropriately-timed TA stimuli would increase the impact of disinhibition (Figure 3-3B).

To test this idea, we examined the net effect of DA during epochs of high-frequency stimulation (HFS). We made extracellular field recordings from the TA-CA1 synapses, before, during and after two epochs of HFS (100 Hz, 100 pulses); the second epoch was delivered after DA application (Figure 3-3C). To quantify the differences between 1st and 2nd HFS, we measured the field potential evoked by the last (100th) stimulus (referred to as the "steady-state potential"). Under control conditions, the steady-state potentials observed at the 1st and 2nd HFS were almost identical (2nd/1st steady-state potential ratio: 0.96 ± 0.04) (Figure 3-3D). DA application, however, significantly enhanced the 2nd steady-state potential (ratio: 1.98 ± 0.13). To examine whether presynaptic inhibition is sufficient to induce this phenomenon, we lowered the extracellular calcium concentration after 1st HFS (low $[Ca^{2+}]_{ext}$; Figure 3-3C), reducing

the probability of neurotransmitter release. This manipulation mimicked the effect of DA, resulting in a larger steady-state potential at the 2nd HFS (ratio: 1.67 ± 0.15; Figure 3-3D). To exclude the possibility that a smaller fEPSP (induced by DA) may itself induce a larger steady-state potential, independent of release probability, we reduced the stimulus strength to imitate the small fEPSP depressed by DA (reduced stim; Figure 3-3C). This manipulation did not augment the steady-state potential (ratio: 0.60 ± 0.11; Figure 3-3D). Taken together, these data suggest that presynaptic inhibition induced by DA is responsible for the larger steady-state field potential observed during HFS.

To directly examine the synaptic efficacy of TA-pyramidal neuron synapses, we made whole-cell voltage-clamp recordings from CA1 pyramidal neurons and measured current influx evoked by the TA pathway stimulation in control or DA-treated slices (Figure 3-4A). A comparison of the average TA-elicited EPSC waveforms from control vs. DA-treated slices indicated no apparent differences in the EPSC waveform shape or kinetics (Figure 3-4A, left). Input resistance also did not differ between the groups. However, during HFS, current influx was significantly larger in the presence of DA (Figure 3-4A, middle and right), suggesting that synaptic efficacy of TA-pyramidal neuron synapses was enhanced by DA. To confirm that the above differences were caused by a modulation of inhibitory transmission, we made recordings under $GABA_{A \text{ and } B}$ receptor blockade to isolate excitatory inputs. We found that GABA receptor antagonists completely prevented the facilitation of the steady-state current by DA (Figure 3-4B), indicating that the observed difference (Figure 3-4A) was caused by inhibitory modulation. The above results reinforce the idea that DA-induced disinhibition enhances

synaptic efficacy during high-frequency stimulation.

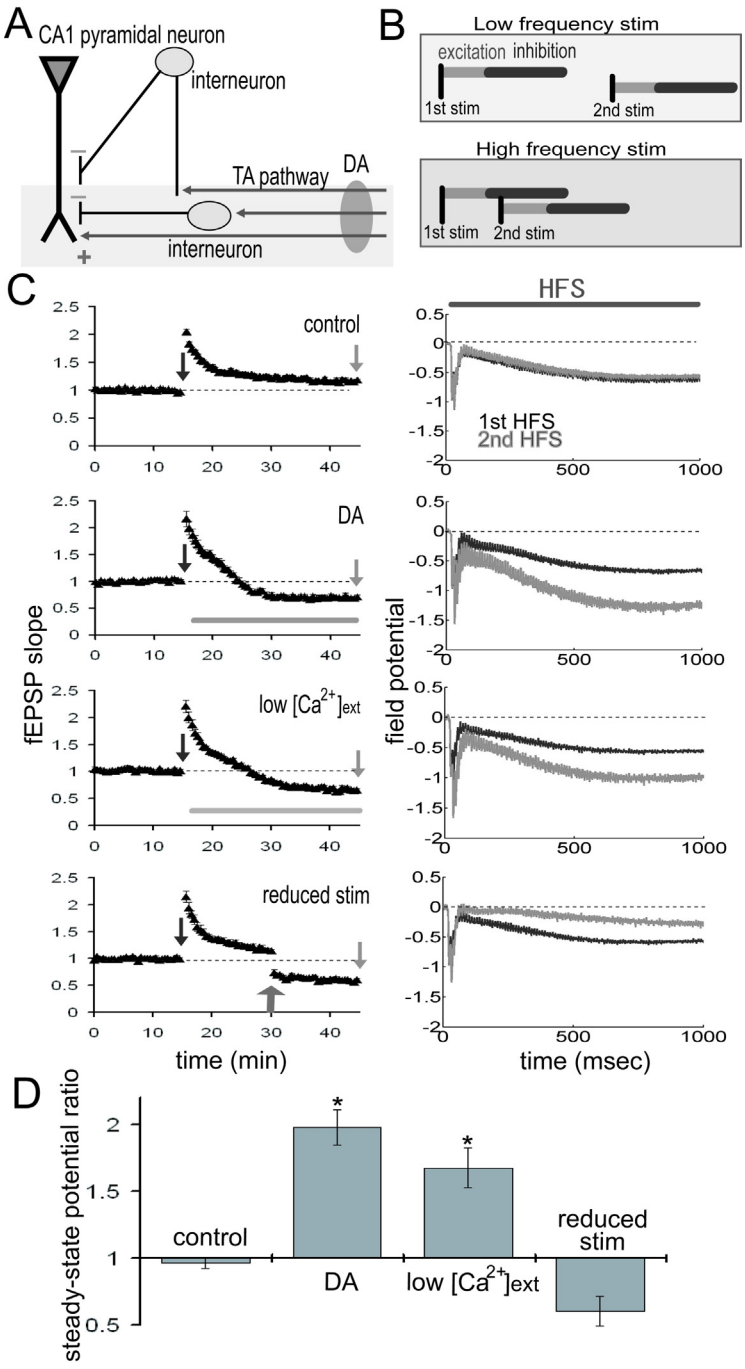

Figure 3-3: DA augments the steady-state field potential induced by HFS

(A) Scheme of the TA-CA1 synapse. The TA axons make excitatory connections with both pyramidal neurons and interneurons. Interneurons in turn inhibit pyramidal neurons

(feed-forward inhibition). Depression of excitatory inputs onto interneurons by DA reduces inhibition of pyramidal neurons. **(B)** Frequency dependent effect of feedforward inhibition. In contrast to the direct excitatory TA-CA1 input, the TA pathway exerts a disynaptic modulation of inhibition. Thus, the inhibition of pyramidal neurons after TA stimulation is delayed, relative to the excitation. In pyramidal neurons, the TA pathway-evoked inhibition does not affect excitation during low-frequency stimulation, because of the delay in inhibition. However, during high-frequency stimulation, inhibition can effectively suppress subsequent excitatory responses. **(C)** Extracellular field recording from TA-CA1 synapses. Left, HFS was applied at 15 min and 45 min (indicated by arrows). Field potential traces during HFS are normalized to the baseline fEPSP amplitude prior to HFS application. The field potential at the end of the HFS (100th stimulus response) was measured (steady-state potential). Right, the average waveforms during HFS are shown. DA: after 1st HFS, DA was applied (indicated by bar). Low $[Ca^{2+}]_{ext}$: after 1^{st} HFS, the extracellular calcium concentration was reduced from 2.5 mM to 1.25 mM (indicated by bar). Reduced stim: at 30 min, the stimulation current was reduced to produce a small fEPSP comparable to that observed during DA application (indicated by arrow) (n = 5 for each group). **(D)** Ratio of steady-state potentials observed during second and first HFS epochs. DA application induced a significantly (*$p < 0.01$) larger steady-state potential that was also mimicked by reduction of $[Ca^{2+}]_{ext}$.

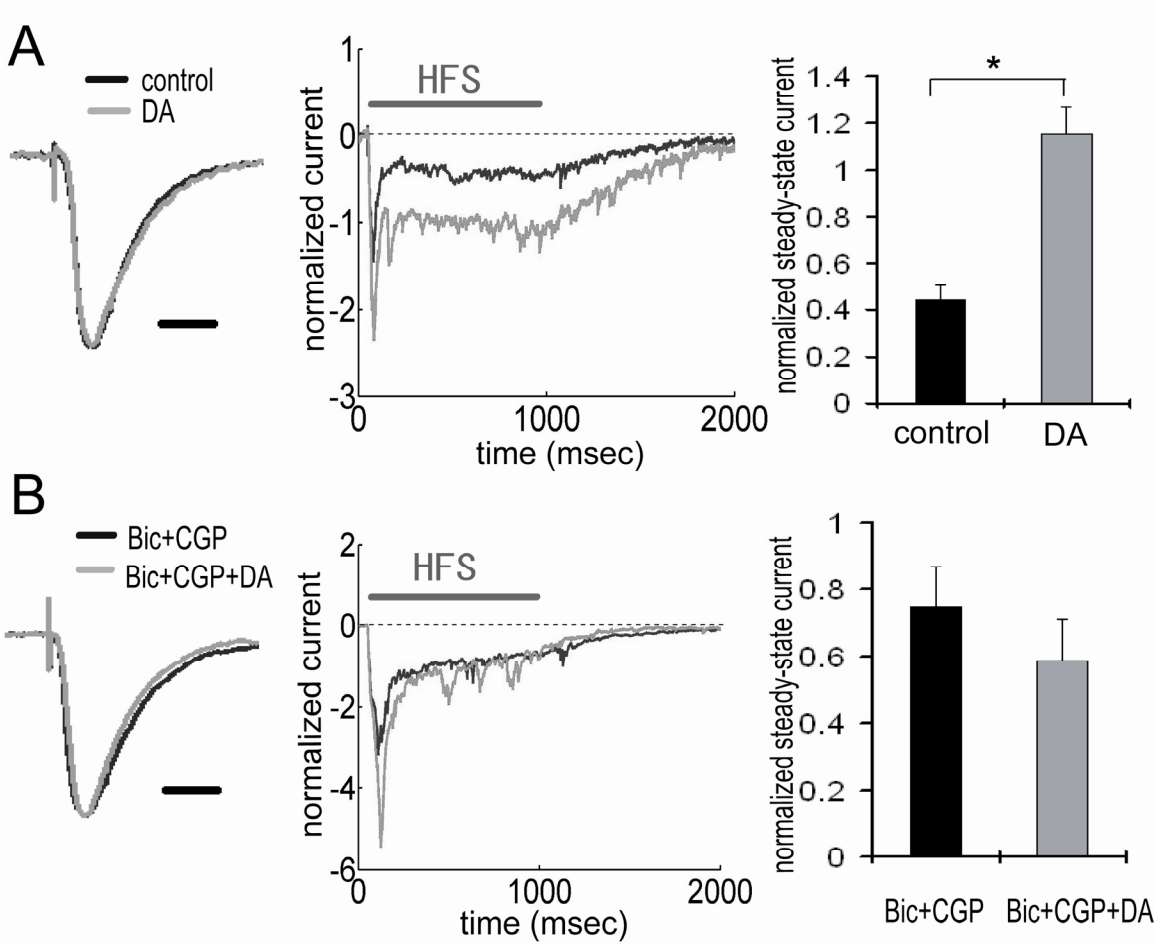

Figure 3-4: Enhancement of TA-CA1 synaptic efficacy during HFS via DA-induced disinhibition

(A) Whole-cell voltage clamp recording from CA1 pyramidal neurons. Waveforms represent the average of all data, showing normalized baseline EPSC (left) and current during HFS (middle). There was no difference in the kinetics of EPSC waveforms obtained with or without DA application. Waveforms during HFS (100 Hz, 100 pulses) were normalized to baseline EPSC amplitude prior to HFS, and the current at the end of HFS (100th stimulus response) was measured (steady-state current). The right figure

shows the analysis of steady-state current, showing that DA induced a significantly (*$p < 0.01$) larger steady-state current. Input resistances were not significantly different (in MΩ); control: 85.8 ± 9.3, DA: 85.0 ± 9.0 (n = 6 for each group) (scale bar = 20 msec). **(B)** Same experimental procedure as **A** under GABA receptor blockade by bicuculline and CGP55845A. GABA blockade attenuated the enhancement of steady-state current by DA. Input resistances were not significantly different (in MΩ); Bic+CGP: 102.0 ± 7.9, Bic+CGP+DA: 98.0 ± 4.6 (n = 5 for each group) (scale bar = 20 msec).

3.3.4 DA imposes a high-pass filter on TA-CA1 synaptic transmission

The oscillatory patterns of neural networks in the mammalian brain cover a wide range of frequencies from approximately 0.05 to 500 Hz (Buzsaki and Draguhn, 2004). We reasoned that the temporal features of disinhibition may interact with oscillatory dynamics of neural networks to produce frequency-dependent modulatory effects of DA. To delineate the frequency profile of DA-induced modulation, we stimulated the TA pathway with 100 pulses at frequencies ranging from 5 to 100 Hz (Figure 3-5A and 3-6A). Under control conditions, steady-state potentials became progressively smaller at stimulation frequencies greater than 10 Hz (Figure 3-6A). On the other hand, under the influence of DA, steady-state potentials were enhanced at all frequencies higher than 10 Hz (Figure 3-6A). Thus, DA exerts a stimulation frequency-dependent modulation of synaptic strength. In another set of analyses, we took into account the DA-induced inhibition of basal transmission by normalizing all potentials to the baseline fEPSP before DA application (Figure 3-5B and 3-6B). Under the influence of DA, steady-state potentials were smaller than control during low-frequency stimulation because of the excitatory depression, however, during high frequency stimulation, the disinhibition overcame the depression and steady-state potentials were larger than control (Figure 3-6B). A similar of results was obtained in a set of experiments conducted at near-physiological temperature (32 – 34 ºC) (Figure 3-6C and 3-6D). These data indicate that the DA-induced disinhibition together with its excitatory depression exhibits an alternate gating of synaptic strength in a frequency-dependent manner – increasing the impact of high-frequency inputs while decreasing the impact of low-frequency signals.

Thus, DA acts as a high-pass filter on TA-CA1 pyramidal neuron signaling.

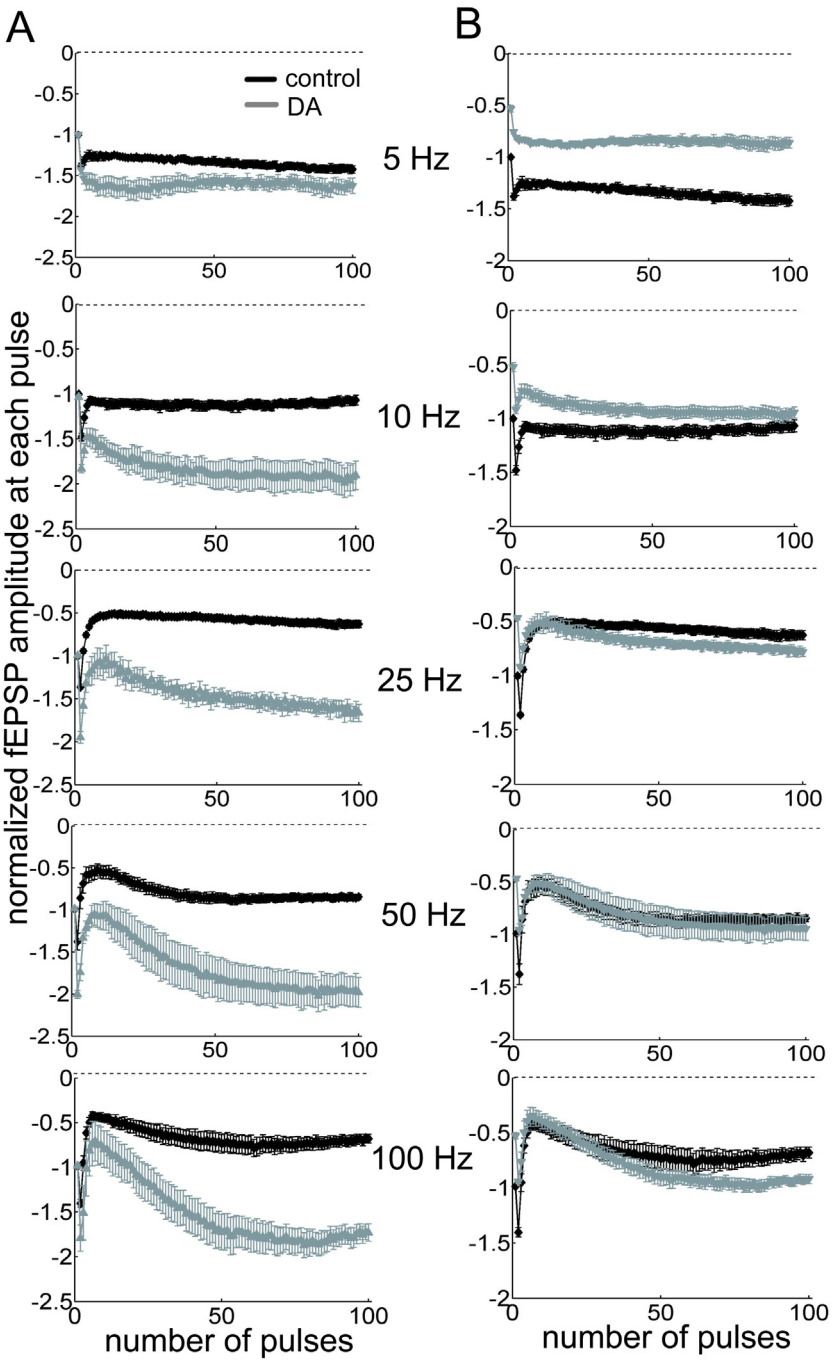

Figure 3-5: High-pass filtering of TA-CA1 synaptic efficacy by DA

(A) Examination of frequency-dependent modulation by DA, using extracellular field recordings. 100 pulses of different stimulation frequencies, as indicated, were applied.

Data were normalized to the baseline fEPSP amplitude prior to stimulation and each mean fEPSP amplitude during 100-pulse stimulation was plotted (from top to bottom; control: n = 5, 5, 7, 6, and 5, DA: n = 5, 5, 5, 5, and 5). **(B)** Same data as in **A**, but normalized to the baseline fEPSP amplitude before, instead of after, DA application.

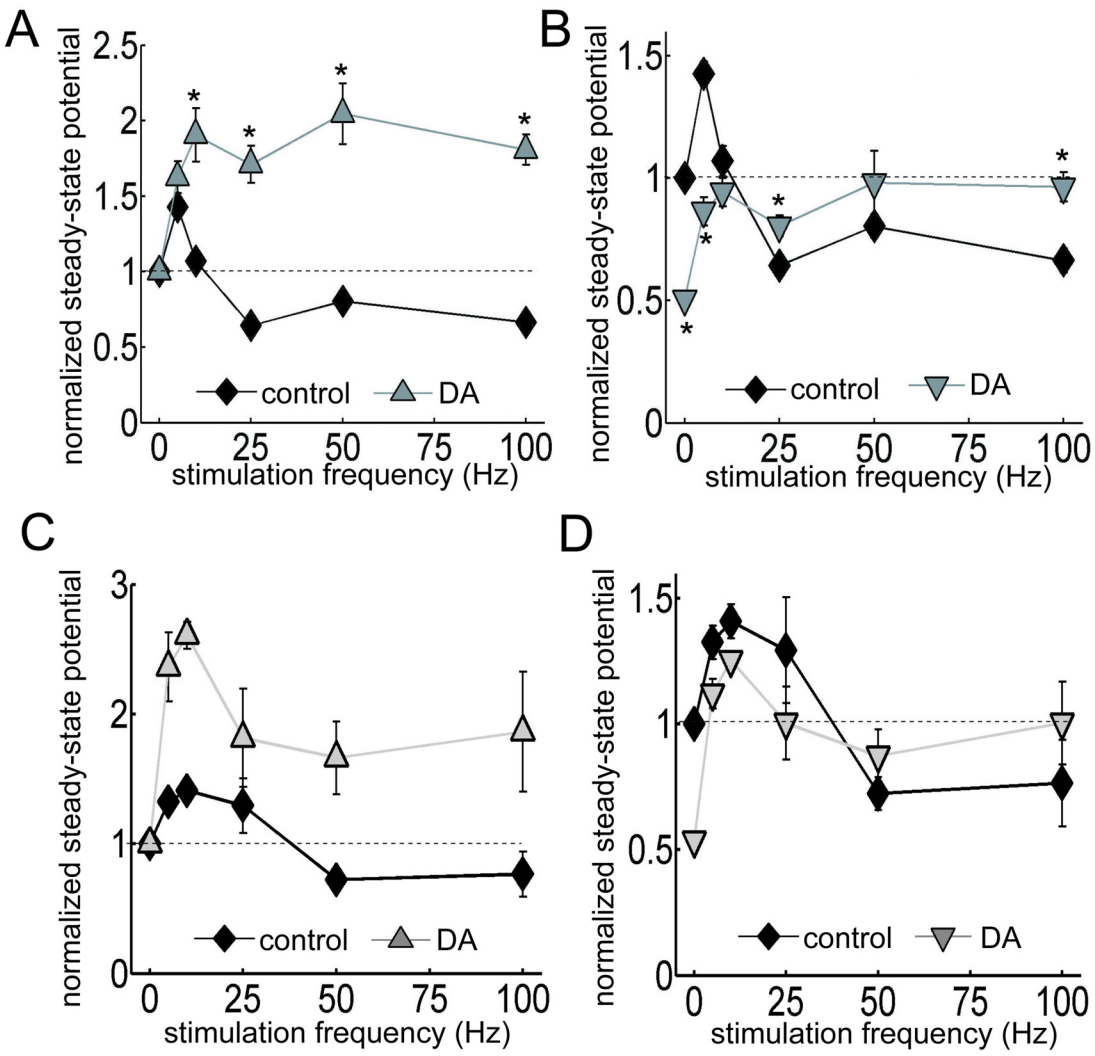

Figure 3-6: Analysis of DA-induced filtering at TA-CA1 synapses at room and near-physiological temperatures

(A) Using same data as in figure 3-5, steady-state potentials were measured. In the presence of DA, the steady-state potential became larger during high-frequency stimulation (*$p < 0.05$ relative to control) (from left to right; control: n = 5, 5, 7, 6, and 5, DA: n = 5, 5, 5, 5, and 5). **(B)** As in figure 3-5B, data were normalized to baseline fEPSP amplitude prior to DA application. Thus, this figure shows the total effect of DA,

including on the depression of basal synaptic transmission. Under DA application, although the steady-state potential was smaller during low-frequency stimulation, it overcame the depression and became larger than control during high-frequency stimulation (*$p < 0.05$ relative to control). Note that control error bars are smaller than the symbol size. **(C)** Similar experiments as **A** conducted at higher temperature (32 – 34 °C). **(D)** Similar analysis as **B**, using data acquired at higher temperature.

3.3.5 DA bi-directionally modulates synaptic plasticity

To assess the functional impact of DA-induced filtering, we next examined the DA's effect on synaptic plasticity, the sign and strength of which is known to be dependent on stimulation frequency. To test this idea, long-term potentiation (LTP) was induced at TA-CA1 synapses with or without DA (Figure 3-7A). LTP, induced by high-frequency stimulation (5 trains of 100 Hz 100 pulses), was significantly enhanced by DA (control: 126.4 ± 7.2%, DA: 172.6 ± 14.3%, 50 – 60 min after LTP induction), which was blocked by dopamine receptor antagonists (Figure 3-7D and 3-7E). On the other hand, long-term depression (LTD), which is induced by low-frequency stimulation, was attenuated by DA (Figure 3-7B; control: 81.7 ± 3.5%, DA: 94.8 ± 2.3%, 30 – 35 min after LTD induction). Thus, the frequency-dependent signal filtering by DA has a profound functional impact on the magnitude of synaptic plasticity. We next examined whether modulation of inhibitory transmission also underlies this phenomena. Under GABA receptor blockade, LTP at TA-CA1 synapses was enhanced, and DA's effect on LTP enhancement was occluded (Figure 3-7C; Bic+CGP: 171.5 ± 18.6%, Bic+CGP+DA: 152.1 ± 9.8%, 50 – 60 min after LTP induction), suggesting an obligatory contribution from the inhibitory network.

How quickly can the network adapt to DA signals? Because dopaminergic neurons show both tonic and burst-like activity patterns *in vivo* (Grace, 1991; Floresco et al., 2003), we examined the sensitivity of this modulation to very brief (10 sec + 1 – 2 min washout) temporally controlled applications of DA (Figure 3-8A and 3-8B). When DA was applied 10 sec before LTP induction, LTP was significantly enhanced when

compared with vehicle applied control (Figure 3-8C; vehicle: 107.0 ± 2.7%, DA: 136.5 ± 8.7%, 50 – 60 min after LTP induction). The application of DA either 3 min before or 10 sec after LTP induction, however, did not enhance TA-CA1 LTP (Figure 3-8D; 3 min before: 111.0 ± 4.0%, 10 sec after: 110.7 ± 5.6%). These data indicate that extremely brief DA application that is coincident with LTP induction is capable of modulating the TA-CA1 plasticity network.

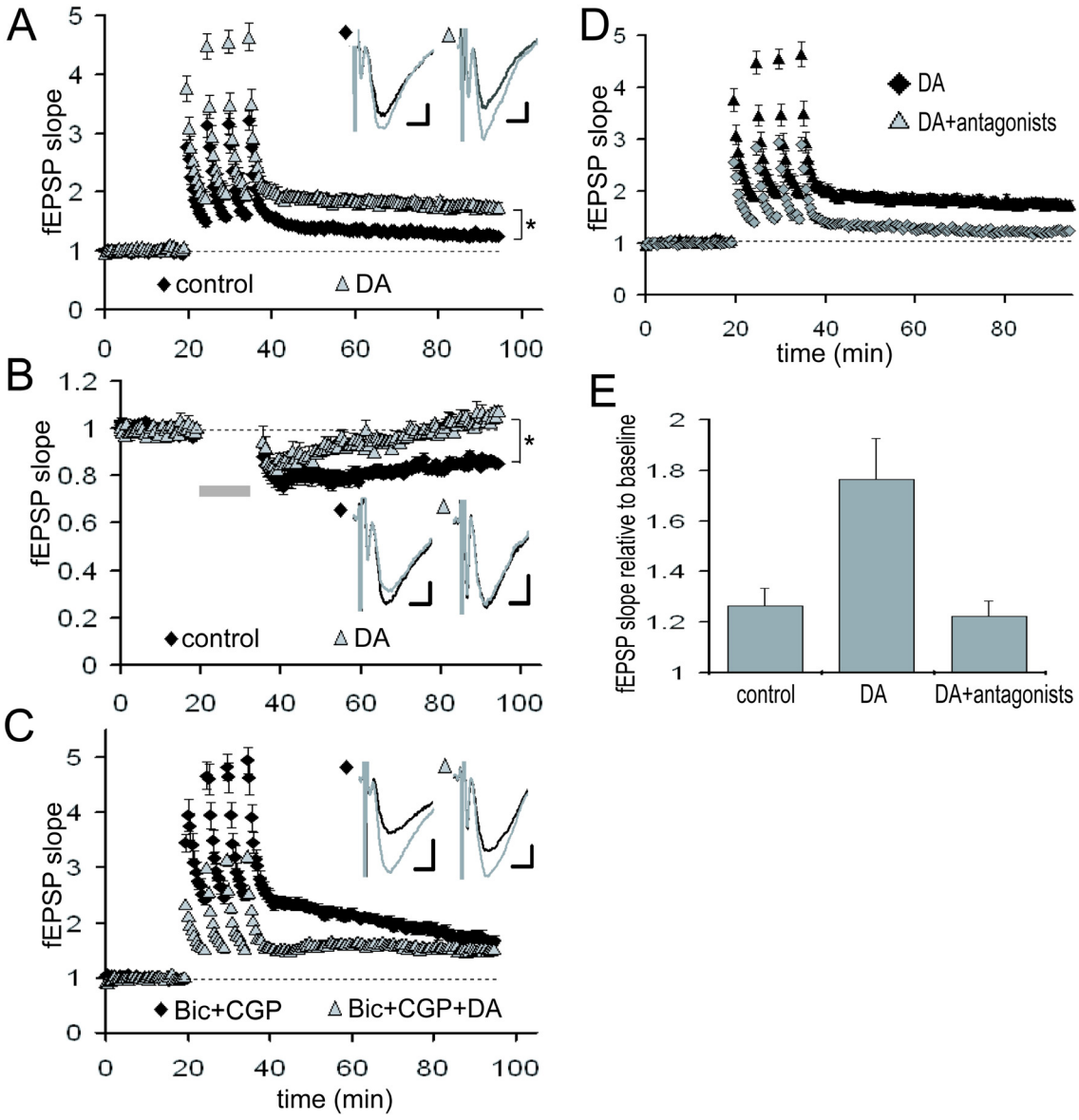

Figure 3-7: DA-induced modulation of synaptic plasticity at TA-CA1 synapses

(A) Enhancement of TA-CA1 LTP by DA. DA was present for the duration of the experiment. Baselines are normalized to 1.0 in order to examine LTP independent of the depression of basal synaptic transmission by DA. For all traces, the baseline (pre-plasticity) trace is black, the post-plasticity trace is grey (*$p < 0.01$) (control: n = 7,

DA: n = 8) (scale bar = 0.1 mV, 5 msec). **(B)** Attenuation of TA-CA1 LTD by DA. Gray bar: LTD induction (*$p < 0.01$) (control: n = 7, DA: n = 6) (scale bar = 0.1 mV, 5 msec). **(C)** Occlusion of DA-induced TA-CA1 LTP enhancement under $GABA_{A \text{ and } B}$ receptor blockade. Under GABA receptor blockade, DA did not significantly enhance LTP (n = 5 for each group) (scale bar = 0.1 mV, 5 msec). **(D)** Blockade of DA-induced enhancement of TA-LTP by dopamine receptor antagonists, SKF 83566 (1 μM) and Sulpiride (10 μM) (DA: n = 8, DA antagonists: n = 5). **(E)** Analysis of LTP at TA-CA1 synapses (50 – 60 min after LTP induction). Dopamine receptor antagonists completely blocked DA-induced enhancement of TA-LTP (control: n = 7, DA: n = 8, DA antagonists: n = 5).

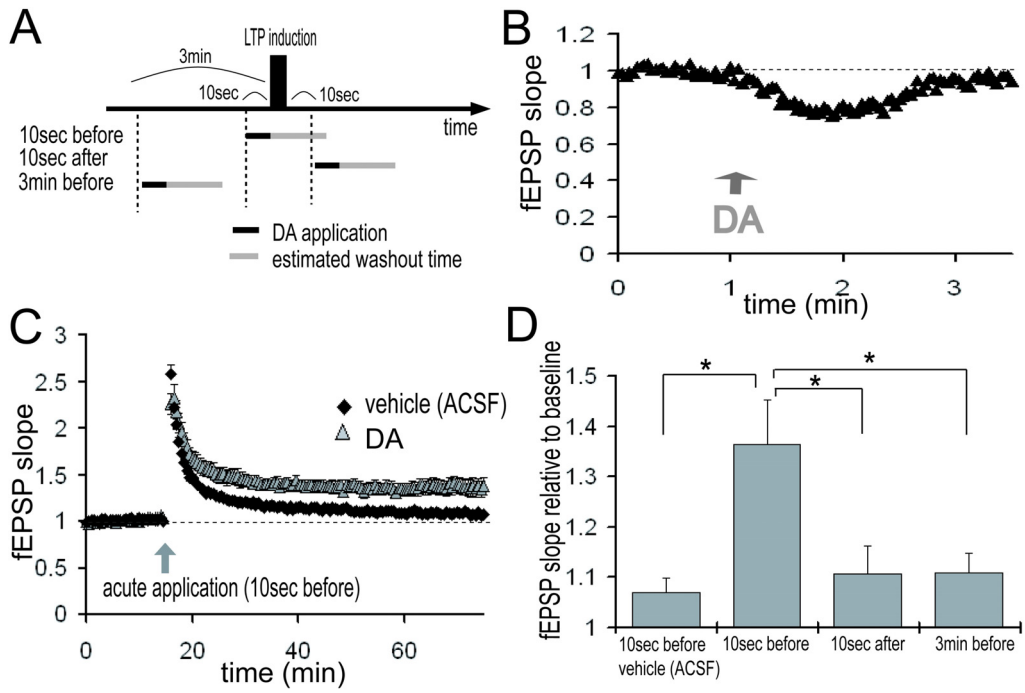

Figure 3-8: Temporally selectivity of LTP enhancement by DA

(A) Acute application of DA. DA was applied for just 10 sec either 10 sec before, 10 sec after, or 3 min before LTP induction. LTP induction protocol was 100 Hz. 100 pulse stimulation, repeated 2 times at an interval of 30 sec. DA was directly applied in the recording chamber for 10 sec and estimated washout time was about 1 – 2 min. **(B)** fEPSP slopes during acute application of DA. TA pathway was stimulated at 0.5 Hz. DA was directly applied into the recording chamber at 1 min (indicated by arrow) and its effects on synaptic transmission were reversible. **(C)** DA application at 10 sec before LTP induction significantly enhanced LTP at TA-CA1 synapses (vehicle: n = 7, DA: n = 8). **(D)** DA application 3 min before or 10 sec after LTP induction did not enhance LTP (n = 6 for each).

3.3.6 DA-induced disinhibition influences synaptic plasticity at SC-CA1 synapses

Although DA-induced excitatory depression is selective to TA-CA1 synapses, the resulting disinhibition may influence another excitatory input to area CA1, the SC pathway. Previous work has shown that TA activity can interfere with LTP induction at SC-CA1 synapses, primarily due to inhibition evoked by the TA pathway stimulation (Levy et al., 1998; Remondes and Schuman, 2002). We reasoned that DA-induced disinhibition may attenuate this LTP interference. We first confirmed that DA had no significant effect on the magnitude of LTP at SC-CA1 synapses up to 1 hr after LTP induction when the SC was stimulated alone either by theta-burst stimulation (TBS) (Figure 3-9C; control: 142.4 ± 5.7%, DA: 139.7 ± 5.3%, 50 – 60 min after LTP induction) or by HFS (Figure 3-9D; control: 179.6 ± 15.5%, DA: 179.5 ± 13.0%). As previously shown, joint TBS applied to both the SC and TA pathways significantly attenuated LTP at SC-CA1 synapses (Figure 3-9E; 112.3 ± 3.0%). To assess the DA-induced disinhibitory effect on LTP interference, the stimulation amplitude was increased after DA application to compensate for the DA-induced excitatory depression (Figure 3-9B). Under this condition, DA significantly attenuated the LTP interference of SC-CA1 synapses elicited by concurrent TA activity (Figure 3-9E; 128.0 ± 1.5%). These results indicate that DA-induced disinhibition has a large impact on plasticity induction not only at TA-CA1 synapses, but also at SC-CA1 synapses.

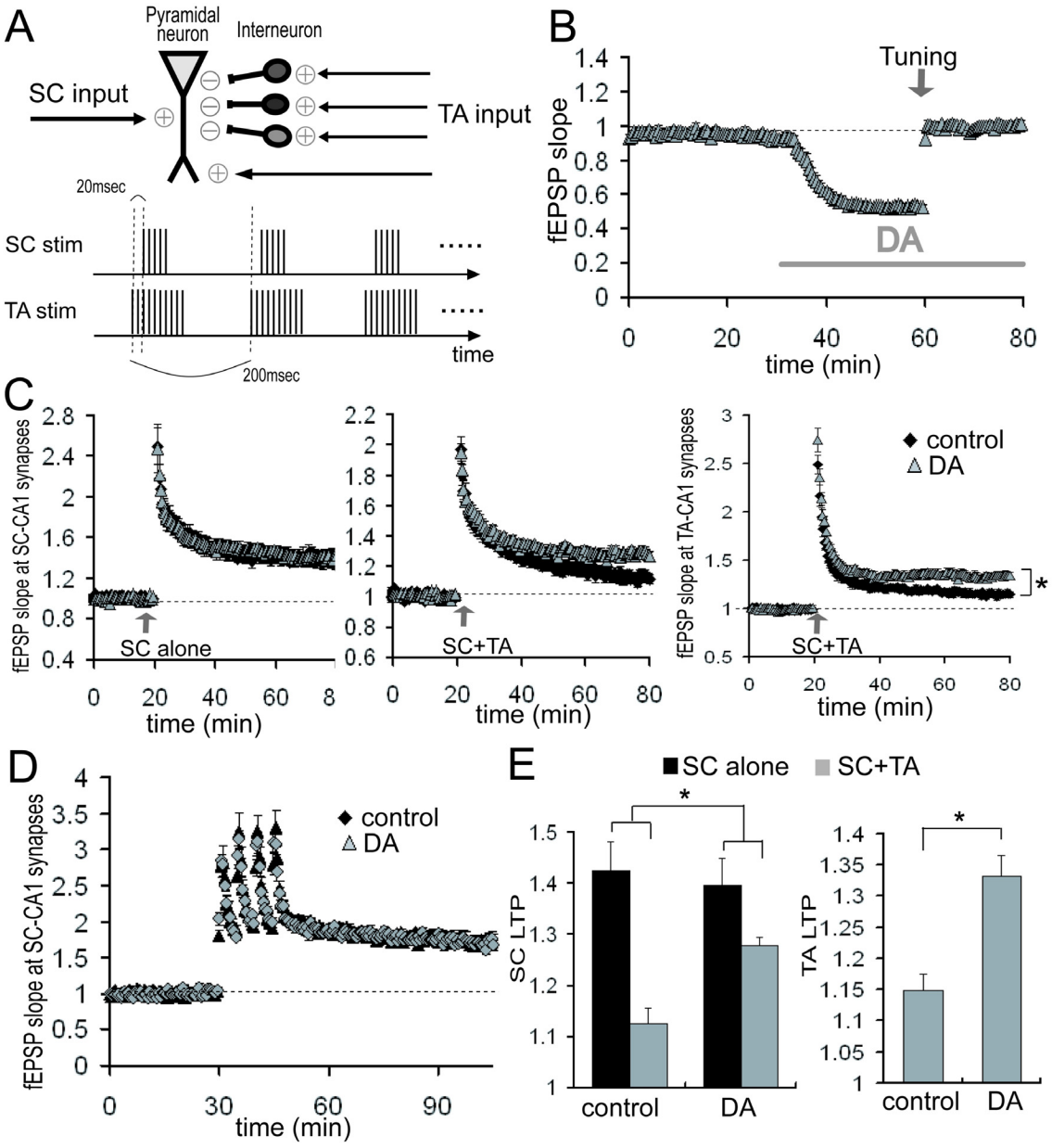

Figure 3-9: Reduction of LTP interference at SC-CA1 synapses by DA-induced disinhibition at TA-CA1 synapses

(A) Scheme of LTP interference protocol. 10 bursts of either 5 (SC) or 10 (TA) at 100 Hz with 200 msec interburst interval, was repeated twice at 30 sec interval. TA-TBS precedes SC-TBS by 20 msec. **(B)** Compensation of DA-induced excitatory depression

by increasing the stimulation current. After DA-induced depression was stabilized, the stimulation current was increased to return the fEPSP to its baseline value (tuning, indicated by arrow). **(C)** Influence of DA on the LTP interference of SC-CA1 synapses elicited by the TA pathway stimulation. TBS was applied to either the SC pathway alone (left; control: n = 8, DA: n = 6) or both the SC and the TA pathways concurrently (middle; n = 9 for each group). Right figure shows the enhancement of LTP at TA-CA1 synapses by DA after concurrent TBS application (n = 9 for each group). **(D)** No significant influence of DA on SC-LTP induced by HFS. LTP induction protocol was 100 Hz (100 pulse) stimulation, repeated 4 times at 5 min intervals (n = 6 for each). **(E)** Analysis of DA's effects on the magnitude of LTP after TBS application, either at SC-CA1 synapses (left) or at TA-CA1 synapses. DA significantly attenuated the LTP interference at SC-CA1 synapses (*$p < 0.05$), and enhanced LTP at TA-CA1 synapses (*$p < 0.01$).

3.4 DISCUSSION

3.4.1 Frequency dependent signal filtering by DA

Our results indicate that DA imposes a high-pass filter on signal propagation at TA-CA1 synapses and dynamically modulates information flow and synaptic plasticity in area CA1. Although previous studies have shown synaptic modulation induced by specific dopamine receptor subtypes in the hippocampus (Huang and Kandel, 1995; Otmakhova and Lisman, 1996; Otmakhova and Lisman, 1998; Chen et al., 1996), it was not clear how DA itself, as a neurotransmitter, modulates the activity of the integrated hippocampal network. Because of complex cooperative and uncooperative interactions among dopamine receptor subtypes (Missale et al., 1998; Taussig et al., 1993; Tucek et al., 2002; Plaznik et al., 1989; Ikemoto et al., 1997; Schmidt and Pierce, 2006; Hopf et al., 2003; Wu and Hablitz, 2005; Lee et al., 2004; Rashid et al., 2007), we decided to examine, primarily, the combined effects resulting from application of DA itself. Here we demonstrate that DA has a profound influence on signal integration of the two pathways in hippocampal area CA1, which may represent an information selection process for learning.

Because both synaptic transmission and action potential generation depend nonlinearly on the input patterns, it is important to understand synaptic function over a wide range of activity frequencies. Indeed, the importance of a frequency-dependent analysis of synaptic transmission was previously suggested (Markram et al., 1998). The frequency-dependent filter at TA-CA1 synapses we describe here, differentially

modulates (i.e., depresses or enhances) signals depending on input frequency, thus transferring qualitatively different information through the synaptic network. This frequency-dependency emerges due to differential responses to synaptic inputs that result from monosynaptic and disynaptic transmission (Figure 3-3B and 3-10). One advantage of this type of alternate gating is the potential for enabling dynamic coupling among different brain areas, because of actively generated oscillatory activities in the brain (Buzsaki and Draguhn, 2004; Siapas et al., 2005). Dynamic modulation of information flow via oscillatory coupling is suggested to have an important role in learning (for review, see Axmacher et al., 2006).

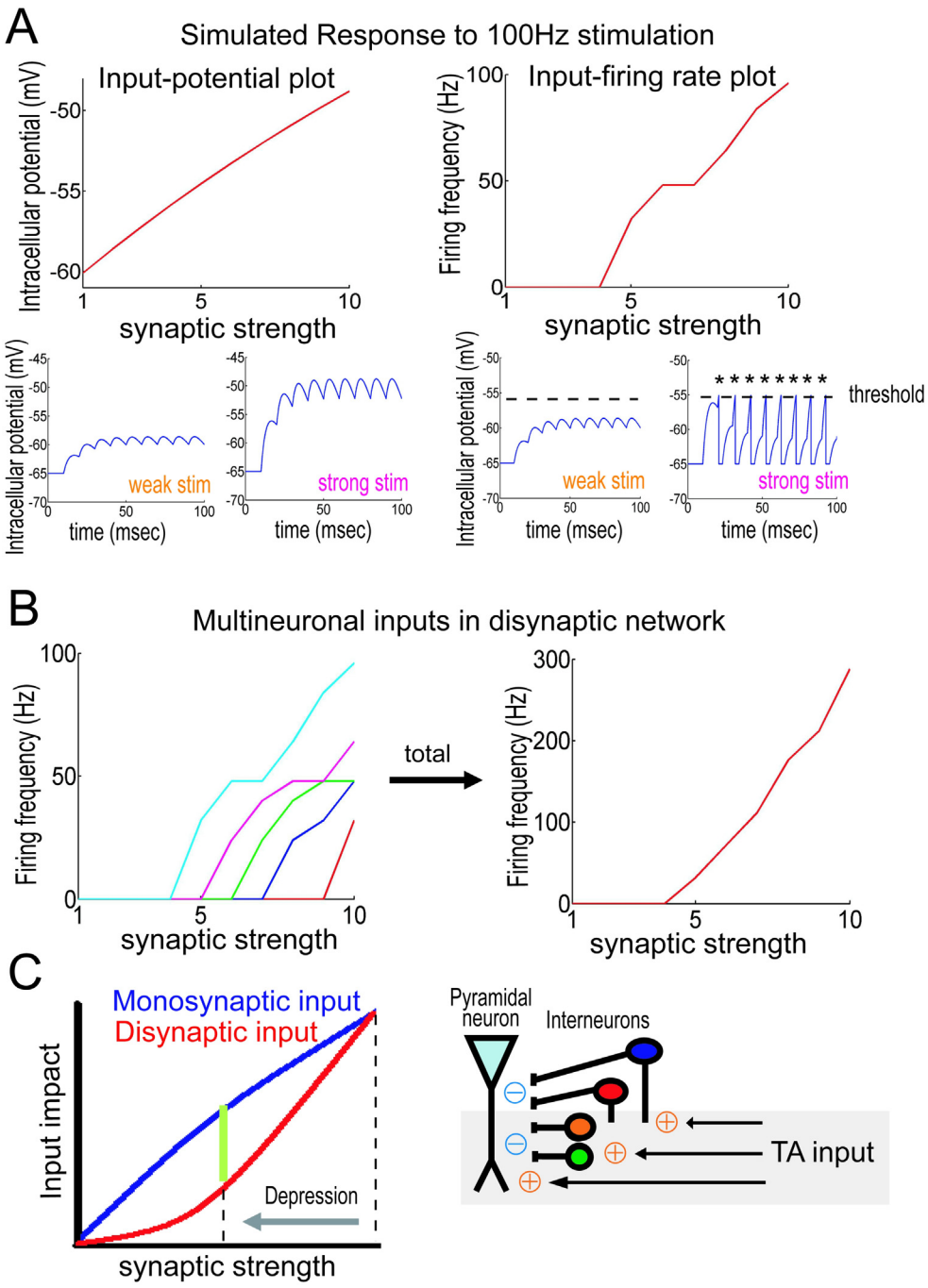

Figure 3-10: Modulation of excitatory/inhibitory balance by DA-induced excitatory depression

(A) Simulation based on an integrate-and-fire model. Excitatory stimuli at 100 Hz are

delivered using EPSPs of different initial strengths. Each plot shows either maximal membrane potential (left) or firing frequency (right) to a given initial input strength. During monosynaptic transmission, maximum membrane potentials depend approximately linearly on input strength (left). Disynaptic transmission, on the other hand, requires action potential generation for the signal propagation, which imposes a nonlinear dependency on input strength (right). **(B)** Total signal output from multiple neurons. Each neuron has a different threshold level as plotted in different colors (left). Summated output depends nonlinearly on input synaptic strength (right). Similarly, at TA-CA1 synapses, a pyramidal neuron receives disynaptic inhibition from multiple number of interneurons, thus inhibition evoked by the TA pathway should nonlinearly depend on the input synaptic strength. **(C)** Differential influence of synaptic depression between monosynaptic and disynaptic transmission. After depression of TA-CA1 synaptic transmission, the reduction of disynaptic inhibition is larger than that of monosynaptic excitation, explaining why the synaptic efficacy is enhanced during HFS, as observed as high-pass filtering, under the DA-induced excitatory depression. Other interneuron classes not studied here may be similarly affected by DA.

3.4.2 Functional impact of high-pass signal filtering on *in vivo* oscillatory activities

Mutual interactions between the dopaminergic system and the hippocampus have been previously suggested (Lisman and Otmakhova, 2001; Lisman and Grace, 2005). Both the hippocampus and the dopaminergic system show differential activation depending on the familiarity of the stimuli (Horvitz, 2000; Vinogradova, 2001; Fyhn et al., 2002; Rutishauser et al., 2006; Kumaran and Maguire, 2006; Schultz, 1998) and influence learning (Buhusi et al., 1998; Katz et al., 2002; Meltzer and Constable, 2005; Wittmann et al., 2005; Adcock et al., 2006). In contrast with short-latency responses (< 100 msec) of dopaminergic neurons to the stimuli (Schultz, 1998; Comoli et al., 2003; Dommett et al., 2005), differential activation of the hippocampus appears from approximately 200 – 400 msec after the stimuli (Knight, 1996; Brankack et al., 1996; Grunwald et al., 1998), suggesting DA may serve as a gate to modulate information flow into the hippocampus (Black et al., 2000; Jurkowlaniec et al., 2003; Orzel-Gryglewska et al., 2006).

Our demonstration of frequency-dependent signal modulation by the neurotransmitter DA has important ramifications for network function *in vivo*, especially when one considers the behavior-dependent oscillatory activities emerging from different brain structures (Buzsaki, 1996; Buzsaki, 2002; Steriade, 2001). For example, during exploratory behavior, the firing patterns of neurons in layer II/III of the entorhinal cortex which send projections to the hippocampus, are characterized by theta (4 - 12 Hz) and gamma frequency volleys (40 - 100 Hz) (Chrobak et al., 2000). Our data predict that

precisely these frequencies will be differentially influenced by DA-induced high-pass filtering. Because signals from the entorhinal cortex (the TA pathway) are thought to relay sensory-bound information (Quirk et al., 1992; Witter and Moser, 2006), in contrast with the associatively-processed information from area CA3 (the SC pathway) (Treves and Rolls, 1994; Nakazawa et al., 2002), the DA-induced frequency-selective enhancement of TA-CA1 signals may modulate the integration of environmental information with previously associated information as it leaves the hippocampus through area CA1. Supporting this idea, a theoretical study suggests that input frequency at TA-CA1 synapses will influence the decoding of information carried via the SC pathway (Yoshida et al., 2002). Furthermore, we demonstrate that DA-induced disinhibition attenuates the TA-evoked interference of plasticity induction at SC-CA1 synapses, possibly boosting information integration in area CA1. Taken together, these data indicate that DA can transform the hippocampal network to an “encoding mode” by reducing the inhibition on CA1 pyramidal neurons and modulating the information flow from the entorhinal cortex, thus facilitating the learning of behaviorally relevant events.

3.5 MATERIALS AND METHODS

3.5.1 Hippocampal slice preparation

Slices were prepared from 25 – 35 day-old Sprague-Dawley rats (Harlan) and microdissected to isolate the TA pathway, as described previously (Dvorak-Carbone and Schuman, 1999a). In brief, a vibrating microtome (EMS OTS4000 or Leica VT1000S) or a tissue chopper (Stoelting) was used to cut hippocampal slices (500 μm thickness, except 300 μm for figure 3-1C and 3-1D) in ice-cold oxygenated artificial cerebrospinal fluid (ACSF) containing (in mM) 119 NaCl, 2.5 KCl, 1.3 $MgSO_4$, 2.5 CaCl, 1.0 NaH_2PO_4, 26.2 $NaHCO_3$, 11.0 glucose. Slices were recovered at room temperature for at least 1 hour in an interface chamber, and transferred to a submerged recording chamber perfused with ACSF at 24.5 – 25.5 °C. The dentate gyrus and CA3 were removed to eliminate the possible activation of the trisynaptic pathway or perforant path projection to area CA3. Concentric bipolar tungsten electrodes (FHC) and stimulus isolators (Axon Instruments) were used for the stimulation.

3.5.2 Electrophysiology

Extracellular field potential recordings were made with 1 – 3 MΩ resistance microelectrodes filled with 3 M NaCl using a bridge amplifier (Axoclamp 2B, Axon Instruments). Whole-cell voltage-clamp recordings from CA1 pyramidal neurons were made without visualization with an Axopatch 1D or 200B (Axon Instruments). Internal solution of patch pipettes was (in mM) 115 potassium gluconate, 20 KCl, 10 sodium

phosphocreatine, 10 HEPES, 2 MgATP, 0.3 NaGTP (pH 7.3). In addition, to minimize possible postsynaptic current modulation by DA, pipette solutions contained (in mM) 5 QX314, 10 TEA, 1 4AP. Membrane voltage was clamped at -60 mV (without liquid junctional potential correction, absolute value of holding current were < 100 pA in all recordings). Membrane capacitance was cancelled and series resistance was compensated (70 – 80%). Recordings were discarded when the series resistance was over 20 MΩ or either series or membrane resistance changed more than 20% during data acquisition. For sharp-electrode intracellular recordings from CA1 interneurons, electrodes were blindly advanced at the border of SR and SLM and neurons were penetrated with a short buzz with an Axoclamp 2B amplifier. Interneurons were identified by both spike activities and morphology using biocytin staining after the recording. Sharp electrodes were 90 – 150 MΩ in resistance and contained 2 M potassium acetate. No tonic current was injected during recordings. Input resistance and membrane potential were monitored and recordings were discarded when either of them changed more than 20 % during data acquisition. In our recordings from interneurons (n = 5), average input resistance: 45.2 ± 7.8 MΩ and average membrane potential: -66.6 ± 3.0 mV. In the experiments using low $[Ca^{2+}]_{ext}$, extracellular calcium concentration was 1.25 mM, instead of 2.5 mM, and the total divalent cation was compensated for by adding magnesium. For frequency dependent modulation analysis, 100 pulses stimulation at the indicated frequencies were applied after baseline responses were stable for at least 10 min. The following stimulation protocols were used: For LTP induction, 100 Hz, 100 pulses, repeated 4 times at 5 min intervals; For LTD induction, 1 Hz, 900 pulses. For joint TBS application, 10 bursts of

either 5 (SC) or 10 (TA) at 100 Hz with 200 msec interburst interval, was repeated twice at 30 sec interval (the onset of TA TBS precedes SC TBS by 20 msec). All stimulus pulses were of the same length and amplitude as test pulses. Test pulses were applied once every 30 sec for extracellular field recordings, every 15 sec for whole cell recordings and every 10 sec for sharp electrode intracellular recordings. Drugs were applied by dilution of concentrated stock solutions into the perfusion medium. The final concentration of bath-applied DA was 20 μM (e.g., Otmakhova and Lisman, 1999). In acute DA application experiments, 500 μL of ACSF-diluted DA (60 μM) was directly applied into the recording chamber. The volume of recording chamber is ~ 1 mL, thus estimated final concentration of DA is ~ 20 μM. The flow-rate of ACSF was ~ 1.5 mL/min.

3.5.3 Data analysis

Data were collected by a custom program using the LabView data acquisition system (National Instruments) for extracellular recordings, or DigiData 1200 and pClamp 9 (Axon Instruments) for intracellular recordings. All numerical values listed represent mean ± s.e.m. Depression and potentiation were measured at 30 – 35 min and 50 – 60 min after plasticity induction, respectively, relative to baseline (average of the slopes of the fEPSPs for 15 min prior to plasticity induction). For plasticity experiments under DA application, the baseline fEPSP was normalized to the depressed state. For analysis of the waveforms during 100 pulses stimulation, stimulation artifacts (and fiber volleys in field recordings) were excluded and the gaps were linearly connected, and the last excitatory

potential or current (100th stimulus response) was measured by a custom program in Matlab (MathWorks). Steady-state potentials or currents were measured to exclude the influence of initial states of the network at the beginning of stimulation. Wilcoxon rank sum test was performed for all statistical analysis except figure 3-9E, for which an ANOVA was performed.

Chapter 4. Functional Division of Hippocampal Area CA1 via Modulatory Gating of Entorhinal Cortical Inputs

4.1 SUMMARY

The hippocampus receives two streams of information, spatial and nonspatial, via major afferent inputs from the medial (MEC) and lateral (LEC) entorhinal cortexes. The MEC and LEC projections in the temporoammonic pathway are topographically organized along the transverse-axis of area CA1. The potential for functional segregation of area CA1, however, remains relatively unexplored. Here, we demonstrated differential novelty-induced c-Fos expression along the transverse-axis of area CA1 corresponding to topographic projections of MEC and LEC inputs. In hippocampal slices, we found distinct presynaptic properties between LEC and MEC terminals, and application of either DA or NE produced a largely selective influence on one set of inputs (LEC). Finally, we demonstrated that differential c-Fos expression along the transverse-axis of area CA1 was largely abolished by an antagonist of neuromodulatory receptors, clozepine. Our results suggest that neuromodulators can control topographic TA projections allowing the hippocampus to independently control spatial and nonspatial information processing.

4.2 INTRODUCTION

The brain has the capacity for parallel information processing, in which sensory information received from the environment is segregated and independently processed

based on particular features. For example, it is generally accepted that visual information is processed in two distinct information streams (Ungerleider and Haxby, 1994): A ventral stream that subserves object recognition, or "what" perception, and a dorsal stream that primarily represents spatial information, or "where" perception. Separately processed information must be integrated somewhere in the brain for coherent perception (Engel and Singer, 2001). A number of studies indicate that the hippocampus, a brain structure important for episodic/declarative memory formation (Scoville and Milner, 1957; Squire et al., 2004), is one such integrative area that combines the two streams of information (Witter and Amaral, 2004; Manns and Eichenbaum, 2006).

As initially described by Ramon Cajal (Cajal, 1911), the hippocampus receives its major afferent inputs from the entorhinal cortex (EC). Detailed anatomical studies suggest that the EC can be further divided into two subdivisions, the medial and lateral areas (MEC and LEC), based on cytoarchitecture and projection patterns (Witter and Amaral, 2004; Canto et al., 2008). Recent data suggest that the MEC and LEC may be functionally distinct: *in vivo* recording studies show strong spatial modulation in MEC neurons (Fyhn et al., 2004), but not in LEC neurons (Hargreaves et al., 2005). Other studies suggest that the LEC is likely to be involved in nonspatial information processing about specific objects or cues in the environment (Knierim et al., 2006).

The projections from the MEC and LEC terminate in distinct parts of the hippocampus (Witter and Amaral, 2004) (see Figure 4-2). In the perforant pathway (originating from layer II EC neurons), the fibers from the LEC terminate in the outer third of the molecular layer in the dentate gyrus (DG), but the axons from the MEC make

synapses in the middle third of the molecular layer. On the other hand, in the temporoammonic (TA) projection (originating from layer III EC neurons) to area CA1, the fibers from the LEC make synapses in the distal part of area CA1 (close to the subiculum), and the axons from the MEC terminate in the proximal part (close to area CA3). The topographic organization of LEC and MEC inputs suggests that neurons in proximal or distal CA1 receive predominantly one set of entorhinal-cortical inputs via the TA pathway. If this is true, there may exist a functional division along the transverse axis of area CA1. This contrasts with the laminar organization of the perforant pathway, where each neuron in the DG or area CA3 receives both MEC and LEC inputs at different dendritic locations. Thus, these organized laminar and topographic projections may play a key role in controlling information transfer from the EC to the hippocampus.

Although many studies have demonstrated the involvement of the hippocampus in learning (Eichenbaum, 2000; Squire et al., 2004), its precise role is not yet clear. One of the prominent features of hippocampal neurons is its differential activation depending on stimulus novelty (Stern et al., 1996; Knight, 1996; Dolan and Fletcher, 1997; Vinogradova, 2001; Rutichauser et al., 2006), suggesting that the hippocampus may act as a novelty detector (Parkin, 1997; Kumaran and Maguire, 2007). The novelty-dependent activation of hippocampal neurons is likely to be a critical feature for learning, allowing circuit modifications that optimize stimulus prediction. How the hippocampus acquires information about the novelty of stimulus or context is still unclear, but a number of studies have indicated a critical role of neuromodulators (Hasselmo and Schnell, 1994; Ranganath and Rainer, 2003; Lisman and Grace, 2005).

Neuromodulators play a key role in controlling information flow among brain areas (Ito and Schuman, 2008). Midbrain dopaminergic neurons in ventral tegmental area and substantial nigra compacta show increased activity after exposure to novel stimuli (Schultz, 1998, Horvitz, 2000). The axons of dopaminergic neurons project to the hippocampus (Gasbarri et al., 1997) and release dopamine (DA) after animals are exposed to a novel environment (Ihalainen et al., 1999). In addition, a number of studies have indicated that DA plays an important role in hippocampal-dependent learning (Gasbarri et al., 1996b; El-Ghundi et al., 1999).

Another major neuromodulator in the brain, norepinephrine (NE), is primarily released from neurons in the locus coeruleus (Siegel et al., 1999), a brain-stem nucleus. Similar to dopaminergic neurons, these neurons also show novelty-dependent activation (Vankov et al., 1995; Harley, 2004; Aston-Jones and Cohen, 2005; Sara, 2009). Many noradrenergic neurons send their fibers to the hippocampus (Swanson, 1987) and release NE when animals are exposed to a novel environment (Ihalainen, 1999). The NE signals are thought to play an important role in eliciting exploratory behaviors in a novel environment (Sara et al., 1995). In addition, a subtype of NE receptors in the hippocampus, the beta-1 adrenergic receptors, appears to be selectively required for the retrieval of hippocampal-dependent memory (Murchison et al., 2004).

The interactions between neuromodulators and the hippocampus may be crucial for constructing or updating representations of environmental context, which requires the integration of spatial and nonspatial information. Here, we investigated how neurons in the hippocampus are activated by spatial or nonspatial novelty and examined if there is a

functional division in area CA1 afforded by the anatomical organization of LEC and MEC inputs. We then examined the effects of NE and DA at entorhinal-cortical inputs as a potential mechanism for the independent control of spatial and nonspatial information processing in the hippocampus.

4.3 RESULTS

4.3.1 Differential activation of distal and proximal CA1 by exposure to novel object or place

Neurons in the hippocampus exhibit differential firing based on the novelty or familiarity of stimuli encountered in the environment. We examined whether exposure to novel stimuli leads to activation of neurons in area CA1, and if so, whether there is differential activation along the transverse-axis of area CA1, due to the topographic organization of LEC and MEC projections in the TA pathway. Following home cage exposure for several days, pairs of individually housed rats were subjected to one of the following conditions: exposure to novel objects in the home cage (experimental group: EXP) or sham exposure (cage opened but no objects introduced, control group: CON). After 2 hrs of novel object exposure, animals were sacrificed and immunohistochemistry was performed on brain slices. To observe activation of CA1 neurons we stained with antibodies for an immediate early gene product, c-Fos (Morgan and Curran, 1991), together with a neuronal nuclear marker protein, NeuN (Figure 4-1A). Animals exposed to the novel objects exhibited a significantly higher number of c-Fos-positive neurons in

area CA1, when compared to control animals. As the LEC has been proposed to process nonspatial information about objects, we counted the number c-Fos-positive neurons in distal (LEC) vs. proximal (MEC) CA1. We observed a larger number of c-Fos positive neurons in distal CA1 (LEC) compared to proximal CA1 (Figure 4-1C) in brain slices from EXP but not control animals.

To further examine the potential topographic representation of environmental signals in CA1 inputs, we examined c-Fos expression after animals were exposed to a novel environment. Using the same design as above, one animal was removed from his home cage and placed in a new cage ("EXP" group), and the paired control was removed and then re-introduced to his home cage ("CON" group). Exposure to a novel place significantly enhanced c-Fos expression in neurons in both proximal and distal CA1 (Figure 4-1B and 4-1D). These data indicate that proximal (MEC) and distal (LEC) CA1 can be differentially activated depending on whether animals are exposed to novel spatial or nonspatial information.

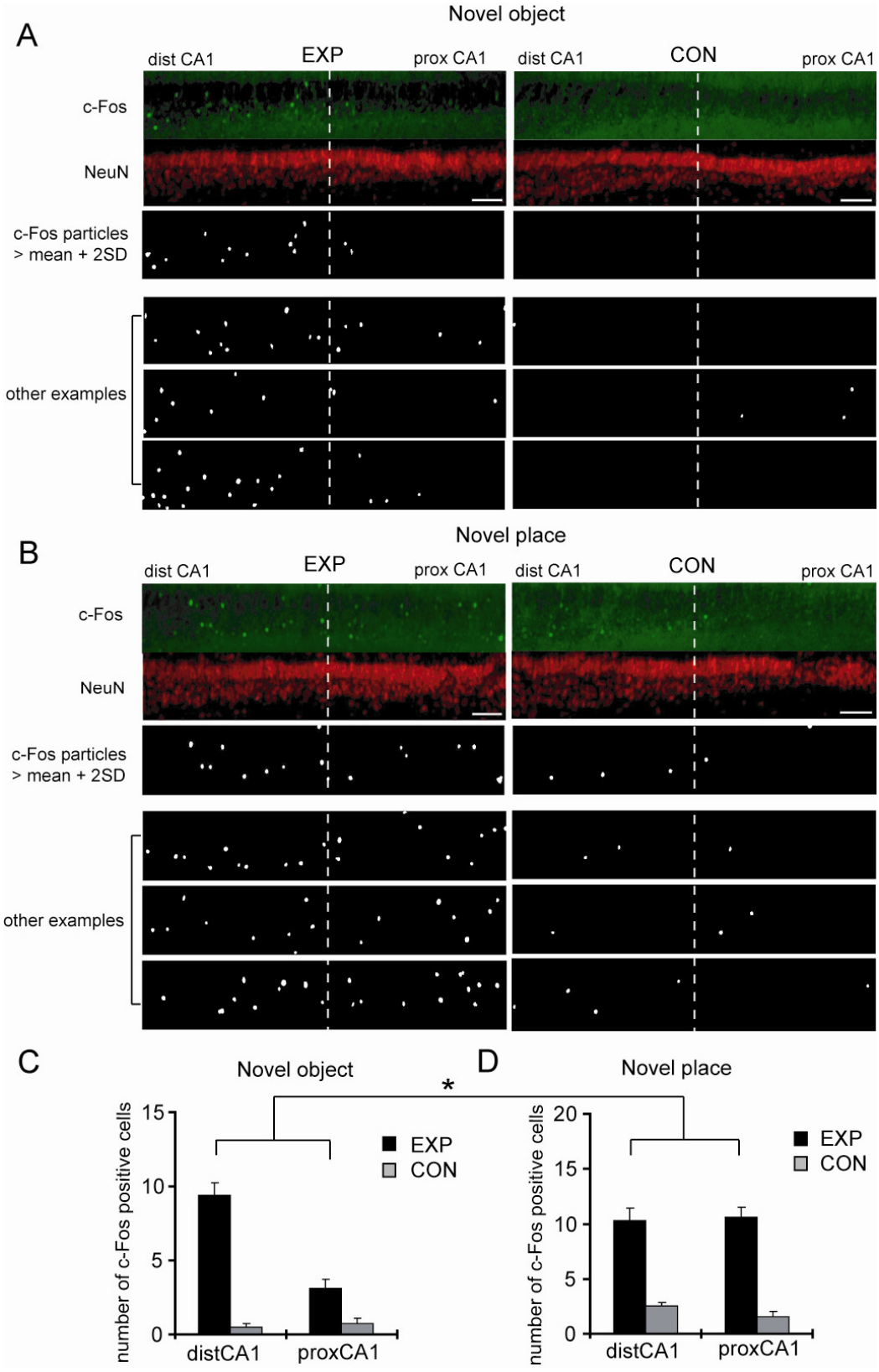
A
Novel object
dist CA1
EXP
prox CA1
dist CA1
CON
prox CA1
c-Fos
NeuN
c-Fos particles
> mean + 2SD
other examples
B
Novel place
dist CA1
EXP
prox CA1
dist CA1
CON
prox CA1
c-Fos
NeuN
c-Fos particles
> mean + 2SD
other examples
C
Novel object
number of c-Fos positive cells
15
10
5
0
EXP
CON
distCA1
proxCA1
D
Novel place
*
number of c-Fos positive cells
20
15
10
5
0
EXP
CON
distCA1
proxCA1

Figure 4-1: Differential c-Fos expression between proximal and distal CA1 after exposure to a novel object or place

(A) Pairs of animals were individually housed in a home cage for at least 2 days. For the experimental animal, the cage was opened and 3 toys were placed inside ("EXP"). For the control animal, the cage was opened, but no object was inserted ("CON"). After 2 hours, hippocampal slices were prepared from both animals, fixed and immunostained with c-Fos and NeuN antibodies. c-Fos particles were detected and analyzed (see methods). Representative images shown are at the pyramidal layer of area CA1 of "EXP" and "CON" animals (scale bar = 100 μm). **(B)** A pair of animals was individually housed in a home cage for at least 2 days. For one of animals, the cage was opened and the animal was carried up and placed in a different cage ("EXP"). For another animal, the cage was opened and the animals was carried up but placed back in the original cage ("CON"). After 2 hours, slices were prepared and immunstained as in **A**. Images shown are from the pyramidal layer of area CA1 of "EXP" and "CON" animals (scale bar = 100 μm). **(C)** The number of c-Fos positive cells was analyzed in the pyramidal layer of area CA1 in each 50 μm slice. Area CA1 was equally divided into two parts, representing distal and proximal CA1. The number of c-Fos positive cells was significantly higher in distal CA1 following exposure to novel objects, when compared to proximal CA1 (n = 6 pairs of animals). The total integrated NeuN signal in same areas used for c-Fos expression analysis did not differ between groups (Supplementary Figure 4-2A). **(D)** The number of c-Fos positive cells was analyzed in the pyramidal layer of area CA1 in each slice. The number of c-Fos positive cells was high in both distal and proximal CA1

following exposure to a novel place (n = 6 pairs of animals). The total integrated NeuN signals in same areas used for c-Fos expression analysis did not differ between groups (Supplementary Figure 4-2A). For the analysis of novelty-induced c-Fos expression, a two-way ANOVA was performed with two variables: novelty type (object vs. place) and CA1 subregion (distal vs. proximal), and revealed a significant interaction ($p = 0.0008$).

4.3.2 Differences in presynaptic properties between LEC and MEC inputs

The above difference in c-Fos immunoreactivity between proximal and distal CA1 indicates that topographic projections in the TA pathway are behaviorally relevant. We next investigated whether any differences can be detected between LEC and MEC inputs at the synaptic scale. We performed immunohistochemistry on hippocampal slices to observe differences in synaptic protein expression between LEC and MEC synapses. When compared to a postsynaptic protein (GluR2/3) expression pattern, we found that some of presynaptic proteins (synapsin I, bassoon or synaptophysin) we examined showed differential expression between either the SLM of distal CA1 vs. proximal CA1, or the outer third vs. middle third of the molecular layer of the DG. These differences mapped onto the anatomical distinction between areas receiving LEC and MEC inputs (Figure 4-2). These immunostaining results suggest that LEC and MEC presynaptic terminals possess different complements of presynaptic proteins.

Next, we examined paired pulse facilitation to assess the presynaptic function of LEC and MEC terminals. In the TA pathway, paired-pulse facilitation was significantly larger at proximal TA-CA1 synapses, compared to distal TA-CA1 synapses (proximal TA: 1.79 ± 0.08, distal TA: 1.24 ± 0.07) (Figure 4-3A). In the perforant pathway, lateral PP synapses showed larger facilitation than medial PP synapses (mPP: 0.76 ± 0.05, lPP: 1.51 ± 0.10) (Figure 4-3B). Thus, our results indicate that LEC and MEC terminals have distinct functional properties, providing a potential substrate for the differential control of LEC and MEC synapses *in vivo*.

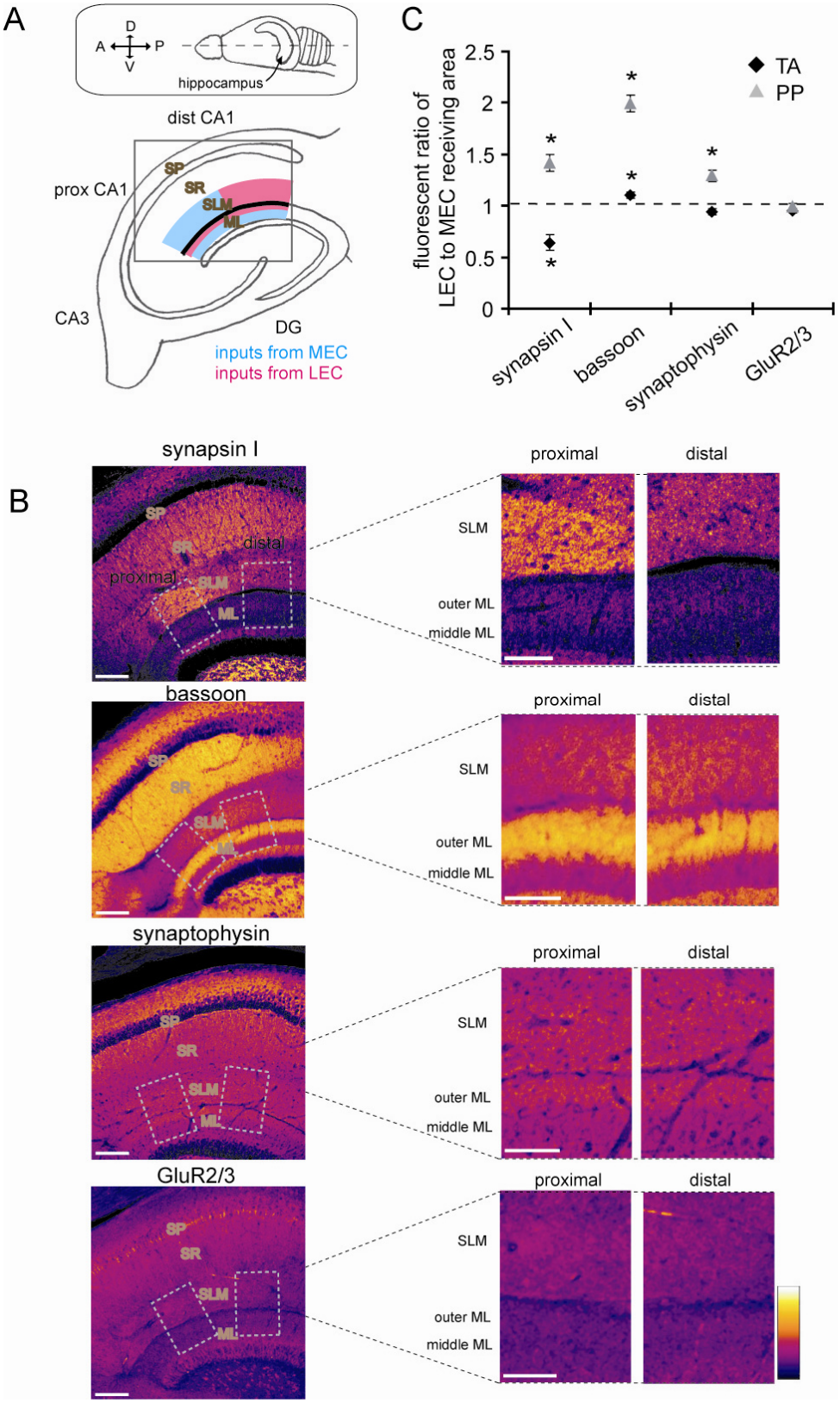
A
D
A
P
V
hippocampus
dist CA1
prox CA1
SP
SR
SLM
ML
CA3
DG
inputs from MEC
inputs from LEC
C
fluorescent ratio of LEC to MEC receiving area
2.5
2
1.5
1
0.5
0
TA
PP
synapsin I
bassoon
synaptophysin
GluR2/3
B
synapsin I
bassoon
synaptophysin
GluR2/3
proximal
distal
SLM
outer ML
middle ML

Figure 4-2: Differences in presynaptic protein expression in synaptic regions that receive inputs from MEC or LEC

(A) Scheme of topographic or laminar projection of MEC and LEC inputs to area CA1 or DG., respectively. The inset shows an approximate section level of hippocampal slices used for c-Fos expression analysis, immunohistochemistry and electrophysiology. **(B)** Distribution of presynaptic proteins (synapsin I, bassoon and synaptophysin) and a postsynaptic protein (GluR2/3) in the hippocampus. Differential protein expression was observed in the SLM of distal vs. proximal CA1 as well as the outer vs. middle ML of the DG (scale bar = 200 μm in the left figures, 100 μm in the right enlarged figures). **(C)** Fluorescent signal ratios of areas receiving LEC inputs to areas receiving MEC inputs in either the TA or perforant pathway. The ratio of some presynaptic proteins (synapsin I, bassoon, or synaptophysin) was significantly different from the ratio of GluR2/3 ($n = 5, 11, 6, 4$ for each) ($*p < 0.05$).

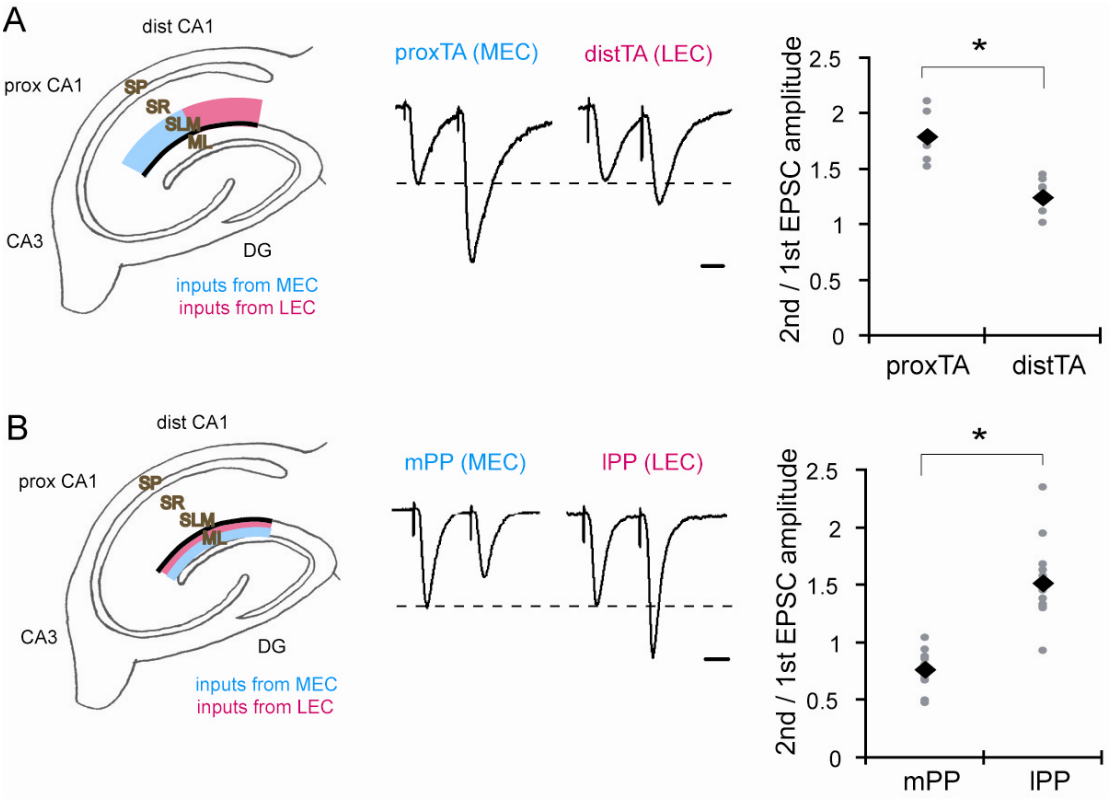

Figure 4-3: Differences in paired-pulse facilitation between LEC and MEC synapses

(A) Whole cell voltage-clamp recordings from pyramidal neurons in proximal or distal CA1 under blockade of fast inhibitory transmission (bicuculline; 10 μM). Internal pipette solution contained QX314 (5 mM), TEA (10 mM), and 4AP (1 mM) to block sodium and potassium channels. A paired-stimulus was applied to either proximal or distal TA pathways and paired pulse facilitation was quantified (2nd / 1st EPSC amplitudes, inter-stimulus interval: 50 ms; n = 7 for each) (scale bar = 20 ms) (*$p < 0.05$). **(B)** Whole cell voltage-clamp recordings from granule cells in the DG. Recording conditions were same as in **A**. A paired-stimulus was applied to either medial or lateral PP and paired pulse facilitation was quantified (2nd / 1st EPSC amplitudes, inter-stimulus interval: 50

ms; n = 13 for each) (scale bar = 20 ms) (*$p < 0.05$).

4.3.3 Differential influence of DA and NE on inputs from the LEC and MEC

Novel signals or stimuli in an animal's environment are known to influence the firing of DA and NE-releasing neurons (Harley, 2004; Kitchigina et al., 1997). The relative short latency of dopaminergic neuron activation after a exposure to a novel stimulus (< 70 to 100 ms; Comoli et al., 2003; Dommett et al., 2005) compared to that of the hippocampus (> 200 ms; Knight, 1996; Brankack et al., 1996; Grunwald et al., 1998) is consistent with the idea that DA exerts a feed-forward influence on hippocampal novelty processing. Thus, we asked whether DA and/or NE modulate LEC and MEC inputs to bring about the observed differences between distal and proximal CA1 activation. To examine this, we obtained extracellular field potentials from distal (close to subiculum) and proximal (close to CA3) TA-CA1 synapses in hippocampal slices (Figure 4-4A). When DA (20 μM) was bath applied, the fEPSP at distal TA-CA1 synapses was largely depressed (55 ± 3%, mean percent of baseline 15 – 20 minute after drug application) (Otmakhova and Lisman, 1999; Ito and Schuman, 2007), but the fEPSP at proximal TA-CA1 synapses was only marginally influenced (95 ± 3%) (Figure 4-4B). We also tested another neuromodulator, NE, and found that bath application of NE (10 μM) also induced significantly larger depression at distal TA-CA1 synapses (40 ± 7%), compared to proximal TA-CA1 synapses (89 ± 2%) (Figure 4-4B). The influence of NE on Schaffer-collateral (SC)-CA1 synapses was significantly smaller (93 ± 2%) (Figure 4-5A), as has also been observed for DA (Otmakhova and Lisman, 1999; Ito and Schuman, 2007). Thus, bath application of DA or NE primarily modulated distal TA-CA1 synapses, while their influence on other synapses in area CA1 was minimal. We

hypothesized that this differential modulation by neuromodulators is due to the different origins of synaptic inputs (MEC vs. LEC). To test this idea, we also examined the neuromodulators' effect on the perforant path (PP) – dentate gyrus (DG) synaptic transmission.

We placed both stimulating and recording electrodes in either the outer or middle third of the molecular layer of the DG (Figure 4-4C). When DA was bath applied, the fEPSP at lateral PP-DG synapses was depressed to 75 ± 4% of baseline, however fEPSP at medial PP-DG synapses was not depressed and rather slightly enhanced (111 ± 6%) (Figure 4-4D). Similarly, NE also largely depressed synaptic inputs from lateral PP (52 ± 5%), but had lesser effects on medial PP-DG synapses (88 ± 5%) (Figure 4-4D). As previously demonstrated, DA- and NE-mediated synaptic depression at distal TA-CA1 synapses is reversible after the washout of neuromodulators (Otmakhova and Lisman, 1999; Ito and Schuman, 2007; Otmakhova et al., 2005). Here, we confirmed that neuromodulator-mediated control of PP-DG synapses was also reversible (Figure 4-5B). Taken together, our results indicate that the neuromodulators, DA and NE, primarily influence synapses made with LEC inputs, providing differential and temporally-controlled regulation of two streams of information, (e.g., spatial and nonspatial), from the EC to the hippocampus.

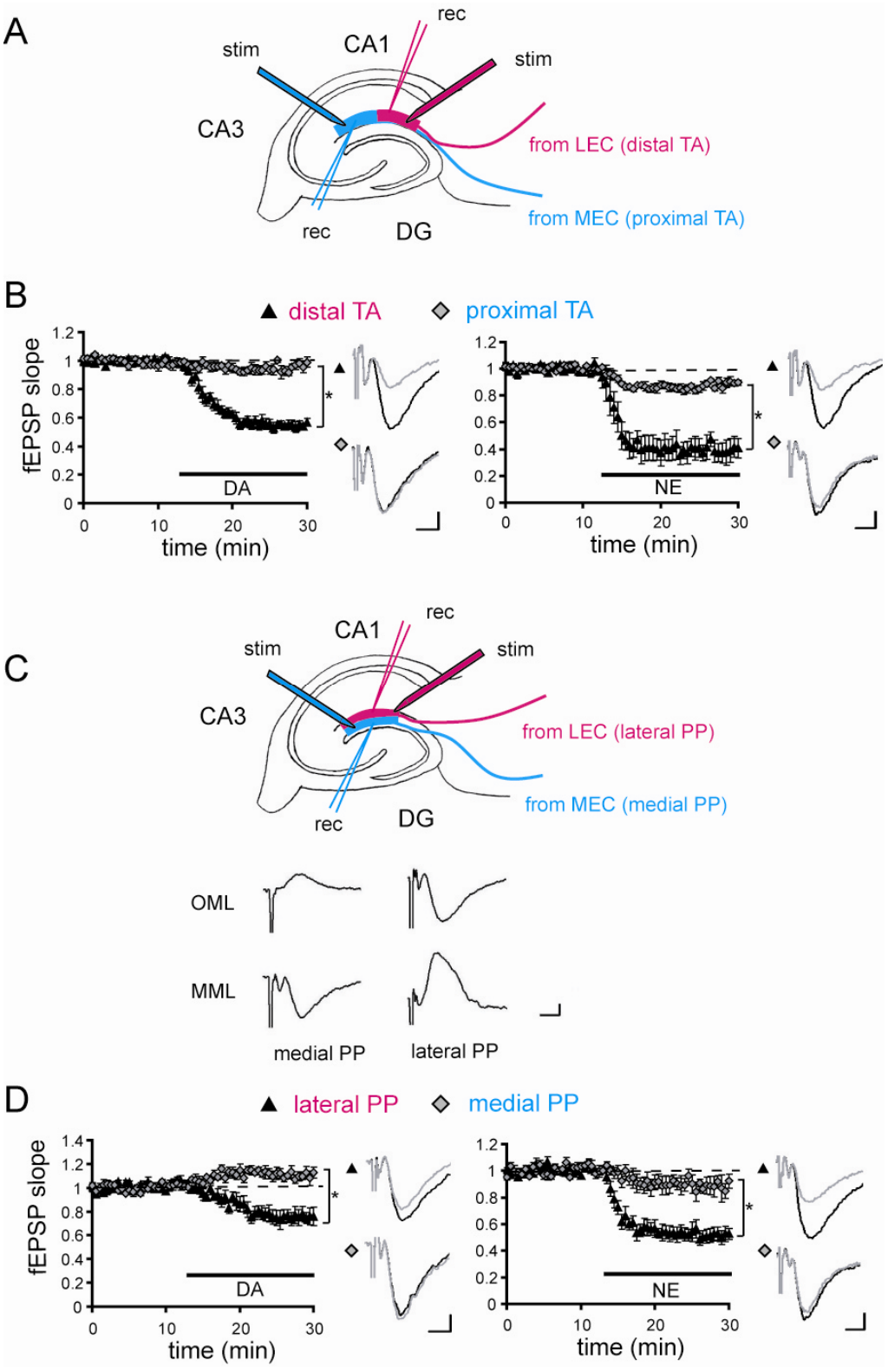
A
stim
CA1
rec
stim
CA3
from LEC (distal TA)
from MEC (proximal TA)
rec
DG
B
distal TA
proximal TA
fEPSP slope
DA
NE
time (min)
C
stim
CA1
rec
stim
CA3
from LEC (lateral PP)
from MEC (medial PP)
rec
DG
OML
MML
medial PP
lateral PP
D
lateral PP
medial PP
fEPSP slope
DA
NE
time (min)

Figure 4-4: Differential modulation of LEC inputs by DA and NE in two different hippocampal pathways

(A) Scheme of entorhinal cortical inputs to SLM of area CA1. MEC inputs make synapses at proximal (relative to CA3) CA1, but LEC inputs project to distal CA1. Appropriate positioning of stimulating and recording electrodes allows the measurement of synaptic responses from each input. **(B)** Either DA (20 μM) or NE (10 μM) application caused a large depression of the field EPSP resulting from LEC, but not MEC activation (DA: n = 7, NE: n = 5). Field EPSP waveforms before (black) and after (gray) DA or NE application are shown (scale bar = 0.1 mV, 5 ms). **(C)** Scheme of entorhinal cortical inputs to the molecular layer of DG. LEC inputs make synapses in the outer molecular layer (OML; lateral PP), but MEC inputs project the middle molecular layer (MML; medial PP). Appropriate positioning of stimulating and recording electrodes allows the measurement of synaptic responses from each pathway. Pathway selectivity was further confirmed by sink-source waveform analysis of field potentials. Representative field potentials depict negative-going potentials in MML and positive-going potentials in the OML in response to medial PP stimulation. On the other hand, lateral PP stimulation induces a negative-going potential in the OML and a positive-going potential in the MML (scale bar = 0.1 mV, 5 ms). **(D)** Either DA or NE application induced large synaptic depression at the lateral PP-DG, but not in medial PP-DG synapse (DA: n = 6, NE: n = 5). Field EPSP waveforms before (black) and after (gray) DA or NE application are shown (scale bar = 0.1 mV, 5 ms).

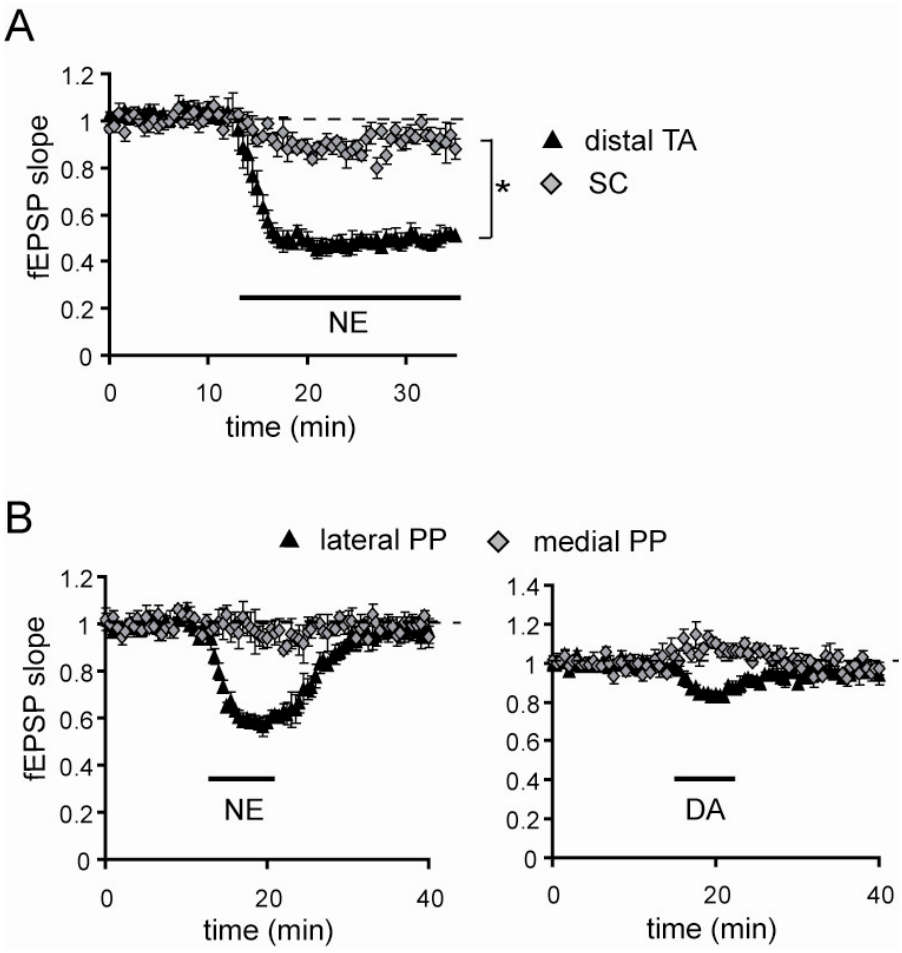

Figure 4-5: Pathway selective and reversible modulation by DA and NE

(A) NE's effects on Schaffer-collateral-CA1 and distal TA-CA1 synapses. NE had a signficantly greater influence on distal TA-CA1 synapses when compared to SC-CA1 synapses (n = 5) (*$p < 0.05$). **(B)** Reversibility of NE and DA's effects on synaptic transmission in the perforant pathway. After the removal of NE or DA, the fEPSP recovered back to the original baseline value (NE: n = 4, DA: n = 4).

4.3.4 Presynaptic inhibition of LEC inputs by DA and NE

To examine the synaptic locus of this differential modulation of LEC vs. MEC inputs, we conducted whole-cell voltage clamp recordings from distal CA1 pyramidal neurons and measured the synaptic responses evoked by stimulation in stratum lacunosum moleculare (SLM) (Figure 4-6A). When fast inhibitory synaptic transmission (bicuculline: 10 μM) as well as postsynaptic voltage-gated sodium/potassium channels (intracellular QX 314: 5 mM, TEA: 10 mM, 4AP: 1 mM) were blocked, NE still significantly depressed the distal SLM-elicited EPSC (45 ± 8%, mean percentage of baseline 7 – 10 minute after drug application) and enhanced paired-pulse facilitation (1.22 ± 0.08 to 1.76 ± 0.20), suggesting a mechanism of presynaptic inhibition. We previously examined DA's influence on these synapses (Ito and Schuman, 2007) and found similar results (EPSC amplitude: 58 ± 2%, paired-pulse facilitation: 1.47 ± 0.05 to 1.90 ± 0.08 after DA application), suggesting that DA also reduces presynaptic release probability. We also conducted whole-cell voltage clamp recording from granule cells in the DG and measured synaptic responses from lateral and medial PP inputs (Figure 4-6B). Both NE and DA largely depressed the EPSC evoked by lateral PP stimulation (NE: 46 ± 5%, DA: 71 ± 6%), but only slightly depressed EPSC from medial PP (NE: 88 ± 10%, DA: 90 ± 4%). Paired-pulse facilitation was significantly increased by both DA and NE at lateral PP synapses (NE: 1.51 ± 0.20 to 2.29 ± 0.38, DA: 1.51 ± 0.09 to 1.83 ± 0.14) but not at medial PP synapses (NE: 0.74 ± 0.6 to 0.66 ± 0.04, DA: 0.77 ± 0.07 to 0.79 ± 0.07) (Figure 4-6C). Taken together, our results suggest that neuromodulators act on LEC inputs via, at least in part, a presynaptic mechanism.

We also examined the receptor subtype contribution to the neuromodulator-mediated control of entorhinal-hippocampal connections, using a variety of receptor antagonists. These studies suggest the contribution of both dopamine D1-like and D2-like receptors to DA-induced synaptic depression, and the alpha-2 adrenergic receptor to NE-induced depression, at both the TA and perforant pathway synapses (Figure 4-7). Thus, the TA and perforant pathway appear to utilize a similar signal transduction pathway for the neuromodulator-mediated control of LEC inputs, irrespective of the origin differences between the TA pathway (layer III of the EC) and the perforant pathway (layer II of the EC).

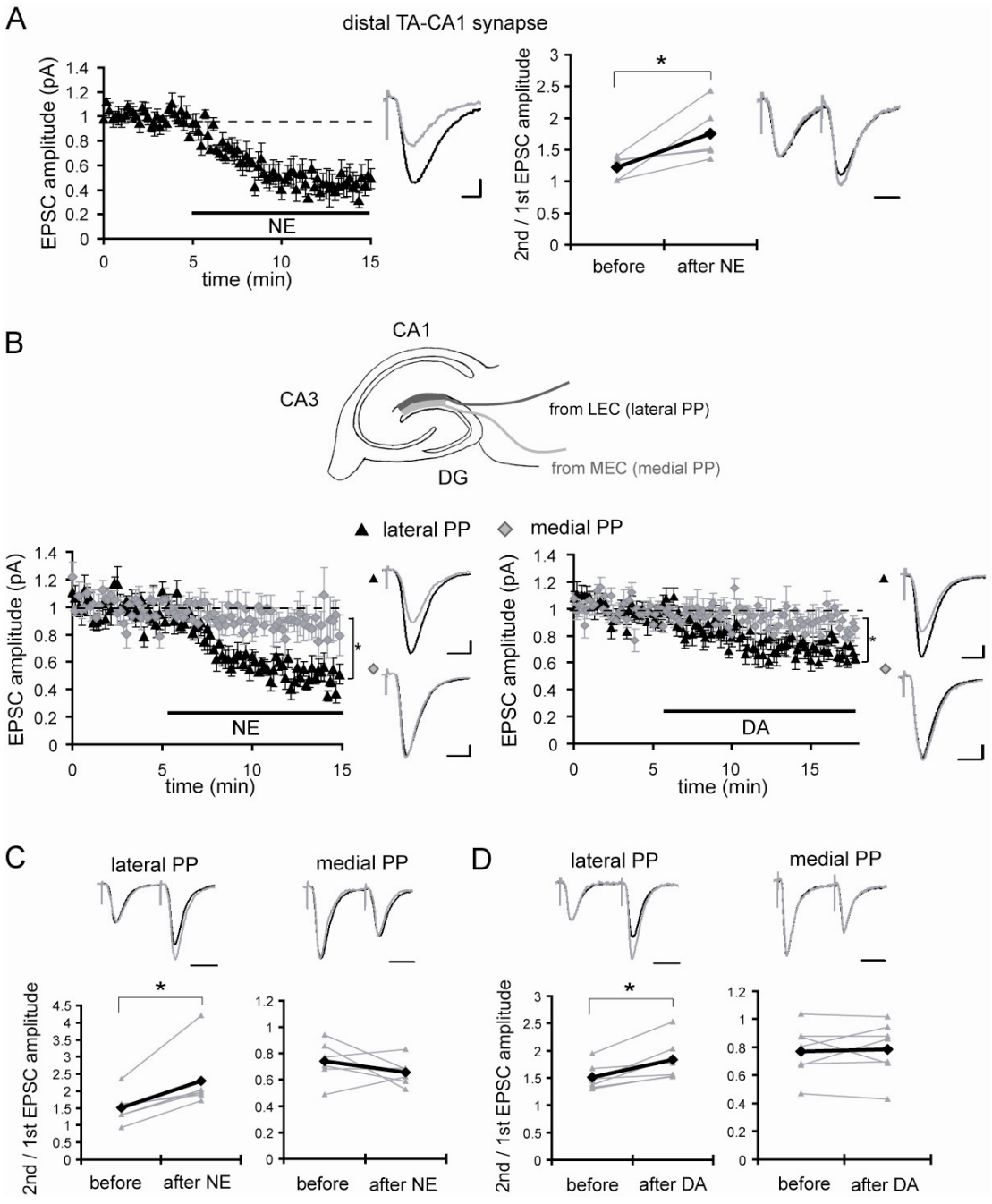

Figure 4-6: DA and NE induce presynaptic inhibition of LEC inputs

(A) Whole cell voltage-clamp recordings from pyramidal neurons in distal CA1 under blockade of fast inhibitory transmission (bicuculline; 10 μM; n = 5). Internal pipette

solution contained QX314 (5 mM), TEA (10 mM), and 4AP (1 mM) to block sodium and potassium channels. NE application significantly depressed the EPSC evoked by distal TA pathway stimulation and enhanced paired pulse facilitation (2nd / 1st EPSC amplitudes (inter-stimulus interval: 50 ms). EPSC waveforms before (black) and after (gray) NE application are shown (scale bar = 20 pA, 10 ms) (*$p < 0.05$). **(B)** Whole cell voltage-clamp recordings from granule cells in the DG. Recording conditions were same as in **A**. NE application significantly depressed the lateral, but not medial PP inputs (n = 6). DA application also selectively depressed lateral PP inputs (n = 7). EPSC waveforms of before (black) and after DA or NE application (gray) are shown (scale bar = 20 pA, 10 ms). **(C)** NE application selectively enhanced paired pulse facilitation (inter-stimulus interval: 50 ms) (gray: individual experiment, black: average). EPSC waveforms before (black) and after (gray) NE application are shown (scale bar = 20 ms) (*$p < 0.05$). **(D)** DA application selectively enhanced paired pulse facilitation (inter-stimulus interval: 50 ms) (gray: individual experiment, black: average). EPSC waveforms before (black) and after (gray) DA application are shown (scale bar = 20 ms) (*$p < 0.05$).

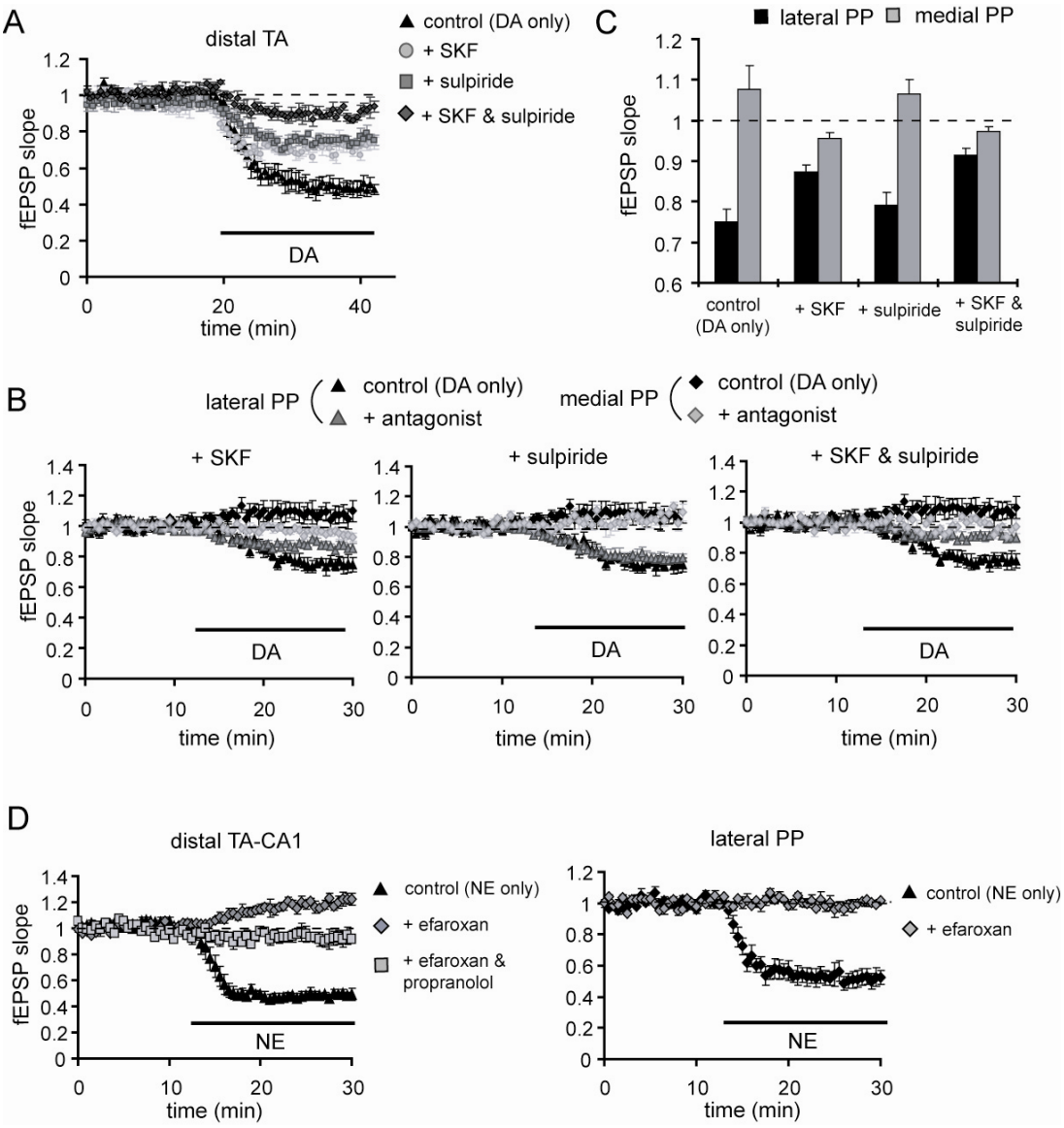

Figure 4-7: Receptor subtype contribution to DA or NE-mediated depression of LEC inputs

(A) Cooperative action of D1-like and D2-like receptors in DA-induced depression at distal TA-CA1 synapses. Either D1-like or D2-like receptor antagonists, SKF83566 (1 μM) or sulpiride (10 μM), partially blocked DA-induced depression (SKF 83566: 71 ± 6%, sulpiride: 76 ± 5%, mean percentage of baseline 10 – 25 minute after drug

application), and simultaneous application of both antagonists almost completely blocked DA's effects (91 ± 6%) (control: n = 8, SKF: n = 5, sulpiride: n = 5, SKF & sulpiride: n = 5). **(B)** D1-like and D2-like receptor contribution to DA's influence on synaptic transmission at the lateral and medial PP (control: n = 6: SKF: n = 6, sulpiride: n = 5, SKF & sulpiride: n = 4). **(C)** Analysis of dopamine receptor subtype contribution at lateral and medial PP synapses. The D1-like receptor antagonist, SKF83566, largely blocked DA's effects on PP (control: mPP: 108 ± 6%, lPP: 75 ± 3%; SKF83566: mPP: 96 ± 1%, lPP: 87 ± 1%; sulpiride, mPP: 106 ± 4%, lPP: 79 ± 3%). **(D)** Adrenergic receptor subtype contribution to NE-induced depression of distal TA-CA1 synapses. The alpha-2 adrenergic receptor antagonist, efaroxan (10 μM), converted NE-effects on synaptic transmission from depression to a slight enhancement (120 ± 3%, mean percentage of baseline 15 – 20 minute after drug application) (n = 6). This enhancement was completely blocked by the simultaneous application of beta adrenergic receptor antagonist, propronolol (20 μM) (92 ± 4%) (n = 4). **(E)** Adrenergic receptor subtype contribution to NE-induced depression of lateral PP. Simultaneous application of the alpha-2 adrenergic receptor antagonist, efaroxan, completely blocked the NE-induced depression (99 ± 2%) (n = 3).

4.3.5 Differential modulation of high-frequency signal transmission by DA or NE at distal TA-CA1 synapses

Signal transmission in neuronal networks is intrinsically nonlinear and strongly influenced by the frequency of the input signals (Markram et al., 1998). Dynamic changes in the amplitude, frequency and phase-coordination of oscillations *in vivo* appear to be functionally linked to animal behavior (Buzsaki and Draguhn, 2004), suggesting that oscillatory activities may participate in signal gating (Laurent, 2002; Ito and Schuman, 2008). We previously showed that DA significantly changes frequency-dependent signal transmission at distal TA-CA1 synapses, by enhancing high-frequency input signals but depressing low-frequency inputs (Ito and Schuman, 2007). Here, we examined how NE influences frequency-dependent signal transmission at these same synapses.

We applied 100 pulses of stimulation to the TA pathway at different ranges of stimulation frequency from 5 to 100 Hz (Figure 4-8A). As in our previous report (Ito and Schuman, 2007), we focused on the analysis of steady-state potentials, because transient potentials during the first few stimuli can be influenced by the pre-stimulus state of the neuronal network. When low-frequency (< 50 Hz) stimulation was applied, NE strongly depressed the steady-state potentials when compared to control. However, as the stimulation frequency increased, the difference between control and NE became smaller (Figure 4-8B), with no modulation observed at high frequencies (> 50 Hz). Although the depression of low-frequency signals by NE is similar to DA-induced modulation, a major difference appeared during high frequency stimulation: only DA enhanced

high-frequency signals.

Thus, although no difference between DA- and NE-mediated synaptic modulation was evident in our analysis of basal synaptic transmission (0.033 Hz) (Figure 4-8B), the frequency-response analysis revealed a clear difference in high-frequency signal modulation by DA and NE at distal TA-CA1 synapses.

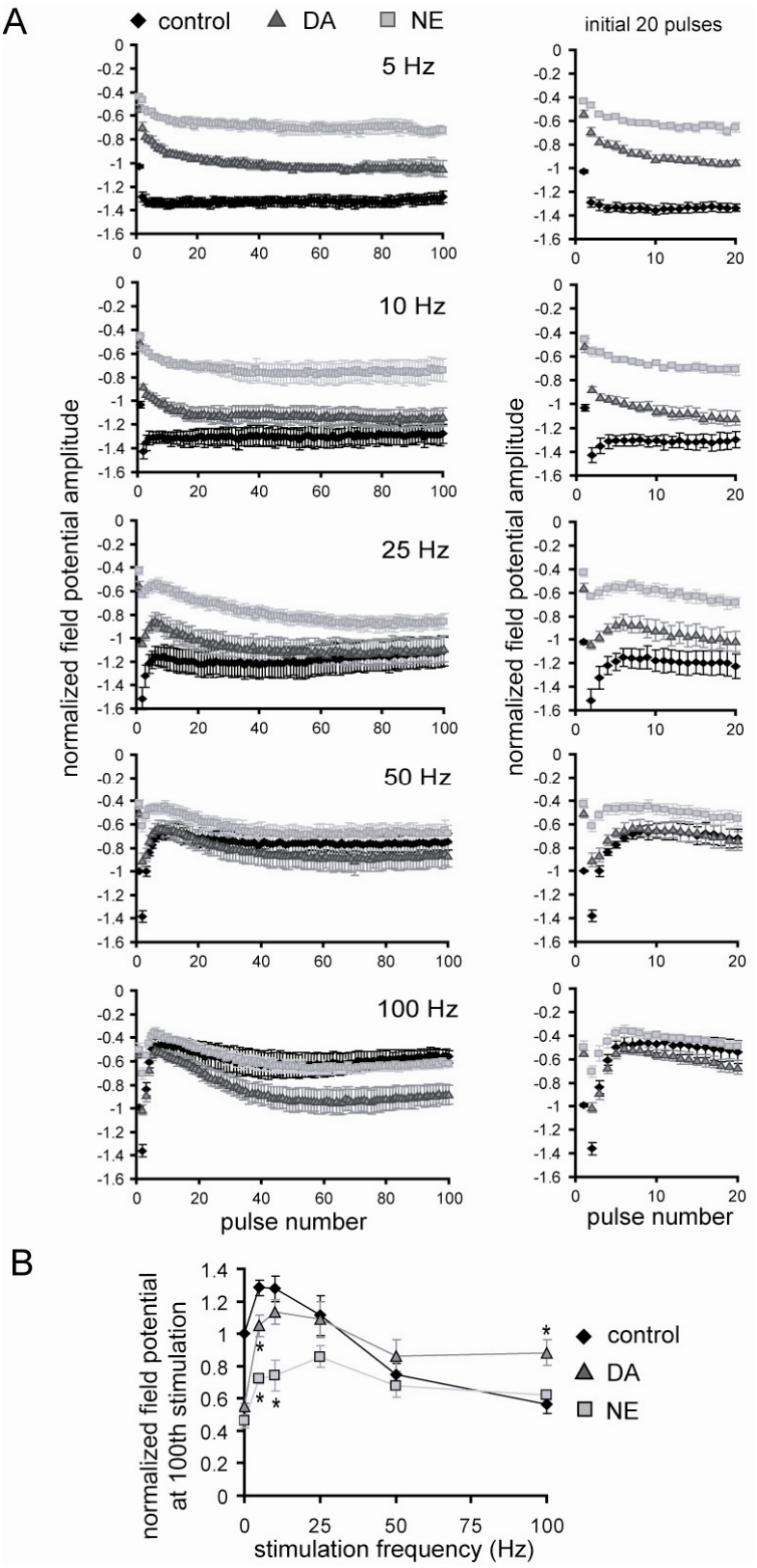
A
control
DA
NE
initial 20 pulses
5 Hz
10 Hz
25 Hz
50 Hz
100 Hz
normalized field potential amplitude
pulse number
B
normalized field potential at 100th stimulation
stimulation frequency (Hz)
control
DA
NE

Figure 4-8: Differences in DA or NE elicited frequency dependent modulation at distal TA-CA1 synapses

(A) Normalized peak field potentials (at each pulse of a 100 pulse stimulation epoch) at frequencies ranging from 5 to 100 Hz. All experiments were done at near physiological temperature (32 – 34 °C). Field potentials were normalized to the baseline fEPSP amplitude before neuromodulator application. (from 5 to 100 Hz, n = 6, 5, 6, 7, 8 for control; n = 7, 5, 5, 5, 8 for DA; n = 6, 4, 4, 4, 7 for NE). **(B)** Analysis of normalized peak field potentials at the 100th pulse. Both DA and NE depressed responses during low-frequency stimulation, but only DA enhanced responses during high-frequency stimulation, when compared to control.

4.3.6 Selective influence of DA or NE on LTP at proximal and distal TA-CA1 synapses

The above differences in frequency-response modulation between NE and DA may influence synaptic plasticity induction, due to the differential handling of high frequency signals like those commonly used to elicit long-term potentiation (LTP) (e.g., 100 Hz). We tested this idea by recording from distal TA-CA1 synapses (Figure 4-9). The application of high-frequency (100 Hz) stimulation induced LTP of a modest magnitude at these synapses (control: 112 ± 3%, mean percent of baseline 55 – 60 minute after LTP induction). On the other hand, slices exposed to DA exhibited LTP of a greater magnitude, as we previously reported (Ito and Schuman, 2007) (DA: 149 ± 4%; Figure 4-9 upper right). On the contrary, NE application did not enhance LTP magnitude, when compared to control (NE: 114 ± 3%; Figure 4-9 lower right). This is predicted by the differences in high-frequency signal modulation between DA and NE that we observed (Figure 4-9). We also tested whether neuromodulators influence LTP induction at proximal TA-CA1 synapses, but neither DA nor NE altered LTP magnitude at these synapses (control: 119 ± 3%, DA: 122 ± 3%, NE: 122 ± 3%; Figure 4-9 left). Thus neither DA nor NE influences basal synaptic transmission or plasticity at proximal TA-CA1 synapses. Whereas DA, but not NE, modulated synaptic plasticity at distal TA-CA1 synapses.

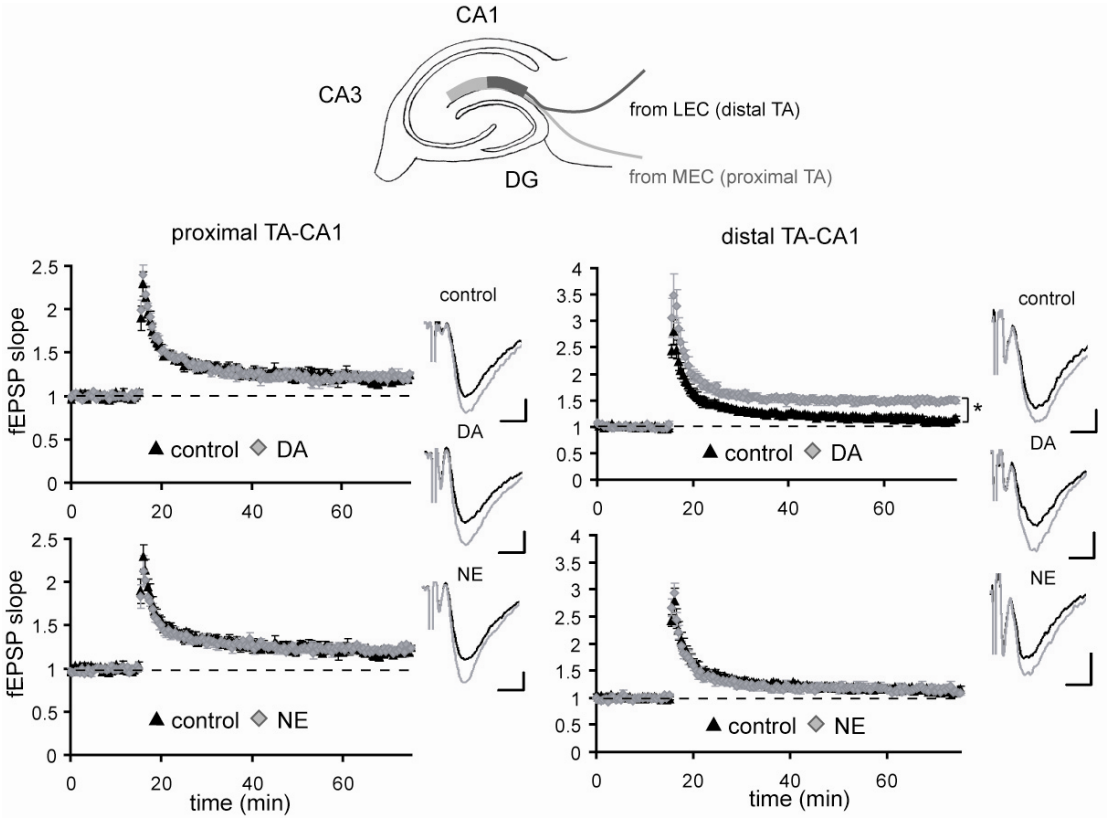

Figure 4-9: Differential influence of DA or NE on LTP induction at TA-CA1 synapses

LTP was induced at proximal (MEC) or distal (LEC) TA-CA1 synapses. Neuromodulators were present throughout the experiments. The LTP induction protocol was 100 pulses at 100 Hz, repeated twice at a 30 s interval (n = 5 for each experimental group). Field EPSP waveforms before (black) and after (gray) NE or DA application are shown (scale bar = 0.1 mV, 5 ms) (*$p < 0.05$).

4.3.7 Clozapine reduces novelty-induced differential activation of distal and proximal CA1

Our slice electrophysiology results suggest that neuromodulators primarily modulate synaptic transmission at distal TA-CA1 synapses, raising the possibility that the novelty-induced enhancement of c-fos transcription is mediated by this influence. Thus, we asked whether an antagonist of neuromodulators influences the differential c-Fos expression along the transverse-axis of area CA1 observed in our behavioral experiments (Figure 4-1). To test this, we examined c-Fos expression in animals treated with a broad spectrum receptor antagonist that blocks both DA and NE-mediated signaling, clozapine (Stahl, 2008), prior to novelty exposure. We housed pairs of animals in the same cage for a baseline period of several days. Then, either saline or clozapine (10 mg/kg) was injected intraperitoneally in each animal. After 4 hrs, novel objects were placed in the home cage (novel object exposure), or both animals were transferred to a new cage (novel place exposure). We found that clozapine-treatment caused a significant reduction in the global c-Fos expression in the hippocampus (Supplementary Figure 4-1C and 4-1D), consistent with previous studies suggesting that DA plays an important role in novelty-induced hippocampal activation (Lisman and Grace, 2005; Li et al., 2003; Adcock et al., 2006). But more importantly, clozapine-treatment appeared to have differential effects on c-Fos expression depending on whether the animals were exposed to novel objects or a novel place. At distal CA1, c-Fos expression after the novel object exposure was significantly reduced by clozapine-treatment, however, c-Fos expression after novel place exposure did not show a significant decrease in clozapine-treated

animals (Figure 4-10B and 4-10C). The strong clozapine sensitivity of c-Fos expression at distal CA1 synapses suggests that neuromodulators are important in signifying the novelty of nonspatial information processing in the hippocampus. Furthermore, because clozapine largely abolished the difference in c-Fos expression between proximal and distal CA1, neuromodulators are likely to play a key role in the differential activation of pyramidal neurons along the transverse-axis of area CA1.

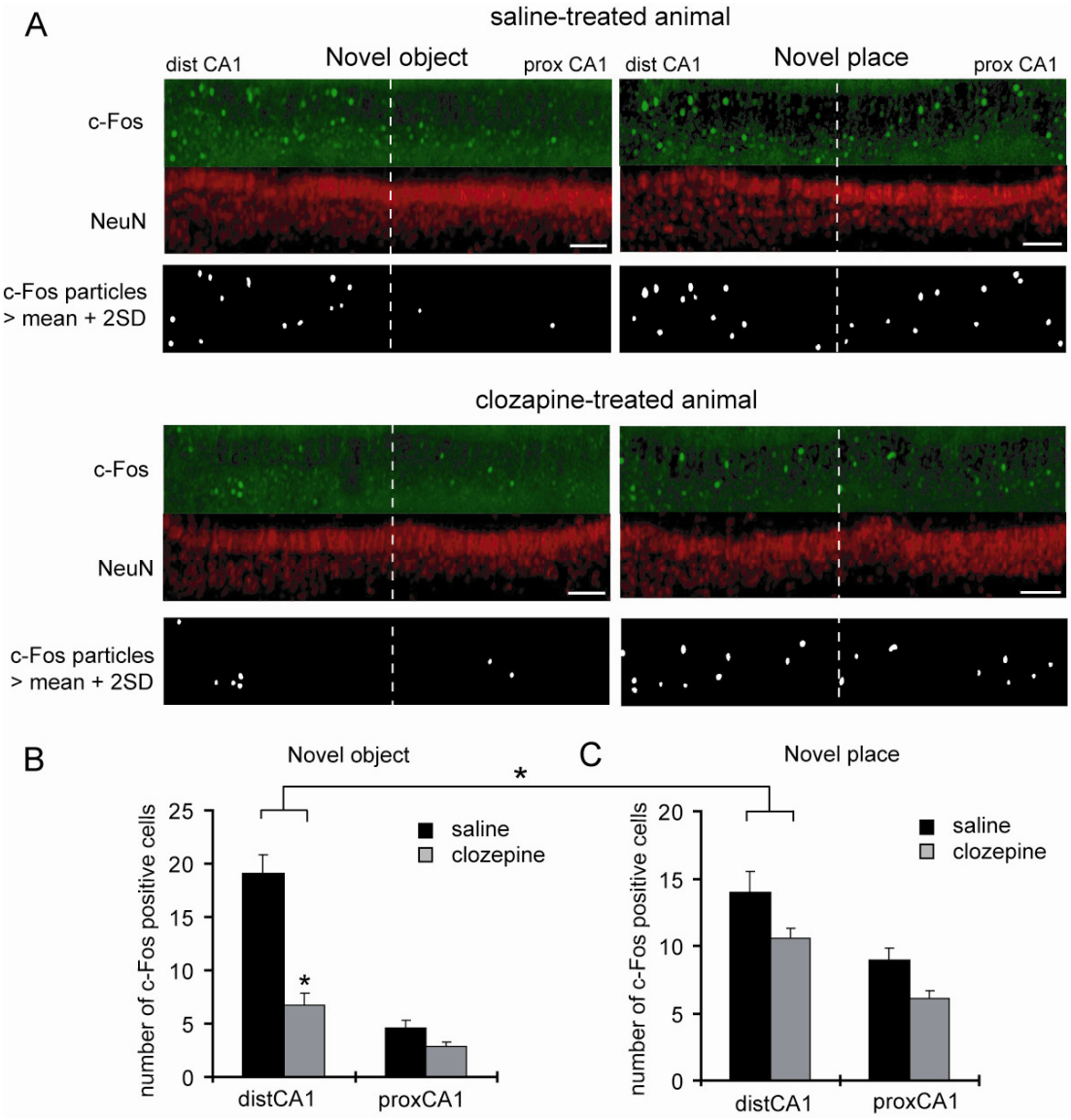

Figure 4-10: A dopamine receptor antagonist prevents the enhanced c-fos immunostaining observed at distal CA1 following novel object exposure

(A) Pairs of animals were housed in the same home cage for at least 2 days. Then, either saline or clozapine (10 mg/kg) was intraperitoneally injected in each animal. After 4 hours, both animals were exposed to either novel objects or novel place, as described in the figure 4-1 legend. After 2 hrs, slices were prepared and stained as previously

described. Images shown are from the pyramidal layer of area CA1 of saline-treated and clozapine-treated animals (scale bar = 100 μm). **(B)** The number of c-Fos positive cells after novel object exposure was analyzed in area CA1 as described in Figure 4-1. The total integrated NeuN signals in same areas used for c-Fos expression analysis did not differ between groups (Supplementary Figure 4-2B). The number of c-Fos positive cells at distal CA1 was significantly reduced by clozapine-treatment (*$p < 0.05$). **(C)** The number of c-Fos positive cells after novel place exposure was analyzed in area CA1. The total integrated NeuN signals in same areas used for c-Fos expression analysis did not differ between groups (Supplementary Figure 4-2B). The number of c-Fos positive cells at distal CA1 did not show a significant decrease by clozapine-treatment. For the comparison of c-Fos expression in distal CA1 after novel object and place exposure, a two-way ANOVA was performed with the two variables, novelty type (object vs. place) and drug treatment (saline vs. clozapine), showing a significant interaction ($p = 0.0015$).

4.4 DISCUSSION

4.4.1 Roles of the TA pathway

The hippocampal area CA1 receives two distinct excitatory inputs either from area CA3 (the SC pathway) or from the EC (the TA pathway). For many years the TA input was dwarfed by studies of the SC input, but many recent studies highlight the significance of this input. For example, the stimulation of the TA pathway influences spike probability or synaptic plasticity induced by SC stimulation (Levy et al., 1998; Dvorak-Carbone and Schuman, 1999b; Remondes and Schuman, 2002). As such, precisely-timed TA inputs relative to SC inputs cause nonlinear signal amplification in dendrites, influencing dendritic signal propagation and synaptic plasticity (Jarsky et al., 2005; Ang et al., 2005; Dudman et al., 2007).

Furthermore in behaving animals, the TA pathway appears to play a major role in particular hippocampal functions. For example, following lesions of SC inputs, animals still maintain spatial recognition memory and CA1 neurons still show location-specific activities (Brun et al., 2002). In addition, the TA pathway is essential for memory consolidation (Remondes and Schuman, 2004). On the other hand, the SC pathway is likely to be necessary for remote navigation memory or one-time contextual learning (Nakashiba et al., 2008; Brun et al., 2008). Thus, each pathway may play a distinct role in animal behavior and learning.

Since the TA pathway itself can maintain spatial recognition memory, the interaction between the EC and area CA1 may be sufficient to carry out certain

hippocampal functions. In support of this idea, reciprocal anatomical interactions between the EC and area CA1 have been described (Tamamaki and Nojyo, 1995; Amaral and Lavenex, 2007). Neurons in proximal CA1, which receive MEC inputs via the TA pathway, send their projections back primarily to the MEC; on the other hand, neurons in distal CA1, which receive LEC inputs, project their efferents back to the LEC. Thus, two distinct information trajectories exist between the EC and area CA1 when we consider the TA pathway; i.e., MEC – proximal CA1 – MEC, and LEC – distal CA1 – LEC. These functional loops could support the independent processing of spatial and nonspatial information. In contrast, granule cells in the DG or CA3 pyramidal neurons integrate both LEC and MEC inputs in their dendrites because of the laminar projection of the perforant pathway. Thus, the EC–CA1 loop circuit allows for the differential handling of nonspatial and spatial information in the hippocampus, which is in clear contrast to the trisynaptic circuit (Andersen et al., 1971) (i.e., EC – DG – CA3 – CA1).

Indeed, many studies have indicated distinct neuronal activities between area CA3 and CA1, which cannot not simply be explained by one-way feed-forward synaptic connections. For example, location-specific activities in area CA3 and CA1 neurons are differentially modulated by spatial geometry changes (Guzowski et al., 2004). Furthermore, Vinogradova and her colleagues described different responses to repeated sensory stimuli between neurons in area CA3 and CA1 (Vinogradova, 2001).We observed differences in c-Fos expression between proximal and distal CA1 depending on whether animals are exposed to novel object or place (Figure 4-1). Thus, both anatomical studies and our results indicate an important role of the TA pathway in distinct information

transfer to distal and proximal CA1, allowing for differential handling of spatial and nonspatial information in the hippocampus.

4.4.2 Neuromodulators in the hippocampus

A number of studies have indicated key roles for neuromodulators in hippocampal function (Lisman and Grace, 2005; Harley, 2004; Hasselmo, 1995). How neuromodulators exactly influence information processing is, however, unclear. The activities of many neuromodulator releasing neurons change when behaviorally relevant events occur (Schultz, 1998; Vankov et al., 1995; Aston-Jones and Cohen, 2005; Acquas et al., 1996). Because of the broadcast nature of their fibers, neuromodulators have the capacity to control many brain areas and synapses simultaneously. Many studies in slices have focused on long-term synaptic modifications elicited by neuromodulators (Dahl and Sarvey, 1989; Huang and Kandel, 1995; Otmakhova and Lisman, 1996; Katsuki et al., 1997), without considering the potential short-term dynamic control of synaptic efficacy. We examined the short-term influence of the neuromodulators, DA and NE, on the entorhinal-hippocampal connections, and found that both DA and NE differentially and reversibly influenced inputs from the MEC and LEC in both the TA and perforant pathways.

In area CA1, neuromodulators primarily act on distal TA-CA1 synapses, which are the synapses made with LEC inputs. We previously showed that DA induces the disinhibition in area CA1 via reducing TA-pathway-mediated excitation of interneurons, resulting in a frequency-dependent signal modulation and the enhancement of LTP at

both TA- and SC-CA1 synapses (Ito and Schuman, 2007). The TA pathway stimulation is known to evoke strong inhibitory responses in CA1 pyramidal neurons in slices (Dvorak-Carbone and Schuman, 1999b; Empson et al., 1995), thus disinhibition in this pathway will have a great impact on area CA1 output.

The entorhinal cortex, the origin of the TA pathway, is a major source of theta (4-12 Hz) and gamma (40-100 Hz) oscillatory activities (Chrobak et al., 2000), thus the frequency-dependent effects we observed will modulate information flow in the circuit. We demonstrated the differential modulation of frequency-dependent signal transmission between DA and NE at distal TA-CA1 synapses. Although both DA and NE similarly depressed low frequency signals, only DA enhanced high-frequency signal transmission when compared to control. We speculate this difference is due to the enhancement of spontaneous inhibition in area CA1 by NE (Bergles et al., 1996). Thus, DA and NE may differentially gate a high-frequency range of oscillatory activities (e.g., gamma oscillations) *in vivo*.

In our c-Fos expression analysis, we demonstrated the differential activation of distal and proximal CA1 depending on whether animals need to process primarily nonspatial or spatial information (Figure 4-1). We further observed a differential clozapine-sensitivity of c-Fos activation at distal CA1 synapses, depending on whether animals are exposed to novel objects or a novel place (Figure 4-10). These data suggest that the hippocampus may utilize distinct encoding modes for nonspatial and spatial information. The main sites of clozapine's action are not clear since it was administered systemically. We did not observe, however, any apparent differences in

clozapine-sensitivity in proximal CA1 or area CA3 under novel object and place exposure (Supplementary Figure 4-1C and 4-1D). Because DA primarily influences distal TA-CA1 synapses in area CA1 these data are consistent with the idea that DA may allow differential encoding of nonspatial information in the hippocampus via selectively controlling LEC inputs.

The hippocampus and its associated medial temporal lobe structures are though to represent information about the environmental context (Myers and Gluck, 1994; Clark and Martin, 2005; Smith and Mizumori, 2006). To acquire such a representation, individual sensory inputs must be associated with the spatial geometry of the environment. Our data demonstrate that neuromodulators differentially control spatial and nonspatial information flow in entorhinal-hippocampal connections. This differential modulation reveals a clear functional division along the transverse-axis of area CA1, emphasizing the importance of the EC-CA1 circuit. Our results further imply that the neuromodulators may allow the hippocampus to utilize different encoding modes for nonspatial and spatial information.

4.5 MATERIALS AND METHODS

4.5.1 Hippocampal slice preparation

Slices were prepared from 21 – 30 day-old Sprague-Dawley rats (Charles River), as described previously (Remondes and Schuman, 2002). In brief, a vibrating microtome (Leica VT1000S) was used to cut hippocampal slices (500 μm thickness for extracellular recordings and 300 μm for whole-cell recordings) in ice-cold oxygenated artificial cerebrospinal fluid (ACSF) containing (in mM) 119 NaCl, 2.5 KCl, 1.3 $MgSO_4$, 2.5 CaCl, 1.0 NaH_2PO_4, 26.2 $NaHCO_3$, 11.0 glucose. Slices were recovered at room temperature for at least 2 hour in an interface chamber, and then transferred to a submerged recording chamber perfused with ACSF at 24.5 – 25.5 °C or 32 – 34 °C (for frequency-dependent analysis). For TA pathway recordings, the DG and CA3 were removed to eliminate the possible activation of the trisynaptic pathway or perforant path projection to area CA3. Concentric bipolar tungsten electrodes (FHC) and stimulus isolators (Axon Instruments) were used for the stimulation.

4.5.2 Electrophysiology

Extracellular field potential recordings were made with 1 – 3 MΩ resistance microelectrodes filled with 3 M NaCl using a bridge amplifier (Axoclamp 2B, Molecular Devices). Whole-cell voltage-clamp recordings from CA1 pyramidal neurons or DG granule cells were obtained without visualization with an Axopatch 200B (Molecular Devices). Internal solution of whole-cell patch pipettes was (in mM) 115 cesium

gluconate, 20 KCl, 10 sodium phosphocreatine, 10 HEPES, 0.2 EGTA, 2 MgATP, 0.3 NaGTP (pH 7.3). In addition, to minimize the possible postsynaptic current modulation by DA or NE, pipette solutions contained (in mM) 5 QX314, 10 TEA, 1 4AP. Membrane voltage was clamped at -60 mV (without liquid junction potential correction). Membrane capacitance was cancelled and series resistance was compensated (60 – 70%). Recordings were discarded when the series resistance was over 20 MΩ or either series or membrane resistance changed more than 30% during data acquisition. For the analysis of frequency-dependent signal modulation, 100 pulses were applied at the indicated frequencies after baseline responses were stable for at least 10 min. The LTP induction protocol was 100 pulses at 100 Hz, repeated twice with a 30 sec interval. All stimulus pulses were of the same length and amplitude as test pulses. Test pulses were applied once every 30 sec for extracellular field recordings and every 10 sec for whole cell recordings. Drugs were applied by dilution of concentrated stock solutions into the perfusion medium. The final concentration of bath-applied DA or NE was 20 μM or 10 μM, respectively. Dopamine and norepinephrine were obtained from Sigma. All other drugs were obtained from Tocris.

4.5.3. Behavioral analysis

Animals used for behavioral analysis were male Sprague-Dawley rats, 24 – 30 day-old. All the behavioral manipulations were carried out at night (0 – 4 am) to maximize active exploration of the environment. The objects used for novel object exposure were three small children's toys, made of either plastic or wood. The new home

cage for novel place exposure was in the same color and shape as the original cage, but had new woodchip flooring and did not have a food box on the ceiling. In dopamine-antagonist experiments, 250 μL of saline or clozapine (10 mg/kg, diluted in saline) was injected intraperitoneally in animals. Clozapine blocks every subtype of dopamine receptors, but also has a small antagonistic effect on serotonin receptors and alpha-2 adrenergic receptors (Stahl, 2008).

4.5.4 Data analysis

Electrophysiology:

Data were collected using a custom-written program (LabView data acquisition system; National Instruments) for extracellular recordings, or DigiData 1200 and pClamp 9 (Molecular Devices) for whole-cell recordings. All numerical values listed represent mean ± s.e.m. For synaptic plasticity experiments, the baseline fEPSP was normalized to the depressed state. For analysis of the waveforms during 100 pulse stimulation, stimulation artifacts and fiber volleys were excluded and the gaps were linearly connected, and the last excitatory potential or current (100th stimulus response) was measured by a custom program in Matlab (MathWorks). Student's t-test was performed to analyze the signficance of the data.

Immunohistochemistry:

Slices (500 μm thickness) were prepared using the same procedure as for

electrophysiology recordings. After cutting, slices were quickly fixed in 4% paraformaldehyde in phosphate-buffered saline (PBS) for at least 2 days. Thin (50 μm) sections were cut with a vibrating microtome (Leica VT1000S).

The sections were incubated overnight with either of 1:250 concentration of anti-c-Fos (sc-52) (Santa Cruz), 1:1000 of anti-NeuN (Millipore), 1:1000 of anti-Synapsin I (Millipore), 1:1000 of anti-Bassoon (Stressgen), 1:1000 of anti-Synaptophysin (Millipore) or 1:100 of anti-GluR2/3 (Millipore) antibodies. The incubation was carried out at room temperature in Tris-buffered saline containing 0.2% Triton X-100, BSA 2%, NGS 4%, followed by 4 hrs of secondary-antibody incubation with 1:1000 of Alexa 488-conjugated anti-rabbit and 1:1000 of Alexa 543-conjugated anti-mouse antibodies (Invitrogen).

For the analysis of immunohistochemistry experiments, images were obtained with Zeiss LSM 510 laser scanning confocal microscopes using a Plan-Neofluor 10×/0.3 air objective. Alexa 488 and 546 were visualized by excitation with the 488 line of an argon ion laser and the 543 nm line of a HeNe laser, respectively. The optical section was 20 μm and fluorescent signals were acquired throughout the slice thickness (50 μm). Each 50 μm slice was obtained from a different 500 μm section and two slices were analyzed from each animal. Slices were obtained from the same septo-temporal position in all experiments. To count the number of c-Fos positive neurons, fluorescent signals less than the mean + 2SD were excluded and, if necessary, an additional thresholding was applied to reduce background signals in dendritic areas. Then, automated particle analysis was carried out using ImageJ (NIH) based on that the following criteria: the particle size

was larger than 56 μm^2 and the circularity was larger than 0.5. For the analysis of dentate granule cells, particle sizes larger than 39 μm^2, instead 56 μm^2, were used due to the smaller size of granule cells. Statistical differences between animals groups were assessed by ANOVA. Regional differences in supplementary figure 4-1C and 4-1D were statistically analyzed by a Student's t-test.

4.6 SUPPLEMENTARY FIGURES

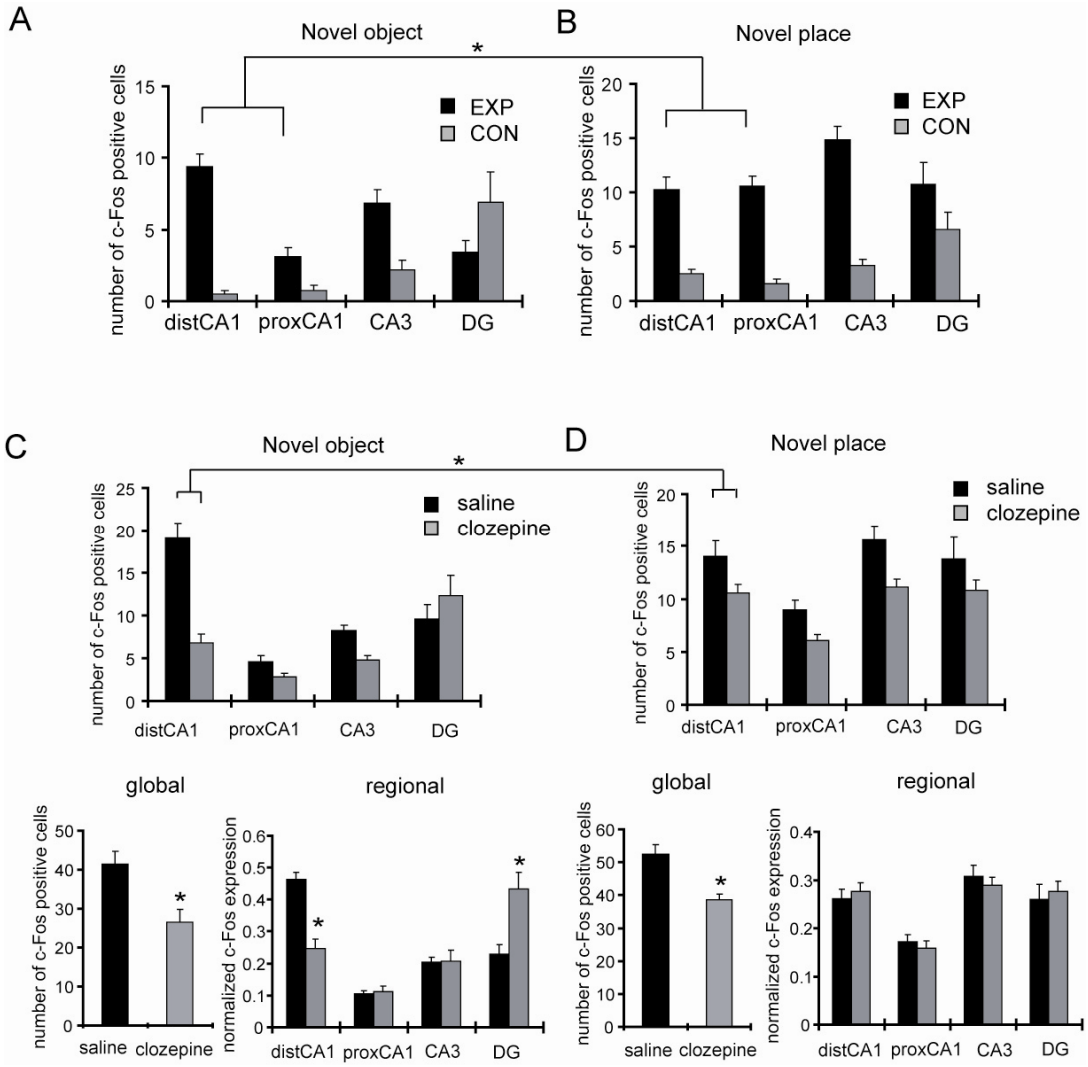

Supplementary Figure 4-1: Analysis of c-Fos expression in each area of the hippocampus after novelty exposure

(A) The number of c-Fos positive cells after novel object exposure was analyzed in the pyramidal layers of area CA1 and CA3 and the granular layer of the DG in the slices (50 μm thickness) used in figure 4-1A (n = 6 pairs of animals). The total integrated NeuN

signal in same areas used for c-Fos expression analysis did not differ between groups (Supplementary Figure 4-2A). **(B)** The number of c-Fos positive cells after novel place exposure was analyzed in the pyramidal layers of area CA1 and CA3 and the granular layer of the DG in the slices (50 μm thickness) used in figure 4-1B (n = 6 pairs of animals). Total integrated NeuN signals in same areas used for c-Fos expression analysis did not differ between groups (Supplementary Figure 4-2A). For the analysis of novelty-induced c-Fos expression, a two-way ANOVA was performed with 2 variables: novelty type (object vs. place) and CA1 subregion (distal vs. proximal), and revealed a significant interaction ($p = 0.0008$). **(C)** The number of c-Fos positive cells after novel object exposure was analyzed in each area of the hippocampus on the slices used in figure 4-10A. In the bottom graphs, c-Fos expression was separately analyzed for global and regional expression. In the global c-Fos expression analysis, the total number of c-Fos positive cells in the hippocampus (CA1, CA3, DG) was analyzed. In the regional expression analysis, the number of c-Fos positive cells in each area was normalized to the total number of c-Fos positive cells in the hippocampus, thus, it represents a relative ratio of c-Fos expression in each area of the hippocampus. The total integrated NeuN signals in same areas used for c-Fos expression analysis did not differ between groups (Supplementary Figure 4-2B). Student's t-test was performed to analyze the significance of global and regional expression differences ($*p < 0.05$). **(D)** The number of c-Fos positive cells after novel place exposure was analyzed in each area of the hippocampus as described in **C**. The total integrated NeuN signals in same areas used for c-Fos expression analysis did not differ between groups (Supplementary Figure 4-2B). For the analysis of

c-Fos expression in distal CA1, a two-way ANOVA was performed with the two variables, novelty type (object vs. place) and drug treatment (saline vs. clozapine), showing a significant interaction ($p = 0.0015$).

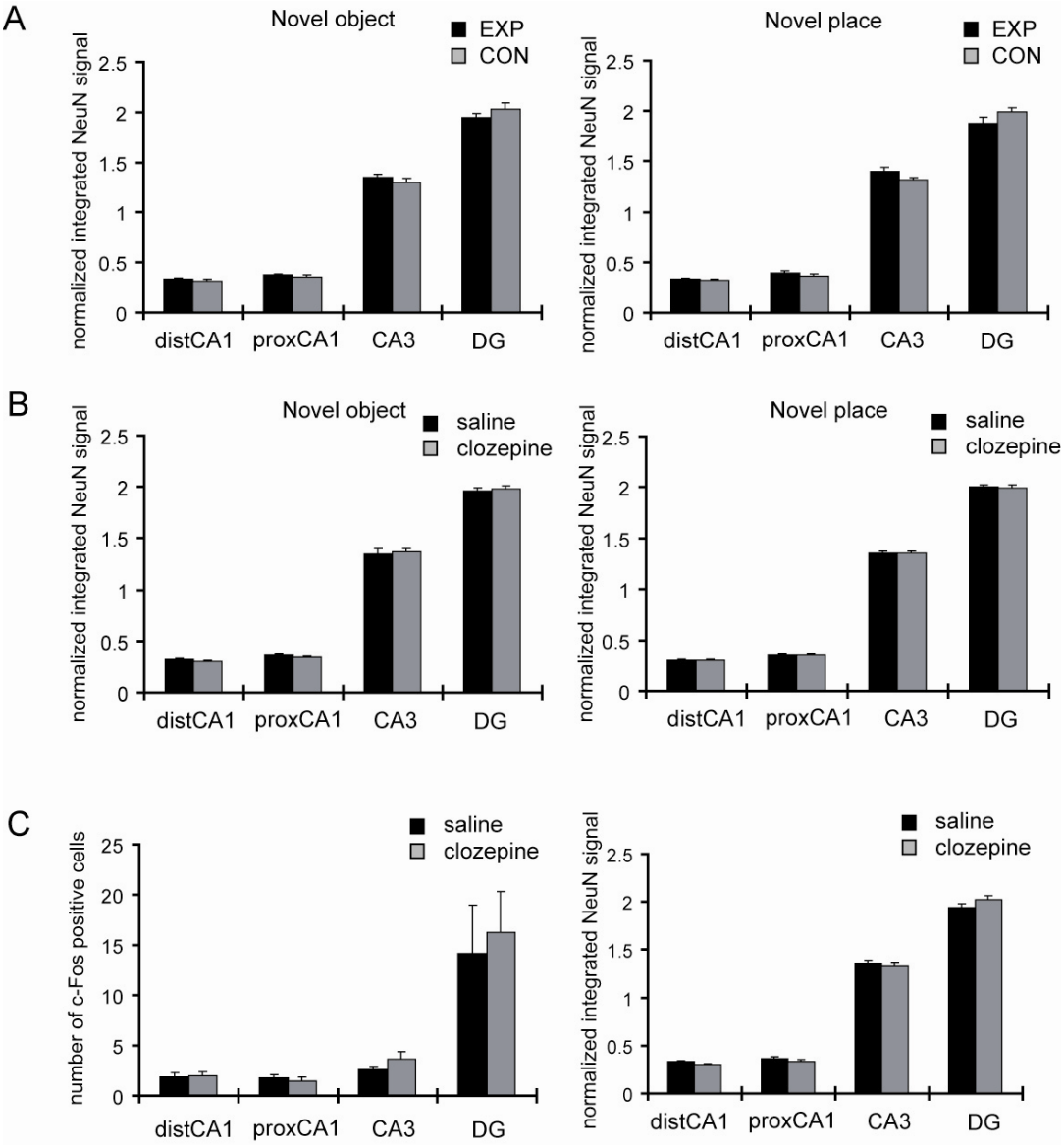

Supplementary Figure 4-2: Control analysis for c-Fos expression experiments

(A) No significant differences were observed in the integrated NeuN signals analyzed same areas as used for c-Fos expression analysis in Figure 4-1. **(B)** No significant differences were observed in integrated NeuN signals in the same areas as used for c-Fos expression analysis in Figure 4-10. **(C)** As a control experiment for the data shown in Figure 4-10, a pair of animals was housed in the same cage for at least 2 days, and then,

either saline or clozapine (10 mg/kg) was intraperitoneally injected in each animal. 6 hrs after the injection (no novelty exposure), animals were sacrificed and immunohistchemistry was performed on fixed slices. Intraperitoneal injection itself did not show any significant enhancement of c-Fos expression in CA1 or CA3 pyramidal neurons. There was no significant difference between saline and clozapine treated animals (n = 4 pairs of animals). The total integrated NeuN signals in the same areas used for c-Fos expression analysis did not differ between groups.

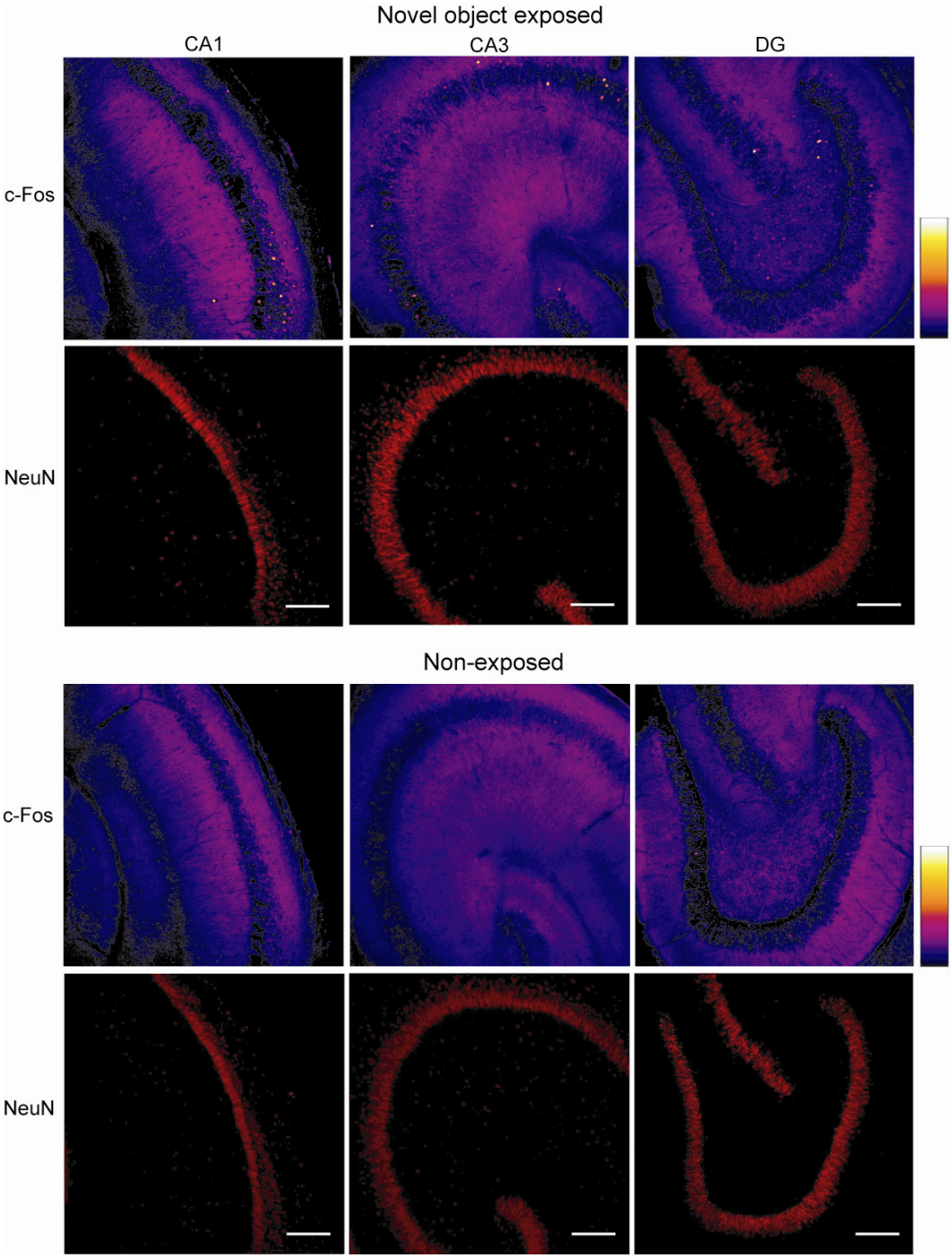

Supplementary Figure 4-3: Slice images of c-Fos and NeuN immunostaining after novel object exposure in each area of the hippocampus

Scale bar = 200 μm

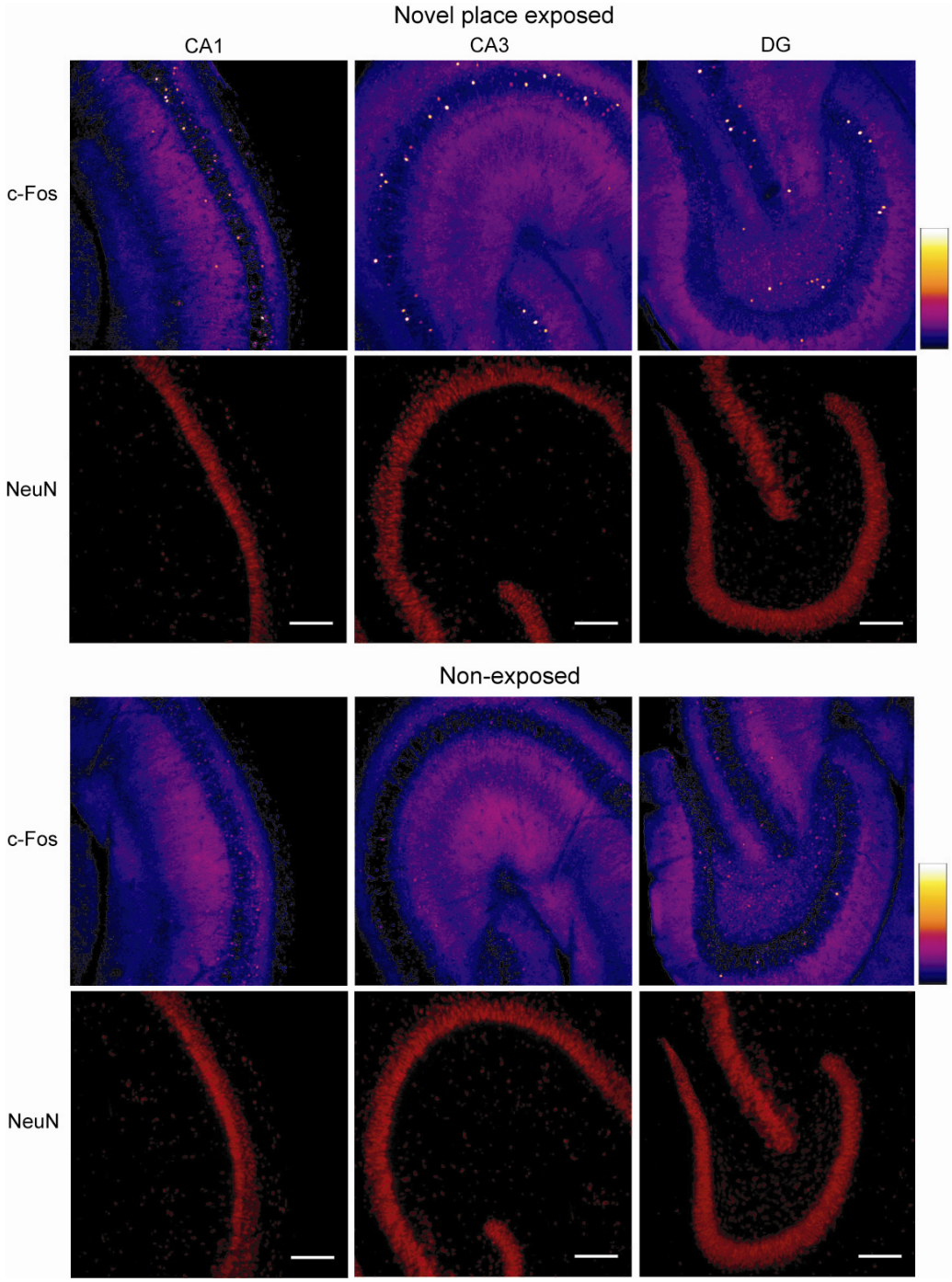

Supplementary Figure 4-4: Slice images of c-Fos and NeuN immunostaining after novel place exposure in each area of the hippocampus

Scale bar = 200 μm

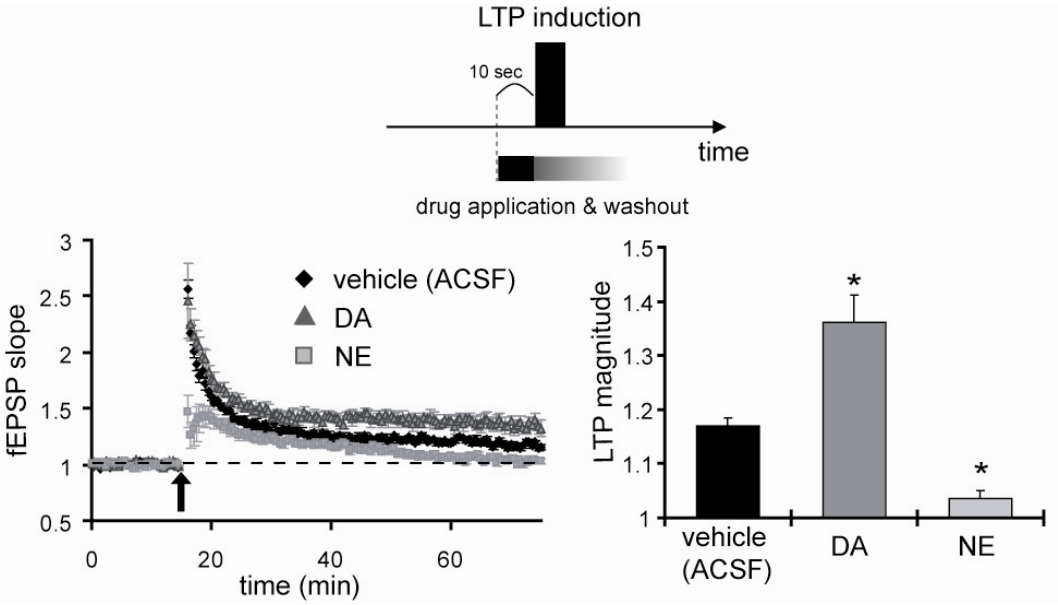

Supplementary Figure 4-5: Acute application of neuromodulators prior to LTP induction

A neuromodulator, DA or NE, was directly applied to the recording chamber 10 sec before LTP induction. The LTP induction protocol was 100 pulses at 100 Hz, repeated twice at a 30 sec interval. Estimated washout time of neuromodulators was about 2 – 3 min. DA and NE differentially modulated the magnitude of LTP at distal TA-CA1 synapses (control: 117 ± 1%, DA: 136 ± 5%, NE: 104 ± 1%, mean percentage of baseline 55 – 60 minute after LTP induction). (n = 7, 6, 6 for each). This is probably due to a reversible baseline shift by acute NE application, and LTP was induced from a depressed baseline level. Then, even if NE's action on LTP induction itself does not differ from control condition (Figure 4-9), the total proportion of LTP-induced synapses will be smaller (*$p < 0.05$ relative to ACSF application).

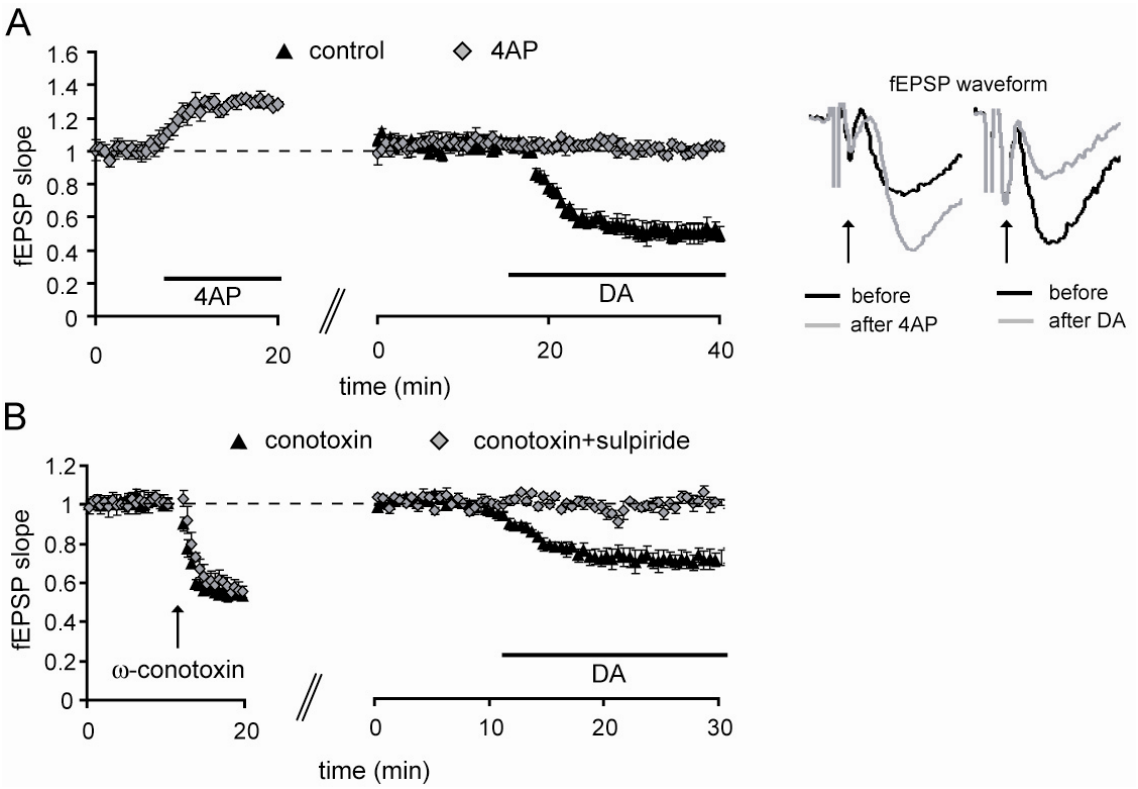

Supplementary Figure 4-6: Presynaptic N-type calcium channel modulation by DA at distal TA-CA1 synapses

(A) Extracellular application of 4-amiopyridine (4AP: 100 μM) completely blocked DA-induced depression at distal TA–CA1 synapses (n = 4). 4AP application itself enhanced fEPSP slope and also changed fEPSP waveform. Note that the fiber volley in fEPSP waveform indicated by arrow became wider after 4AP application. However, DA application did not change a fiber volley waveform, suggesting that the site of DA's action is different from 4AP affecting sites. Instead, 4AP may mask the DA's effect on N-type calcium channels as previously described (Wheeler et al., 1996). **(B)** N-type calcium channel dependent action of D1-like receptors at distal TA–CA1 synapses. Field

EPSP at distal TA–CA1 synapses was significantly depressed after N-type calcium channel blocker, ω-conotoxin GVIA (2.5 μM), application, which was directly applied to the recording chamber. After N-type calcium channel blockade, DA-induced partial depression at TA–CA1 synapses was completely blocked by a D2-like receptor antagonist, sulpiride (n = 4). Disappearance of D1-like receptor effects after N-type calcium channel blockade suggests that N-type calcium channel is likely to be a main target of D1-like receptors at distal TA-CA1 synapses.

Chapter 5. Maternal Immune Activation Alters Hippocampal Information Processing in Adult Offspring

5.1 SUMMARY

The observation that maternal infection increases the risk for schizophrenia in the offspring suggests that the maternal immune system may play a key role in the pathogenesis of schizophrenia. We generated a mouse model of maternal immune system activation at mid-gestation by injecting the dsRNA viral mimic, poly(I:C). The adult offspring of poly(I:C)-treated mothers display behavioral abnormalities in open field exploration, prepulse inhibition and latent inhibition, which are relevant to schizophrenia. As abnormalities in the hippocampal network are a consistent observation in schizophrenia patients, we examined the synaptic properties in hippocampal slices prepared from the off-spring of poly(I:C) treated mothers. Electrophysiological recordings from these slices displayed a reduced frequency and increased amplitude of miniature excitatory postsynaptic currents (mEPSCs) in CA1 pyramidal neurons. We did not find a significant difference in paired-pulse facilitation or LTP at Schaffer collateral–CA1 synapses. However, temporoammonic–CA1 synapses, which mediate object-related information, displayed a significantly increased sensitivity to dopamine (DA) applied to acute slices. To assess hippocampal network function *in vivo*, we used expression of the immediate early gene, c-Fos, as a surrogate measure of neuronal activity. Compared to controls, the offspring of poly(I:C)-treated mothers display a distinct c-Fos expression pattern in area CA1 following novel object exposure. Because DA

differentially influences object and spatial information processing in the hippocampus, our findings indicate that the offspring of immune-activated mothers may have an abnormality in modality-specific information processing. Indeed, preliminary data indicate that the offspring of poly(I:C)-treated mothers display enhanced novelty discrimination in an object switching, but not in a location switching task. Thus, analysis of object and spatial information processing at both synaptic and behavioral levels reveals a largely selective abnormality in object information processing in this mouse model. Our results imply that the altered processing of object-related information may underlie the pathogenesis of some schizophrenia-like cognitive behaviors.

5.2 INTRODUCTION

Schizophrenia is a major psychiatric disorder affecting approximately 1% of the population in the world. The symptoms of schizophrenia, initially described by Kraepelin and Bleuler, are generally categorized as either positive or negative (Cohen, 2003). Positive symptoms include hallucinations and delusions, and negative symptoms include reduction in emotional expression, normal thoughts, speech, and the desire for social and familial connections.

The pathogenesis of this disorder is still unclear. Although many potential genetic factors have been described (Burmeister et al., 2003; Bertolino and Blasi, 2009), epidemiologic evidence indicates that genetic factors alone cannot explain the pathogenesis. For example, the concordance for schizophrenia in monozygotic twins is approximately 48% (Gottesman, 1991). Furthermore, among monozygotic twins who do

not share placenta, the concordance rate drops to 10%, in contrast to 60% concordance when they share a placenta (Davis et al., 1995). These studies suggest the importance of the fetal environment. Supporting this idea, Mednick et al. (1988) reported that fetuses exposed to a viral epidemic during the second trimester of fetal development are at elevated risk for developing schizophrenia. Subsequent analyses have shown that maternal infections of various types increase the risk for schizophrenia in the offspring 3–7 fold (Patterson, 2007, 2008; Penner and Brown, 2007).

Based on this evidence, several animal models of maternal immune activation have been established (Borrell et al, 2002; Shi et al., 2003; Patterson, 2008). Among them, exposure to the synthetic dsRNA, poly(I:C), can effectively induce maternal immune activation, resulting in altered behaviors in adult offspring, including prepulse inhibition, social interaction, latent inhibition, working memory, novel object exploration, and amphetamine-induced locomotion, all of which are relevant to schizophrenia patients (Patterson, 2008). Thus, these animal models are useful for investigating the pathophysiology of schizophrenia-like behaviors.

Clinical studies reveal an important role for dopamine (DA)-mediated signaling in the pathophysiology of schizophrenia. For example, drugs that increase DA release in the brain induce several aspects of schizophrenic psychosis in normal adults, and exacerbate psychotic symptoms in patients with schizophrenia (Lieberman et al., 1987; Angrist and Vankammen, 1984). Moreover, all drugs currently in use for the treatment of schizophrenia block D2 DA receptors (Creese et al., 1976). This evidences led to the hypothesis that schizophrenia is due to a hyperdopaminergic state. This DA hypothesis is,

however, primarily based on the observation of positive symptoms. The drugs primarily acting on DA D2 receptors are ineffective in treating the negative symptoms of schizophrenia. To explain the negative symptoms of schizophrenia, a deficit in dopamine D1 receptor-mediated transmission in prefrontal areas has been suggested (Davis et al, 1991; Toda and Abi-Dargham, 2007). Indeed, imaging studies of schizophrenic patients reveal an increased D2 receptor density in the striatum (Weinberger and Laruelle, 2001) and a decreased D1 receptor density in the prefrontal cortex (Okubo et al., 1997).

Deficits in other cortical regions may also play a key role in the pathophysiology of schizophrenia. Among them, hippocampal abnormalities are commonly found (Heckers and Konradi, 2002). Adult patients with hippocampal damage do not, however, necessarily display schizophrenia-like behaviors, even though they show deficits in learning and memory (Scoville and Milner, 1957; Squire et al., 2004). Lipska et al. (1993) suggested that the important variable is the developmental period in which the hippocampal pathology takes place. Thus, lesions of the rat hippocampus performed in adult animals fail to produce schizophrenia-like alterations, while hippocampal disruption in neonatal stages causes these behavioral alterations to emerge in adulthood (Lispka et al., 1993; Grace, 2000). Furthermore, recent studies show a reciprocal functional interaction between the DA system and the hippocampus (Lisman and Grace, 2005). Together, these studies indicate that hippocampal dysfunction participate in the pathogenesis of schizophrenia.

Considering these findings, we used the maternal immune activation animal model to investigate the pathogenesis of schizophrenia-like behaviors. We focused on the

hippocampal network, conducting experiments at the synaptic-level in acute slices, as well as behavioral level using c-Fos expression as a surrogate for *in vivo* hippocampal activity. We investigated a functional link between synaptic dysfunction and altered behavior.

5.3 RESULTS

5.3.1 CA1 pyramidal neurons in offspring of poly(I:C)-treated mothers display a reduced frequency and increased amplitude of mEPSCs

A number of studies indicate that the brains of schizophrenia patients exhibit a reduction in the volume of the hippocampus (Nelson et al., 1998; Heckers and Konradi, 2002). Although most studies on schizophrenia patients report no significant change in neuronal density in the hippocampus (Dwork, 1997; Harrison, 1999), many post-mortem studies have reported an abnormal expression of synaptic proteins, including synaptophysin (Eastwood and Harrison, 1995; Davidsson et al., 1999), synapsin I (Browning et al., 1993), SNAP-25 (Young et al., 1998) and spinophilin (Law et al., 2004). In addition, Cotter et al. (2000) reported an altered expression of MAP2, a cytoskeletal protein. An elevation in overall MAP2 immunoreactivity in hippocampal dendrites was observed. Therefore, we investigated the effect of maternal immune activation on the expression of synaptic and dendritic proteins in the hippocampus.

We performed immunohistochemistry to examine the expression of synaptophysin, GluR1 and MAP2 in hippocampal area CA1. We did not observe a

significant difference in the relative distribution of the synaptic proteins synaptophysin and GluR1 along the apical dendrites of CA1 pyramidal neurons (Figure 5-1). We did, however, find a significantly higher MAP2 expression ratio in dendritic regions relative to the soma in area CA1 (Figure 5-1). These results indicate that the offspring of poly(I:C)-treated mothers may have an abnormality in the dendritic structure of CA1 pyramidal neurons.

We then asked whether the offspring of immune-activated mothers display abnormalities in synaptic number or efficacy. We observed an increased amplitude, but decreased frequency in CA1 pyramidal neuron mEPSCs (amplitude: saline 8.5 ± 0.3 pA, poly(I:C) 9.9 ± 0.5 pA; frequency: saline 0.95 ± 0.15 Hz, poly(I:C) 0.60 ± 0.05 Hz) (Figure 5-2A). This trend was found in nearly all animals tested (Figure 5-2B). We did not find any difference in the kinetics of mEPSC waveforms (Figure 5-2C) or membrane properties (membrane capacitance: saline 220 ± 36 pA, poly(I:C) 210 ± 33 pA, membrane resistance: saline 194 ± 62 MΩ, poly(I:C) 149 ± 55 MΩ, in mean ± SD), suggesting that the observed differences in mEPSC amplitude and frequency are primarily due to altered synaptic properties. The decrease in mEPSC frequency suggests either presynaptic dysfunction or a reduction of excitatory synapse number per neuron. The increase in mEPSC amplitude may be a compensatory response for the reduction of mEPSC frequency (Turrigiano et al., 1998; Sutton et al., 2006). These results indicate that the offspring of poly(I:C)-treated mothers display altered excitatory synaptic transmission in area CA1.

To examine inhibitory synaptic transmission, we also recorded mIPSCs from

CA1 pyramidal neurons. We do not find a significant difference in either amplitude or frequency of mIPSCs between groups (amplitude: saline 13.9 ± 1.1 pA, poly(I:C) 13.6 ± 1.0 pA, frequency: saline 4.9 ± 0.3 Hz, poly(I:C) 4.3 ± 0.5 Hz) (Figure 5-2D), suggesting that the function of inhibitory synapses is normal in area CA1 of the adult offspring of poly(I:C)-treated mothers.

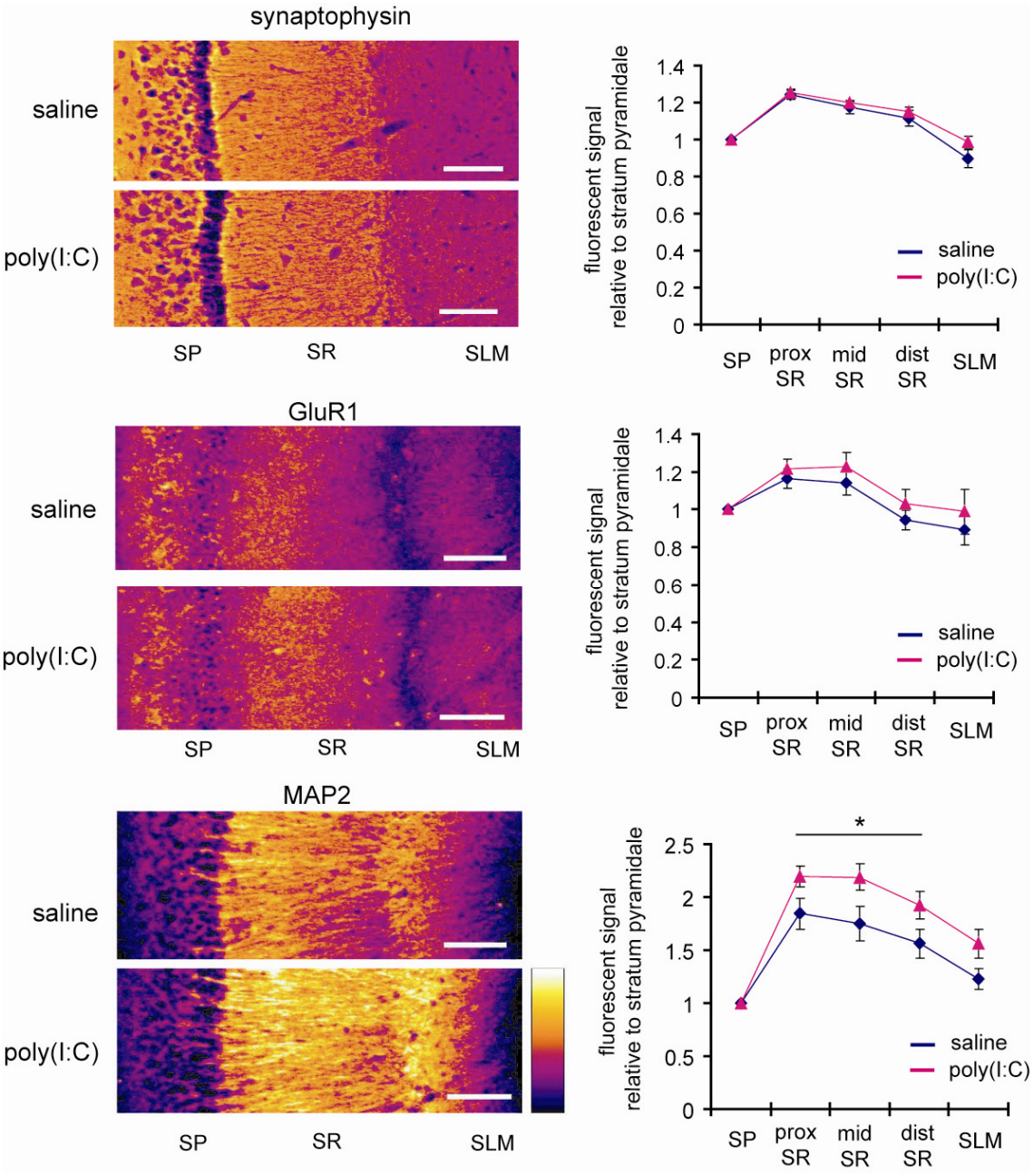

Figure 5-1: The offspring of poly(I:C)-treated mothers display differential MAP2 expression in area CA1

Immunohistochemistry using antibodies raised against synaptophysin, GluR1 and MAP2 was performed on the hippocampal slices from the adult offspring of saline- or

poly(I:C)-treated mothers. The fluorescent signal from the soma (SP, stratum pyramidale) to dendritic regions (SR, stratum radiatum and SLM, lacunosum-moleculare) was analyzed in area CA1. The stratum radiatum was equally divided into 3 regions (proximal, middle and distal) for analysis. To quantitate the levels of MAP2 signal in the different regions, signals were normalized to that detected in stratum pyramidale. An ANOVA reveals a significant main effect of group, indicating that MAP2 staining differs from control and the offspring of poly(I:C)-treated mothers ($p = 0.0014$) ($n = 4$ pairs of animals, 2 slices analyzed from each) (scale bar = 100 μm).

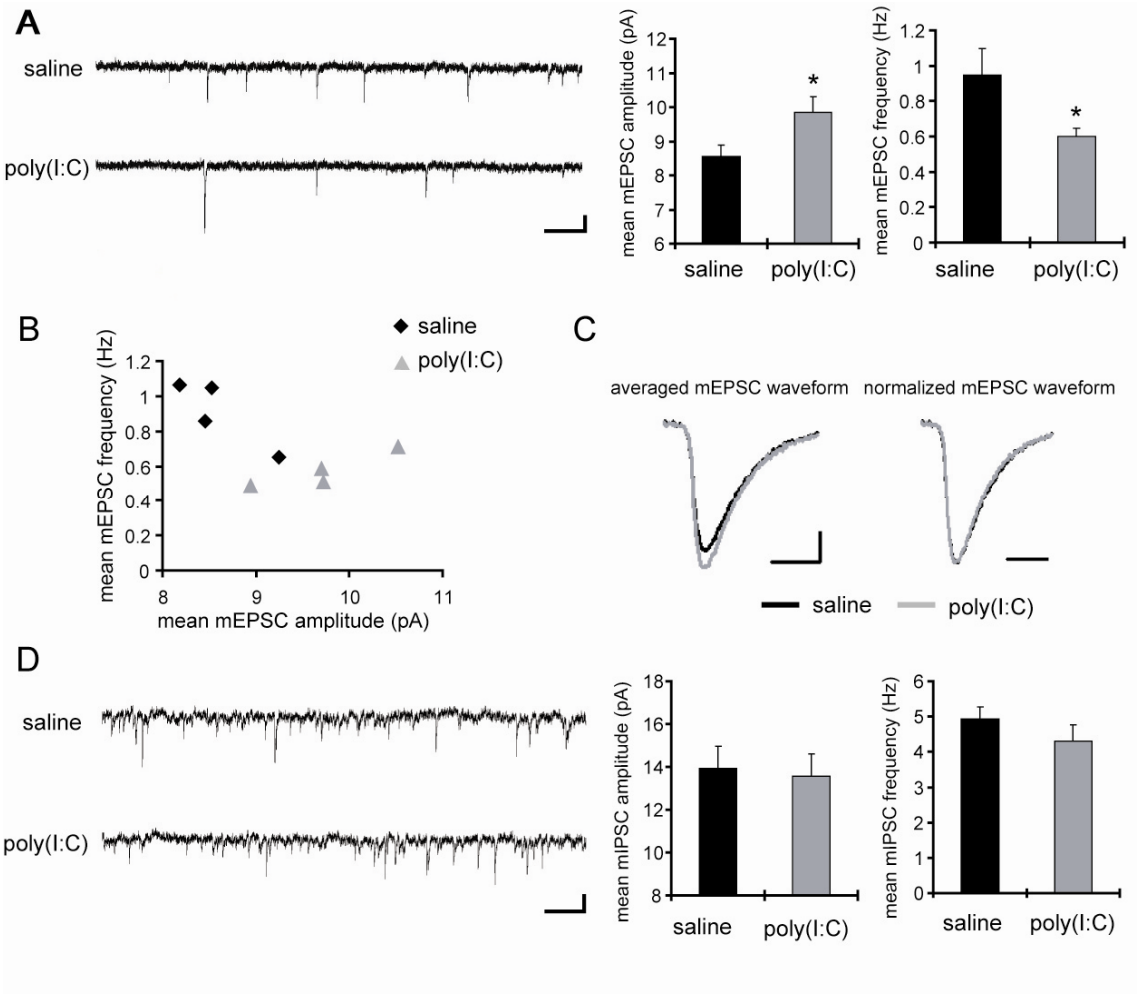

Figure 5-2: CA1 pyramidal neurons in the offspring of poly(I:C)-treated mothers display reduced frequency and increased amplitude of mEPSCs, but no significant difference in mIPSCs

(A) Recording of mEPSCs from CA1 pyramidal neurons are shown (saline: n = 11 neurons, poly(I:C): n = 12 neurons, 4 pairs of animals) (scale bar = 500 ms, 10 pA) (*p < 0.05 relative to control). **(B)** Mean frequency and amplitude of each animal used for the analysis in **A** is plotted. Relative to controls, mEPSCs recorded from slices prepared from offspring of poly(I:C)-treated mothers showed a tendency toward larger amplitude and

smaller frequency in mEPSCs. **(C)** Averaged mEPSC waveforms from animals used for the analysis in **A** are shown on the left. Normalized mEPSCs on the right indicates that there is no significant difference in kinetics of mEPSCs between the groups. **(D)** Recording of mIPSCs from CA1 pyramidal neurons are shown (n = 12 neurons for each group, 3 pairs of animals). A cesium chloride-based solution was used as the internal solution of patch pipettes and recordings were made at 28 °C under TTX (1 μM), NBQX (20 μM) and APV (50 μM) to block excitatory synaptic transmission. Extracellular potassium concentration was increased from 2.5 mM to 5 mM to enhance the frequency of miniature synaptic events. No significant difference was observed in mIPSC amplitude or frequency between the groups.

5.3.2 No significant group differences are observed in paired-pulse facilitation or LTP at Schaffer-collateral-CA1 synapses

Our analysis of mEPSCs suggest that the offspring of poly(I:C)-treated mothers display either a reduced number of excitatory synapses or a reduction in the probability of release at Schaffer-collateral CA synapses. To assess the presynaptic function of these animals, we analyzed paired-pulse facilitation. We did not, however, find a significant difference between the groups (saline: 2.1 ± 0.2, poly(I:C): 2.0 ± 0.2; 2nd to 1st EPSC amplitude) (Figure 5-3A), suggesting that presynaptic function in the experimental group is normal. We also tested synaptic plasticity at Schaffer-collateral-CA1 synapses, examining long-term potentiation (LTP) elicited by a single train of 100 stimuli at 100 Hz. When LTP was induced by a high-frequency stimulation, the magnitude of LTP in slices prepared from the offspring of poly(I:C)-treated mothers was similar to controls (saline: 1.45 ± 0.05, poly(I:C): 1.36 ± 0.07; mean fEPSP at 55 – 60 min after LTP induction relative to the baseline) (Figure 5-3B). Taken together, these data suggest that the offspring of poly(I:C)-treated mothers display a reduced number of normally functioning excitatory synapses on CA1 pyramidal neurons. Our results are consistent with studies using lipopolysaccharide (LPS), instead of poly(I:C), for maternal immune activation. In this study, they observed smaller fiber volleys and larger fEPSP in extracellular field recordings at Schaffer-collateral-CA1 synapses in hippocampal slices prepared from the offspring of LPS-treated mothers (Lowe et al., 2008).

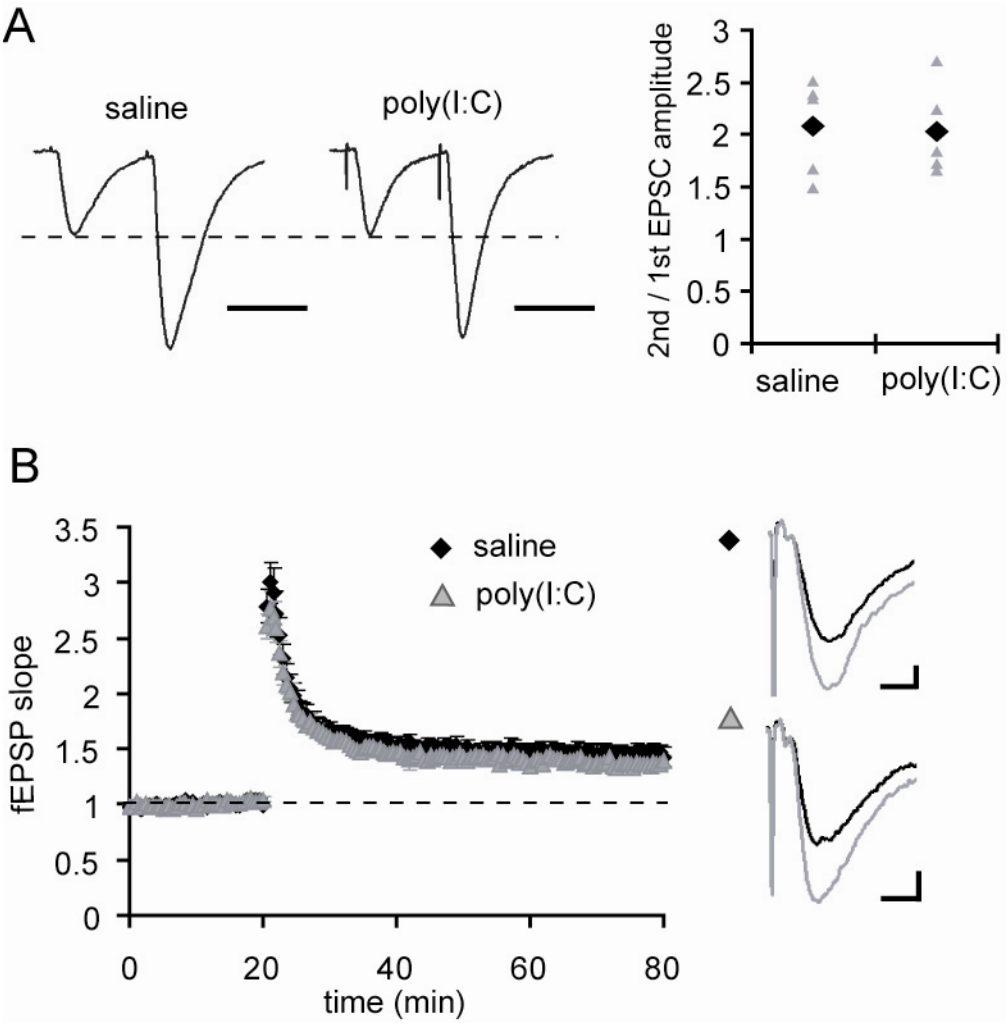

Figure 5-3: The offspring of poly(I:C)-treated mothers display normal paired-pulse facilitation and LTP at Schaffer-collateral-CA1 synapses

(A) Whole-cell voltage-clamp recordings were performed in CA1 pyramidal neurons under the inhibitory blockade with the GABA receptor antagonists bicuculline (10 μM) and CGP55845 (1 μM). Membrane potential was clamped at -60 mV. Paired-pulse facilitation was analyzed at Schaffer-collateral-CA1 synapses (interstimulus interval was 50 ms; n = 5 neurons for each group, 3 pairs of animals; scale bar = 50 ms). **(B)**

Extracellular field recordings were performed at Schaffer-collateral-CA1 synapses under fast inhibitory transmission block with the $GABA_A$ receptor antagonist bicuculline. LTP was induced by a single train of 100 stimuli at 100 Hz (n = 8 slices for each group, 3 pairs of animals; scale bar = 0.2 mV, 5 ms).

5.3.3 Hippocampal slices prepared from offspring of poly(I:C)-treated mothers display increased sensitivity to dopamine at temporoammonic-CA1 synapses

Because DA signaling plays an important role in the pathophysiology of schizophrenia, we investigated DA modulation of synaptic activity in hippocampal area CA1. As previous studies showed a selective influence of DA on the temporoammonic-CA1 synapses versus Schaffer-collateral–CA1 synapses (Otmakhova and Lisman, 1999; Ito and Schuman, 2007), we examined DA modulation of TA–CA1 synapses. The TA pathway includes two axonal populations, from the medial (MEC) and lateral (LEC) entorhinal cortexes. These projections are topographically organized along the transverse axis of area CA1, such that the projections from MEC make synapses at proximal CA1 (close to CA3), but those from the LEC projects to distal CA1 (close to subiculum) (Figure 5-4A; Witter and Amaral, 2004). We recorded fEPSPs simultaneously from proximal and distal TA-CA1 synapses. DA application induced a synaptic depression at both proximal and distal TA-CA1 synapses in the slices prepared from control animals (Figure 5-4B), which is in strong contrast to our prior studies in rat hippocampal slices where the neuromodulators, DA or NE, induced a largely selective influence on the input from the LEC (Ito and Schuman, unpublished data, Chapter 4). Furthermore in mouse hippocampal slices, DA induced a significantly larger depression at proximal TA–CA1 synapses when compared to distal TA-CA1 synapses (proximal TA: 57.6 ± 2.2%; distal TA: 65.3 ± 2.3%, relative to baseline; Figure 5-4C). Taken together, these data indicate that DA differentially controls MEC and LEC inputs via a different mechanism from the rat hippocampus.

Previous anatomical studies in the mouse brain showed a similar, but less clear, topographic projection of the TA pathway as that observed in the rat brain (van Groen et al., 2003). Our immunohistochemistry studies also observed expression differences of presynaptic proteins, synapsin I and bassoon, in the stratum lacunosum-moleculare between distal and proximal regions of mouse area CA1 (Supplementary Figure 5-1). Furthermore, this topographic organization of presynaptic proteins was observed in both animals groups (Supplementary Figure 5-1).

In slices prepared from the offspring of poly(I:C)-treated mothers, DA induced a comparable depression to that observed in control slices at proximal TA–CA1 synapses. At distal TA–CA1 synapses, however, the slices prepared from the offspring of poly(I:C)-treated mother showed a significantly larger depression when compared to control (proximal TA: 55.4 ± 3.1%; distal TA: 56.3 ± 1.4%, relative to baseline; Figure 5-4C). To examine DA sensitivity at distal TA–CA1 synapses, DA was applied sequentially from low to high concentration to acute slices (Figure 5-4D) and DA-mediated depression was quantified. We found that, compared to controls, the amount of depression was significantly larger at each DA concentration examined in the slices prepared from the experimental group (Figure 5-4E). These results indicate that the adult offspring of poly(I:C)-treated mothers display an enhanced sensitivity to DA selectively at LEC inputs.

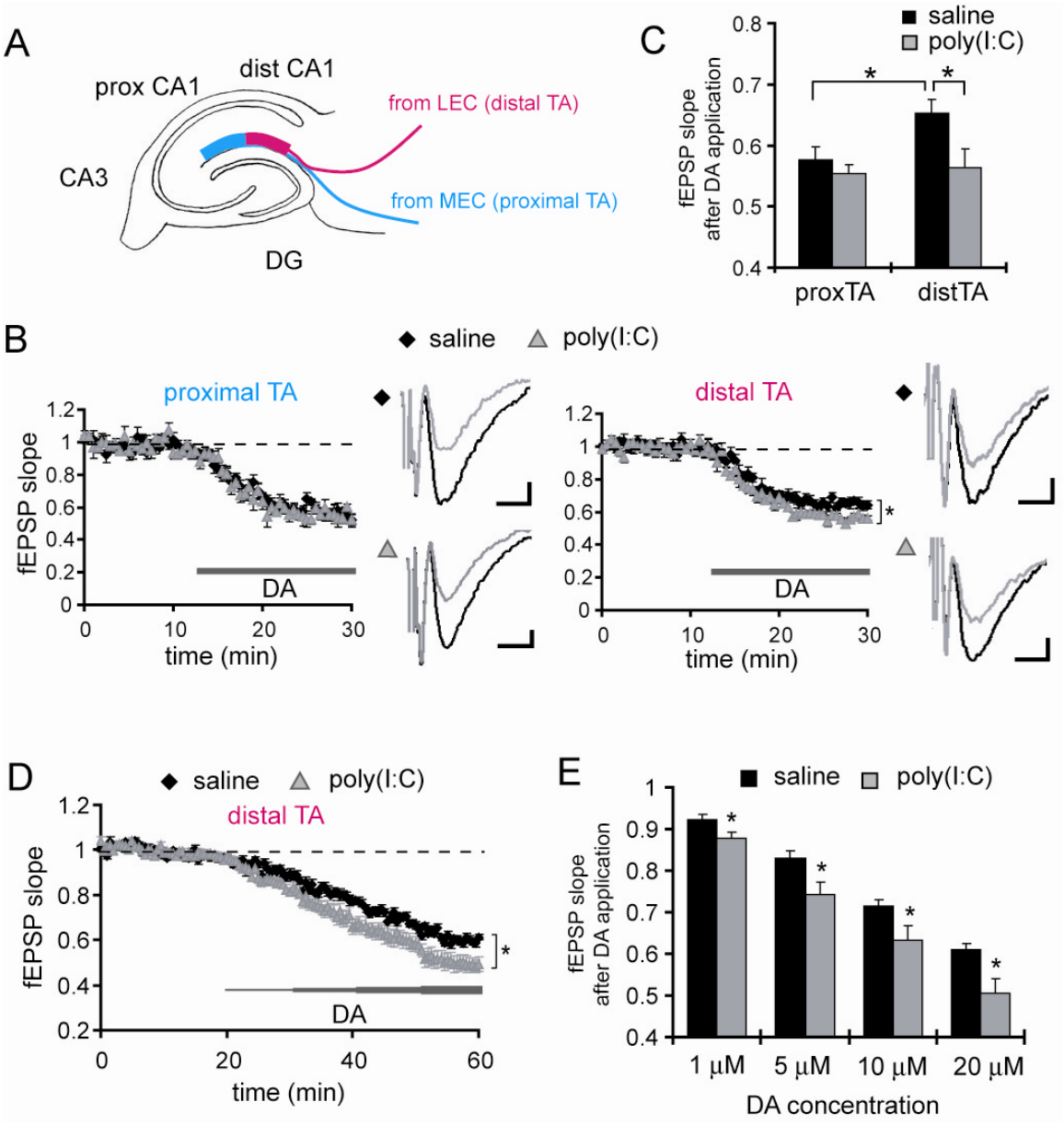

Figure 5-4: The offspring of poly(I:C)-treated mothers display increased DA-induced depression at temporoammonic-CA1 synapses

(A) A schematic diagram depicting the two distinct axonal projections in the temporoammonic pathway, either from MEC or LEC. **(B)** The extracellular field recordings obtained simultaneously from proximal and distal TA–CA1 synapses. The concentration of bath applied DA was 20 µM. The representative traces show fEPSP

waveforms before (black) and after (gray) DA application (scale bar = 0.05 mV, 5 ms) (*p < 0.05 relative to control). **(C)** In hippocampal slices prepared from control animals, DA induced a significantly larger depression at proximal compared to distal TA–CA1 synapses. The slices prepared from the offspring of poly(I:C) mothers showed a normal DA-induced depression at proximal synapses, however, exhibited a significantly larger depression at distal TA-CA1 synapses, compared to control (*p < 0.05). **(D)** Hippocampal slices prepared from the offspring of poly(I:C)-treated mothers show increased DA-induced depression at TA–CA1 synapses. The DA concentration was increased sequentially every 10 min from 1 to 20 μM (*p < 0.05 relative to control). **(E)** Analysis of the data in **D** is shown. Slices prepared from the offspring of poly(I:C)-treated mothers showed a significantly larger depression at each DA concentration examined (n = 12 slices for each group, 8 pairs of animals) (*p < 0.05 relative to control).

5.3.4 The offspring of poly (I:C)-treated mothers display a distinct c-Fos expression pattern in transverse-axis of hippocampal area CA1 following novel object exposure

The hippocampus receives two streams of information from the entorhinal cortex: one is spatial information carried by axons from the medial entorhinal cortex (MEC), and another is nonspatial, or object, information carried by axons from the lateral entorhinal cortex (LEC) (Manns and Eichenbaum, 2006). Because the offspring of poly(I:C)-treated mothers show higher sensitivity to DA on LEC projection to area CA1, these animals may possess abnormal object information processing.

To test this idea, we examined how the hippocampal neurons are activated *in vivo* during novel object exposure by immunostaining for an immediate-early gene product, c-Fos (Morgan and Curran, 1991). Immediate early gene expression in resting animals is very low, but rapidly increases following patterned neuronal activities to induce synaptic plasticity (Cole et al., 1989), suggesting that c-Fos expression can be used as a neuronal activation marker (Guzowski et al., 2005). Following home cage exposure for several days, a pair of animals, a control and an experimental mouse, were exposed to novel objects in the home cage. After 2 hrs of novel object exposure, animals were sacrificed and immunohistochemistry was performed on brain slices. The control mice showed differential c-Fos expression between proximal and distal CA1 pyramidal neurons (Figure 5-5B and 5-5C), consistent with our previous results observed in rats (Ito and Schuman, unpublished data, Chapter 4). The offspring of poly(I:C)-treated mothers, however, did not show a clear differential c-Fos activation between proximal and distal CA1 pyramidal neurons (Figure 5-5B and 5-5C). Because neuromodulatory control of

TA-CA1 synapses likely plays a key role in the differential activation of area CA1 (Ito and Schuman, unpublished data; chapter 4), our results suggest that the offspring of poly(I:C)-treated mothers possess an abnormality in neuromodulator-mediated control of object information processing in the hippocampus.

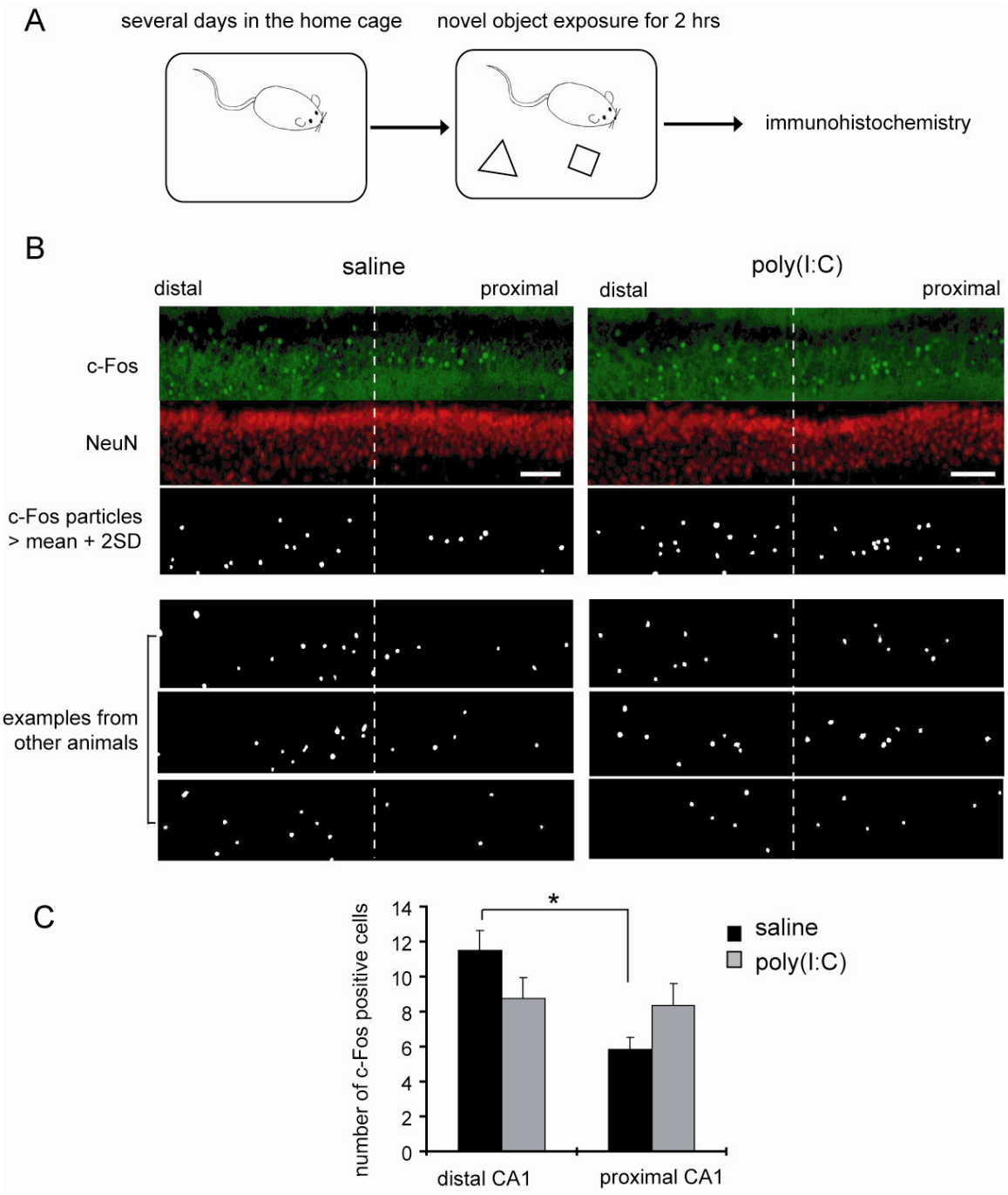

Figure 5-5: The offspring of poly(I:C)-treated mothers display abnormalities in c-Fos expression in area CA1 pyramidal neurons following novel object exposure

(A) A schematic diagram of the behavioral procedure is shown. After mice were

accommodated in the home cage for a few days, two novel objects were placed in the cage. After a 2 hr exposure, animals were sacrificed, brain slices were made and processed for immunohistochemistry. **(B)** Examples of c-Fos expression in the pyramidal layer of area CA1 are shown. The pyramidal layer was equally divided into proximal and distal regions. The c-Fos particles that have signals larger than mean + two times the standard deviation, were analyzed using ImageJ (see methods for details) (scale bar = 100 μm). **(C)** The number of c-Fos signal particles was quantitated in proximal and distal regions of CA1 pyramidal layer (n = 6 pairs of animals, 2 slices analyzed from each).

5.4 DISCUSSION

5.4.1 Reduced excitatory input on CA1 pyramidal neurons

The offspring of poly(I:C)-treated mothers display altered synaptic properties in hippocampal area CA1. First, using immunohistochemical techniques, we observed a relative increase in a dendritic cytoskeletal protein, MAP2 in the stratum radiatum, and second, electrophysiological studies suggest a decreased number of excitatory synapses per neuron.

It has been estimated that each CA3 pyramidal neuron axon makes synapses with 30,000 – 60,000 neurons (Li et al., 1994). Most of these CA3 projections are received by CA1 pyramidal neuron via the Schaffer-collateral pathway. Each CA1 pyramidal neuron, in turn, receives approximately 30,000 excitatory inputs (Megias et al., 2001), which is primarily due to the convergence of thousands of CA3 pyramidal neurons (Sorra and Harris, 1993). This huge divergence-convergence architecture is one of major features of Schaffer-collateral pathway. The reduction in synaptic number suggested in the offspring of poly(I:C)-treated mothers may impair some key functions of the hippocampus based on this architecture.

The observed deficits at Schaffer-collateral–CA1 synapses from the poly(I:C) offspring slices is consistent with previous studies in schizophrenia patients, where abnormal mRNA expression of presynaptic proteins in area CA3 have been reported (Harrison and Eastwood, 2001). We did not observe a significant difference in the mIPSCs amplitude or frequency in the offspring of poly(I:C)-treated animals. Although

several studies have reported a decreased number of GABAergic neurons in the hippocampus, most of these differences were observed in area CA2/3, not in area CA1 (Benes et al., 1996; Benes et al., 1997; Heckers and Konradi, 2002). Thus, GABAergic input to area CA1 pyramidal neurons appears normal.

5.4.2 Increased dopamine sensitivity in the temporoammonic pathway

Compared to the Schaffer-collateral pathway in area CA1, the temporoammonic pathway has been a relatively unexplored connection in the hippocampus. Many recent findings highlight its unique role in the hippocampal function, however (Brun et al., 2002; Remondes and Schuman, 2004; Nakashiba et al., 2008). Some interesting features of this pathway include its topographic projection pattern and its sensitivity to neuromodulators.

A topographic projection in which LEC or MEC-derived axons terminate in different regions, allows the entorhinal cortex to send nonspatial and spatial information to distinct neuronal populations in area CA1. This contrasts with the laminar organization of the perforant pathway projection, from the entorhinal cortex to the dentate gyrus or area CA3, where each neuron receives both LEC and MEC inputs in different dendritic regions (Witter and Amaral, 2004). The efferents from area CA1 are also topographically organized such that neurons in proximal CA1 send projections back to the MEC, while neurons in distal CA1 project back to the LEC (Tamamaki and Nojyo, 1995). Thus, two independent circuit loops for nonspatial and spatial information exist between the entorhinal cortex and area CA1 (Amaral and Lavenex, 2007). This architecture, based on

the TA pathway, may allow for the hippocampus to independently process nonspatial and spatial information, providing a unique role of the TA pathway in the hippocampus.

Sensitivity to neuromodulators is another feature of the TA pathway. In recordings from mouse hippocampal slices, DA induced a larger depression at proximal compared to distal TA-CA1 synapses in hippocampal slices prepared from control animals. However, hippocampal slices prepared from poly(I:C)-treated mothers exhibited a significantly larger DA-induced depression selectively at distal TA-CA1 synapses compared to control, which may abolish the differential control of LEC and MEC inputs by DA. Our present observations, based on both electrophysiology and c-Fos expression in behaving animals, suggest that the offspring of poly(I:C)-treated mothers have altered DA-mediated control of the TA pathway and may have an abnormality in object information processing. It is worth noting that the antipsychotic drug, clozapine, effectively blocks DA-induced depression at TA-CA1 synapses (Otmakhova and Lisman, 1999) and also abolishes differential neuronal activation along the transverse-axis of area CA1 (Ito and Schuman, unpublished data, Chapter 4). This indicates that the TA pathway may be a locus for clozapine action in schizophrenia patients.

5.4.3 Integration of information processed in parallel

One of the major features of the brain is the so-called parallel information processing. For example, visual information is processed in two distinct information streams: a ventral stream that subserves object recognition, or “what” perception, and a dorsal stream that primarily subserves spatial information, or “where” perception

(Ungerleider and Haxby, 1994). The distributed information, processed in different brain areas, must be integrated for coherent perception.

Recent imaging and physiology studies reported abnormal visual object recognition in schizophrenia patients (Doniger et al., 2002; Wynn et al., 2008). Wynn et al. measured the activities in early retinotopically organized areas (V1–V4), motion-sensitive areas (human area MT) and object-recognition areas (lateral occipital complex), and found that schizophrenia patients display more widely-distributed activation in areas involved in object-recognition than controls (Wynn et al., 2008). Thus, the abnormally distributed object-selective cortex in schizophrenia patients may indicate a problem in the integration of spatial and nonspatial information.

In the hippocampus, the integration of spatial and nonspatial information is critical for constructing a neural representation of environmental context. As such, the hippocampus plays an essential role in contextual memory formation. Interestingly, several studies indicate that schizophrenia patients have a severe problem in contextual memory formation (Boyer et al., 2007; Rizzo et al., 1996; Danion et al., 1999), although other types of memory, which do not require contextual information, are relatively intact. In light of our findings, this memory deficit could be due to abnormal DA-mediated control of the TA pathway in the hippocampus.

Using the poly(I:C) maternal immune activation model, we investigated synaptic dysfunction and the accompanying behavior-dependent c-Fos expression in the hippocampus. The altered information processing we observe may underlie some of the

schizophrenia-like behaviors observed in the offspring of poly(I:C)-treated mothers. These studies, together with others, suggest that it is necessary to consider two distinct streams of information, nonspatial and spatial, in understanding hippocampal information processing in schizophrenia patients. Further investigations based on this perspective may shed new light on the pathophysiology of schizophrenia.

5.5 MATERIALS AND METHODS

5.5.1 Animals

Pregnant C57BL/6J mice were injected i.v. with 5 mg/kg poly(I:C) potassium salt freshly dissolved in 0.9% sterile saline on E12.5. Control females were injected with the same volume of saline. The offspring were undisturbed until weaning on P21. Offspring were behaviorally tested from 6 to 11 weeks for pre-pulse inhibition, latent inhibition, open field exploration, Morris water maze, novel location and novel object recognition (data not reported here).

5.5.2 Hippocampal slice preparation

For each experiment, hippocampal slices (400 μm) were made from paired adult offspring (7 – 12 week old, same sex) from saline and poly(I:C)-treated mothers. In brief, a vibrating microtome (Leica VT1000S) was used to cut hippocampal slices (400 μm thickness) in ice-cold oxygenated artificial cerebrospinal fluid (ACSF) containing (in mM) 119 NaCl, 2.5 KCl, 1.3 $MgSO_4$, 2.5 CaCl, 1.0 NaH_2PO_4, 26.2 $NaHCO_3$, 11.0 glucose. Slices were recovered at room temperature for at least 2 hour in an interface chamber, and then transferred to a submerged recording chamber perfused with ACSF. Concentric bipolar tungsten electrodes (FHC) and stimulus isolators (Axon Instruments) were used for the stimulation.

5.5.3 Electrophysiology

Extracellular field potential recordings were made with 1 – 3 MΩ resistance microelectrodes filled with 3 M NaCl using a bridge amplifier (Axoclamp 2B, Molecular Devices). Whole-cell voltage-clamp recordings from CA1 pyramidal neurons or DG granule cells were obtained without visualization with an Axopatch 200B (Molecular Devices). Internal solution of whole-cell patch pipettes was (in mM) 115 cesium gluconate, 20 cesium chloride, 10 sodium phosphocreatine, 10 HEPES, 0.2 EGTA, 2 MgATP, 0.3 NaGTP (pH 7.3). The membrane capacitance was cancelled and series resistance was compensated (60 – 70%) for paired-pulse facilitation experiments, but uncompensated for miniature recordings. Recordings were discarded when the series resistance was over 20 MΩ or either series or membrane resistance changed more than 30% during data acquisition. Test pulses were applied once every 30 sec. Dopamine was obtained from Sigma. All other drugs were obtained from Tocris. For mEPSC recordings, whole-cell patch clamp recordings were obtained from CA1 pyramidal neurons in extracellular solution containing TTX (1 μM) and bicuculline (10 μM) at 25 °C. For mIPSC recordings, the internal solution of patch pipettes was a cesium chloride-based solution (in mM) 115 cesium gluconate, 20 KCl, 10 sodium phosphocreatine, 10 HEPES, 0.2 EGTA, 2 MgATP, 0.3 NaGTP (pH 7.3). The recordings were made at 28 °C under TTX (1 μM), NBQX (20 μM) and APV (50 μM) to block excitatory synaptic transmission, and the extracellular potassium concentration was increased from 2.5 mM to 5 mM to enhance the frequency of miniature synaptic events. Membrane voltage was clamped at -70 mV. For the analysis of paired-pulse facilitation, whole-cell patch clamp recordings were obtained from CA1 pyramidal neurons. The membrane potential was

clamped at -60 mV, and recordings were made at 25 °C under bicuculline (10 μM) and CGP55845 (1 μM) to block inhibitory synaptic transmission. The interstimulus interval was 50 msec. The LTP induction protocol was a single train of 100 pulse stimuli at 100 Hz. All stimulus pulses were of the same length and amplitude as test pulses.

5.5.4 Behavioral analysis

All the behavioral manipulations were carried out at night (0 – 4 am) to maximize active exploration of the environment. The objects used for novel object exposure were two small children's toys, made of either plastic or wood.

5.5.5 Data analysis

Electrophysiology:

Data were collected using a custom-written program (LabView data acquisition system; National Instruments) for extracellular recordings, or DigiData 1200 and pClamp 9 (Molecular Devices) for whole-cell recordings. All numerical values listed represent mean ± s.e.m. Student's t-test was performed to analyze the signficance of the data.

Immunohistochemistry:

Slices (400 μm thickness) were prepared using the same procedure as for electrophysiology recordings. After cutting, slices were quickly fixed in 4% paraformaldehyde in phosphate-buffered saline (PBS) for at least 2 days. Thin (50 μm)

sections were cut with a vibrating microtome (Leica VT1000S).

The sections were incubated overnight with either of 1:250 concentration of anti-c-Fos (sc-52) (Santa Cruz), 1:1000 of anti-Synaptophysin (Millipore), 1:1000 of anti-MAP2 (Sigma) or 1:1000 of anti-GluR1 (Millipore) antibodies. The incubation was carried out at room temperature in Tris-buffered saline containing 0.2% Triton X-100, BSA 2%, NGS 4%, followed by 4 hrs of secondary-antibody incubation with 1:1000 of Alexa 488-conjugated anti-rabbit and 1:1000 of Alexa 543-conjugated anti-mouse antibodies (Invitrogen).

For the analysis of immunohistochemistry experiments, images were obtained with Zeiss LSM 510 laser scanning confocal microscopes using a Plan-Neofluor 10×/0.3 air objective. Alexa 488 and 546 were visualized by excitation with the 488 line of an argon ion laser and the 543 nm line of a HeNe laser, respectively. The optical section was 20 μm and fluorescent signals were acquired throughout the slice thickness (50 μm). Each 50 μm slice was obtained from a different 400 μm section and two slices were analyzed from each animal. Slices were obtained from the same septo-temporal position in all experiments. To count the number of c-Fos positive neurons, fluorescent signals less than the mean + 2SD were excluded and, if necessary, an additional thresholding was applied to reduce background signals in dendritic areas. Then, automated particle analysis was carried out using ImageJ (NIH) based on that the following criteria: the particle size was larger than 39 μm^2 and the circularity was larger than 0.5. Statistical differences between animals groups were assessed by ANOVA.

5.6 SUPPLEMENTARY FIGURES

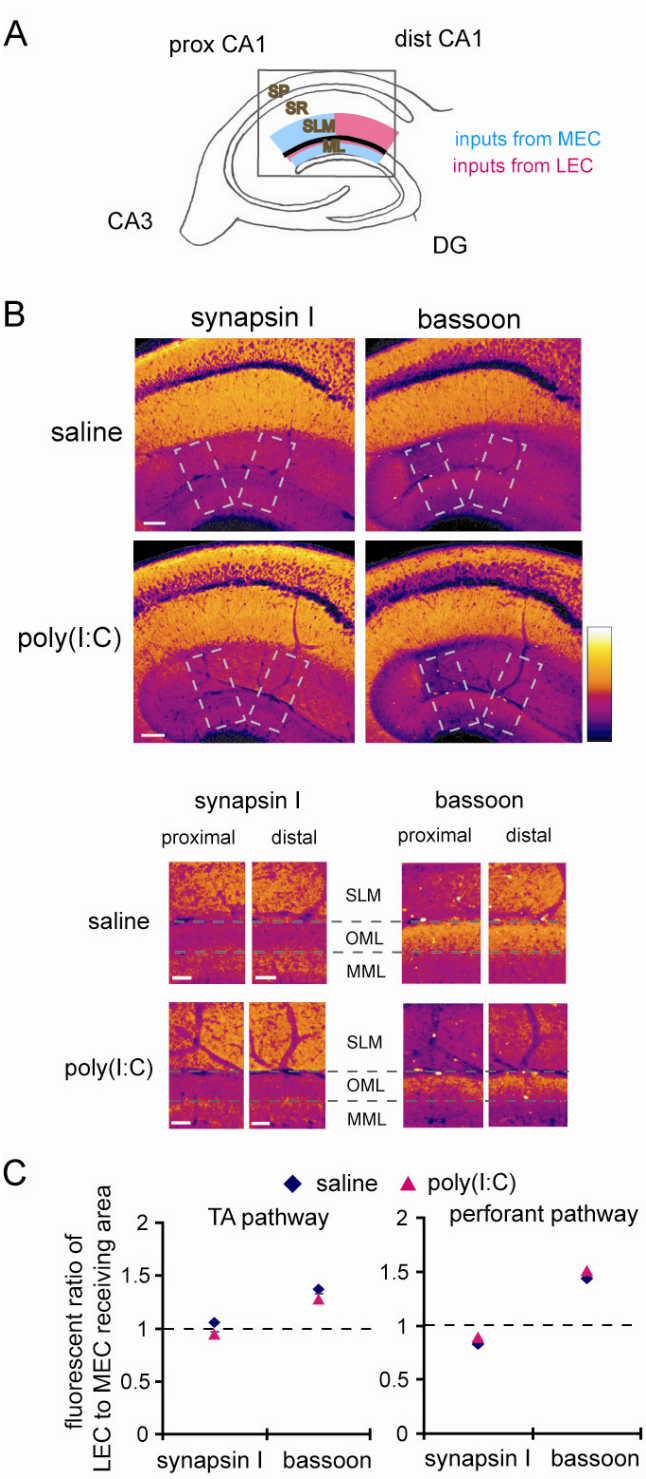

Supplementary Figure 5-1: Differences in presynaptic protein expression in synaptic

regions that receive inputs from MEC or LEC

(A) Scheme of topographic or laminar projection of MEC and LEC inputs to area CA1 or DG, respectively. **(B)** Distribution of presynaptic proteins (synapsin I and bassoon) in the hippocampus of C57BL/6J mice. Differential protein expression was observed in the SLM of distal vs. proximal CA1 as well as the outer vs. middle ML of the DG (scale bar = 100 μm in the top figures, 50 μm in the bottom enlarged figures). **(C)** Fluorescent signal ratios of areas receiving LEC inputs to areas receiving MEC inputs in either the TA or perforant pathway (n = 12 for each group, 6 pairs of animals).

Chapter 6. Discussion

6.1 Neuromodulators and Parallel Information Processing in the Brain

A number of studies suggest that the brain exhibits functional localization, such that some brain regions are specialized to process or integrate certain types of sensory information (Boling et al., 2002; Passingham et al., 2002). Most animal behaviors require the coordinated activity of sensory, integrative and motor brain areas. As the sensory landscape undergoes change, the interactions among brain areas are also dynamic and change depending on the situation and history. For example, when you meet a new person, initially you may try to memorize his or her face (encoding information), but the next time you see this person, you will recognize his or her face and may remember several events associated with this person (retrieving information). Given that synaptic transmission between neurons is the basic unit of information processing, it is crucial to understand how synaptic modulation can change interactions among brain areas.

Neurotransmitters, such as dopamine, norepinephrine, serotonin, or acetylcholine, play an important role in state-dependent modulation of the brain (Kodama et al., 2002; Robbins 2005; Takakusaki et al., 2006). These neurotransmitters, often called neuromodulators, are synthesized and released from a relatively small number of specialized neurons, which are primarily located in distinct nuclei in the basal forebrain, midbrain or brainstem (Siegel et al, 1999). Through long-range connections, these neuromodulator-releasing neurons make synaptic contacts with many different brain areas. Neuromodulators released from synaptic terminals are also capable of diffusing

over substantial distances (> 10 μm) and can act on receptors remote from release sites (volume transmission; Zoli et al., 1998, Venton et al., 2003). Thus, at the apparent cost of spatial selectivity, the information from neuromodulator-releasing neurons can be broadcast to a large area of the brain. As such, activity changes in a small number of neurons can exert a broadcast influence, coordinating a functional change across many brain areas (Hasselmo, 1995).

Our studies demonstrated that the neuromodulators, DA or NE, differentially influence inputs from the LEC and MEC to the hippocampus (Chapter 4), suggesting a role of neuromodulators in coordinating interactions among brain areas. Furthermore, at a local circuit level, neuromodulators exert a frequency-dependent modulation of synaptic transmission (Chapter 3). What is the impact of such frequency-based modulation for brain function?

6.1.1 Nonlinear Synaptic Transmission and Oscillatory Activities in the Brain

In electroencephalograms or local field potential recordings, brain activities are observed as multiple oscillators at different frequencies. A number of studies have described apparent links between specific oscillatory activities and particular brain functions (Laurent and Davidowitz, 1994; Buzsaki and Draguhn, 2004, Osipova et al., 2006, Palva and Palva, 2007). These oscillatory activities are not just epiphenomena, but rather the brain utilizes them for information coding, for example, to bind distributed information in the cortex (Engel et al., 2001; Varela et al., 2001) or to select phase-locked

activities (Laurent, 2002). These studies indicate that oscillatory activities play an important role in regulating information flow in the brain. Thus, it is important to understand how neuronal networks respond to different frequencies of stimulation.

In monosynaptic transmission, the magnitude of the postsynaptic response evoked by presynaptic stimulation is intrinsically dependent on the stimulation frequency (Markram et al., 1998). For example, during the delivery of multiple stimuli at close time intervals, the size of postsynaptic potentials can become larger or smaller, phenomena known as paired-pulse facilitation or depression, respectively (Zucker and Regher, 2002) (Figure 6-1). Both presynaptic and postsynaptic mechanisms have been implicated in these processes. For example, changes in neurotransmitter release probability, the availability of synaptic vesicles (Dobrunz and Stevens, 1997), postsynaptic receptor desensitization (Koike-Tani et al., 2008) or surface mobility of postsynaptic receptors (Heine et al., 2008) have all been proposed to play an important role in frequency-dependent modulation of synaptic transmission.

Differences in neuronal morphology and molecular composition will further extend possible patterns of frequency dependency modulation in signal transmission. The brain is composed of hundreds of types of neurons and each has distinct morphology, channel/receptor density and distribution, which determines differences in the threshold for action potential generation, firing patterns or synaptic plasticity (Shepherd, 2004). Therefore, the same input stimuli applied to different types of neurons can reveal one type of neuron that is sensitive to low-frequency stimulation and another that is sensitive to high-frequency stimulation (Hucheon and Yarom, 2000, Buzsaki and Draghun, 2004).

Frequency-dependent signal transmission by distinct neuronal types has been observed in the hippocampus (Pouille and Scanziani, 2004; Mori et al, 2004).

Signal gating based on input stimulation patterns can also be generated based on differences between monosynaptic and disynaptic transmission. Disynaptic transmission differs from monosynaptic transmission in two ways: i) the temporal delay imposed by the additional synapse, and ii) the nonlinear signal transduction with respect to the strength of input stimulation, due to the requirement for action potential generation at the first synapse. These differences will play an important role in the temporal filtering of input signals because the influence of disynaptic inputs are evident when inputs are delivered close in time (Figure 6-1). Thus, a neuronal network does not pass all signals equally, but rather, has a bias for a certain signal pattern. As such, changing oscillatory activities observed in the brain may lead to dynamic modulation of regional interactions.

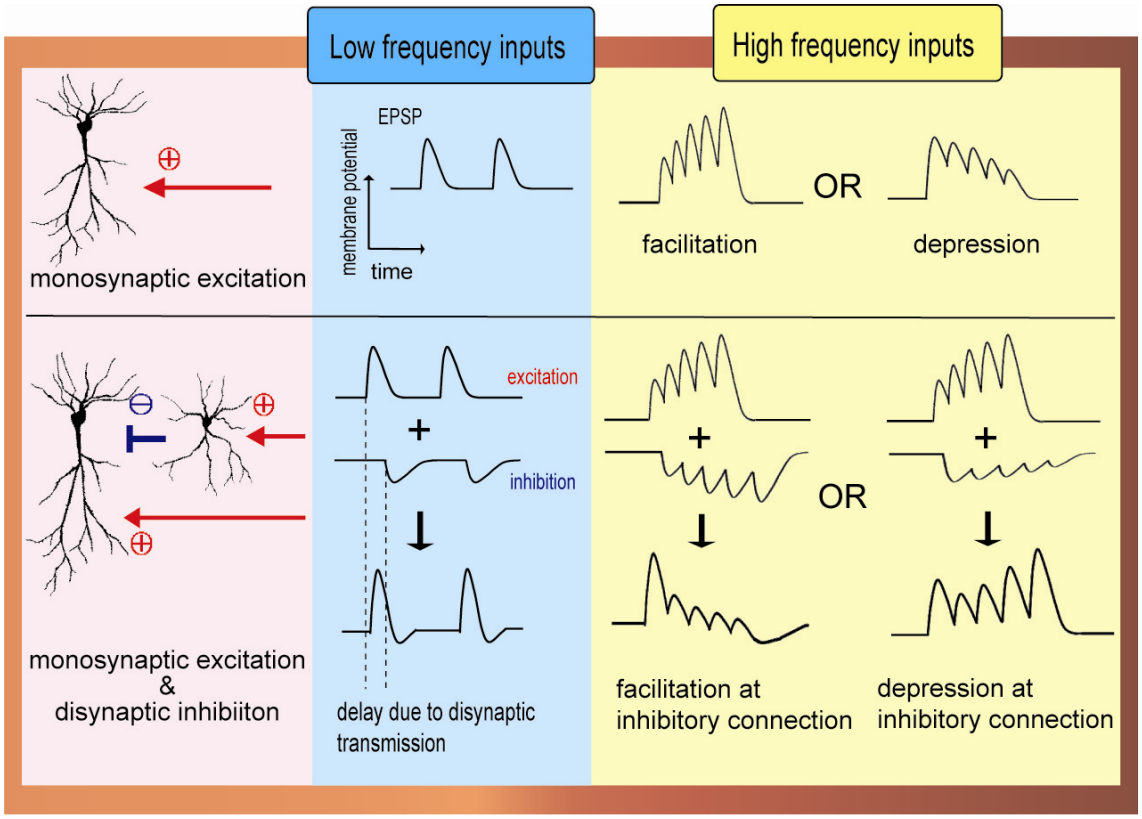

Figure 6-1: Examples of differential signal transmission between low- and high-frequency inputs

In monosynaptic transmission, low-frequency inputs elicit constant postsynaptic responses, however, high-frequency inputs induce facilitation or depression in signal transmission. A simple network composed of monosynaptic excitation and disynaptic inhibition exhibits diverse patterns of signal modulation. The influence of disynaptic transmission on synaptic transmission is not evident during low-frequency inputs, due to the temporal delay imposed by the additional synapse. During high-frequency stimulation, however, disynaptic inhibition effectively influences monosynaptic excitation. Because each neuron shows distinct responses to high-frequency stimuli, disynaptic inhibitory

connections shows facilitation, depression, or some characteristic response, which will, together with modulation in monosynaptic excitation, can magnify the difference of signal transmission between low- and high-frequency stimulation.

6.1.2 Neuromodulator-Mediated Control of Frequency-Dependent Signal Transmission

We examined how the neurotransmitter dopamine can change a frequency-dependent profile of signal transmission at temporoammonic–CA1 synapses in the hippocampus (Chapter 3). The primary effect of dopamine at these synapses is presynaptic depression due to a decrease in the release probability of synaptic vesicles. Surprisingly, however, this simple form of modulation has a large impact on the neuronal circuit as a whole. That is, dopamine depresses low-frequency input signals but enhances high-frequency signals. Thus, dopamine imposes a high-pass filter on this pathway exerting a preference for certain frequency inputs. This is a good example of how a simple synaptic modulatory action can have a large impact at a network level. Here, the difference between monosynaptic and disynaptic transmission plays an important role in generating this effect (Figure 6-1).

The significance of this frequency-dependent signal transmission is exemplified in the temporoammonic pathway, because the entorhinal cortex, which is the origin of this pathway, shows both theta (4–12 Hz) and gamma (40–100 Hz) oscillatory activities in behaving animals (Chrobak et al., 2000). As such, the presence of dopamine will impose a selection bias for the receipt of information, encoded differentially with oscillatory activities in the entorhinal cortex. Thus, dopamine-induced change in frequency-dependent signal transmission is likely to have a significant impact on functional coupling between the entorhinal cortex and the hippocampus.

Although here we specifically focused on neuromodulator-mediated gating of oscillatory

activities, the influence of neuromodulators on the regional interactions of the brain is not limited to this process. For example, individual neurons differ in their preferred oscillatory frequency of membrane potential owing to the type and distribution of ion channels present (i.e., resonance property; Hucheon and Yarom, 2000, Buzsaki and Draghun, 2004, Giocomo et al, 2007). These resonant properties may be differentially controlled by neuromodulators by changing kinetics of voltage-sensitive channels. Such modulation is likely to influence the generation and receipt of oscillatory activities in each brain area. Thus, neuromodulators have many effects and can influence each step of frequency-dependent information transfer among brain areas including the generation, transmission and receipt of oscillatory activities.

6.2 Spatial Remapping and Contextual Representation in the Hippocampus

Our studies demonstrated that the hippocampus utilizes two functional circuits, the trisynaptic and EC–CA1 loop circuits, to encode environmental information (Chapter 4). I will describe the functional implication of these two circuits by comparing them with previous *in vivo* recording studies in the hippocampus of behaving animals.

Many studies have focused on spatial information processing in the rodent hippocampus (Best et al., 2001). When examined *in vivo* in freely moving rodents, hippocampal neurons exhibit place-specific firing. By combining the activities of many such “place cells” the hippocampus creates a spatial map of the environment. Recently, several studies have focused on how the hippocampal spatial map is modified after changes in the geometry or sensory cues of the environment. Moser and his colleagues

reported that two distinct types of remapping were observed in hippocampal place cells, called rate or global remapping (Colgin et al., 2008). When animals experience prominent changes in the same spatial context, the firing rates of place cells are changed, although the preferred location of place cell firings is maintained, this is called rate remapping. In contrast, when animals experience significant changes in the spatial context itself, both location and frequency of place cell firings change, this is called global remapping (Leutgeb et al., 2004). The distinction between two types of remapping in hippocampal place cells may be crucial to understand how animals represent the environment.

In our behavioral experiments using c-Fos expression analysis, exposure to novel objects was designed to represent a prominent cue change in the same spatial context (cf to rate remapping), but the novel place exposure, as a result of changing the home cage was designed to represent a change in spatial context itself (cf to global remapping). Thus, we speculate that the hippocampal activation we observed after novel object or place exposure may correspond to rate or global remapping, respectively. If so, the differences in c-Fos expression patterns may represent some aspects of place cell remapping. After novel object exposure, neurons in area CA1 showed differential c-Fos expression along transverse-axis of area CA1, suggesting a dominant role of EC–CA1 circuit using topographic TA projections. In contrast, after novel place exposure, neurons in distal and proximal CA1 equally expressed c-Fos signals, implying that these neurons are primarily activated by Schaffer-collateral synapses. Thus, the differential activation of two distinct circuits, trisynaptic or EC–CA1, may be key to understanding the distinction between rate and global remapping. In addition, a differential control of MEC and LEC

inputs by neuromodulators may help to coordinate two functional circuits. Supporting this idea, Leutgeb et al. (2008) recently reported that LEC lesions selectively disrupted rate, but not global, remapping.

In area CA3 of the hippocampus, however, many studies suggest that activity patterns in area CA3 remain relatively, constant even with a slight change in input patterns, implying a role for CA3 in pattern completion (Marr, 1971; Nakazawa et al., 2002). However, if the difference in an input pattern exceeds a threshold, CA3 cells suddenly generate a totally different activity pattern (Guzowki et al., 2004). Considering this nonlinear pattern representation, activities in CA3 neurons may represent whether animals perceives the environmental context as the same or different. If this is the case, area CA1 may act as an integrator between contextual information represented in area CA3 (Schaffer-collateral pathway) and more sensory-bound information from the entorhinal cortex (TA pathway). Indeed, we observed significantly more c-Fos positive cells in area CA3 after novel place exposure, when compared to novel object exposure, which may imply that animals perceive the novel place as different context (Chapter 5).

6.3 Neuromodulators and Mental Disorders

Despite many efforts in neuroscience research, we are still far from understanding of the pathophysiology of mental disorders, such as schizophrenia, major depression, bipolar disorder, or autism. One of a few available clues for this problem is that almost all mental disorders are related to dysfunction of neuromodulators (Stahl, 2008). Indeed, drugs that control neuromodulator function can either exacerbate or

alleviate symptoms of many mental disorders. As our studies suggest, if a major role of neuromodulators is to coordinate interactions among brain areas, mental disorders may result from a disturbance in this coordination.

The brain is distributed system and the information acquired from the environment is processed in parallel (Gray et al., 1989). The hippocampus integrates two streams of distributed information from the MEC and LEC (Chapter 4; Manns and Eichenbaum, 2006). In our experiments using a model mouse of schizophrenia, we found that hippocampal slices prepared from these animals displayed a selective abnormality in DA-mediated control of one stream of information from the LEC (Chapter 5). The resulting imbalance in information integration could lead to the deficits in coherent perception associated with schizophrenia.

In addition to pathway selective control, neuromodulators also exert frequency-dependent modulation of synaptic transmission (Chapter 3). Our results indicate that neuromodulators play a key role in filtering specific information based on its frequency range. If patients have an abnormality in frequency-dependent synaptic modulation, they may also exhibit deficits in coordination of oscillatory activities among brain areas, which is an important mechanism to bind distributed information (Grey et al., 1989; Singer, 1999). Recent studies, indeed, support this hypothesis. Examination of auditory and visual responses to repetitive stimulation revealed a specific reduction in the power of beta and gamma frequency oscillations in schizophrenia patients (Kwon et al., 1999; Krishnan et al., 2005; Uhlhaas and Singer, 2006). Moreover, Uhlhaas et al. (2006) reported that schizophrenic patients exhibit deficits in the detection of images which

requires grouping of stimulus elements into coherent object representations (i.e., Gestalt perception). Corresponding to these perceptual deficits, patients display reduced synchrony in beta-band (20 – 40 Hz) oscillations (Uhlhaas et al., 2006).

Our results, together with previous studies, indicate that mental disorders may result from a disturbance in coordination among brain areas, which leads to impairments in coherent perception. Our studies, in addition, provide a possible functional linkage between neuromodulators and coordinated interactions among brain areas. Further investigations on neuromodulators-mediated control of distributed information will yield important insights into the pathophysiology of mental disorders.

REFERENCES

Abbott, L.F., and Nelson, S.B. (2000). Synaptic plasticity: taming the beast. Nat Neurosci *3 Suppl*, 1178-1183.

Abe, K., and Takeichi, M. (2007). NMDA-receptor activation induces calpain-mediated beta-catenin cleavages for triggering gene expression. Neuron *53*, 387-397.

Acquas, E., Wilson, C., and Fibiger, H.C. (1996). Conditioned and unconditioned stimuli increase frontal cortical and hippocampal acetylcholine release: effects of novelty, habituation, and fear. J Neurosci *16*, 3089-3096.

Adcock, R.A., Thangavel, A., Whitfield-Gabrieli, S., Knutson, B., and Gabrieli, J.D. (2006). Reward-motivated learning: mesolimbic activation precedes memory formation. Neuron *50*, 507-517.

Amaral, D., Lavenex, P (2007). Hippocampal Neuroanatomy. In The Hippocampus Book (Oxford: Oxford University Press).

Amaral, D.G., Ishizuka, N., and Claiborne, B. (1990). Neurons, numbers and the hippocampal network. Prog Brain Res *83*, 1-11.

Andersen, P., Blackstad, T.W., and Lomo, T. (1966). Location and identification of excitatory synapses on hippocampal pyramidal cells. Exp Brain Res *1*, 236-248.

Andersen, P., Bliss, T.V., Lomo, T., Olsen, L.I., and Skrede, K.K. (1969). Lamellar organization of hippocampal excitatory pathways. Acta Physiol Scand *76*, 4A-5A.

Andersen, P., Bliss, T.V., and Skrede, K.K. (1971). Unit analysis of hippocampal polulation spikes. Exp Brain Res *13*, 208-221.

Andrasfalvy, B.K., Makara, J.K., Johnston, D., and Magee, J.C. (2008). Altered synaptic and non-synaptic properties of CA1 pyramidal neurons in Kv4.2 knockout mice. J Physiol *586*, 3881-3892.

Andrasfalvy, B.K., Smith, M.A., Borchardt, T., Sprengel, R., and Magee, J.C. (2003). Impaired regulation of synaptic strength in hippocampal neurons from GluR1-deficient mice. J Physiol *552*, 35-45.

Ang, C.W., Carlson, G.C., and Coulter, D.A. (2005). Hippocampal CA1 circuitry dynamically gates direct cortical inputs preferentially at theta frequencies. J Neurosci *25*, 9567-9580.

Angrist, B., and Vankammen, D.P. (1984). Cns Stimulants as Tools in the Study of Schizophrenia. Trends in Neurosciences *7*, 388-390.

Aniksztejn, L., Charton, G., and Ben-Ari, Y. (1987). Selective release of endogenous zinc from the

hippocampal mossy fibers in situ. Brain Res *404*, 58-64.

Aston-Jones, G., and Cohen, J.D. (2005). An integrative theory of locus coeruleus-norepinephrine function: adaptive gain and optimal performance. Annu Rev Neurosci *28*, 403-450.

Axmacher, N., Mormann, F., Fernandez, G., Elger, C.E., and Fell, J. (2006). Memory formation by neuronal synchronization. Brain Res Rev *52*, 170-182.

Bekkers, J.M. (2000). Distribution and activation of voltage-gated potassium channels in cell-attached and outside-out patches from large layer 5 cortical pyramidal neurons of the rat. J Physiol *525 Pt 3*, 611-620.

Benes, F.M., Khan, Y., Vincent, S.L., and Wickramasinghe, R. (1996). Differences in the subregional and cellular distribution of GABAA receptor binding in the hippocampal formation of schizophrenic brain. Synapse *22*, 338-349.

Benes, F.M., Wickramasinghe, R., Vincent, S.L., Khan, Y., and Todtenkopf, M. (1997). Uncoupling of GABA(A) and benzodiazepine receptor binding activity in the hippocampal formation of schizophrenic brain. Brain Res *755*, 121-129.

Bergles, D.E., Doze, V.A., Madison, D.V., and Smith, S.J. (1996). Excitatory actions of norepinephrine on multiple classes of hippocampal CA1 interneurons. J Neurosci *16*, 572-585.

Bertolino, A., and Blasi, G. (2009). The genetics of schizophrenia. Neuroscience.

Best, P.J., White, A.M., and Minai, A. (2001). Spatial processing in the brain: the activity of hippocampal place cells. Annu Rev Neurosci *24*, 459-486.

Bird, C.M., and Burgess, N. (2008). The hippocampus and memory: insights from spatial processing. Nat Rev Neurosci *9*, 182-194.

Black, K.J., Hershey, T., Gado, M.H., and Perlmutter, J.S. (2000). Dopamine D(1) agonist activates temporal lobe structures in primates. J Neurophysiol *84*, 549-557.

Boling, W., Olivier, A., and Fabinyi, G. (2002). Historical contributions to the modern understanding of function in the central area. Neurosurgery *50*, 1296-1309, discussion 1309-1210.

Borrell, J., Vela, J.M., Arevalo-Martin, A., Molina-Holgado, E., and Guaza, C. (2002). Prenatal immune challenge disrupts sensorimotor gating in adult rats. Implications for the etiopathogenesis of schizophrenia. Neuropsychopharmacology *26*, 204-215.

Boyer, P., Phillips, J.L., Rousseau, F.L., and Ilivitsky, S. (2007). Hippocampal abnormalities and memory deficits: new evidence of a strong pathophysiological link in schizophrenia. Brain Res Rev *54*, 92-112.

Brankack, J., Seidenbecher, T., and Muller-Gartner, H.W. (1996). Task-relevant late positive component in

rats: is it related to hippocampal theta rhythm? Hippocampus *6*, 475-482.

Browning, M.D., Dudek, E.M., Rapier, J.L., Leonard, S., and Freedman, R. (1993). Significant reductions in synapsin but not synaptophysin specific activity in the brains of some schizophrenics. Biol Psychiatry *34*, 529-535.

Brun, V.H., Leutgeb, S., Wu, H.Q., Schwarcz, R., Witter, M.P., Moser, E.I., and Moser, M.B. (2008). Impaired spatial representation in CA1 after lesion of direct input from entorhinal cortex. Neuron *57*, 290-302.

Brun, V.H., Otnass, M.K., Molden, S., Steffenach, H.A., Witter, M.P., Moser, M.B., and Moser, E.I. (2002). Place cells and place recognition maintained by direct entorhinal-hippocampal circuitry. Science *296*, 2243-2246.

Buhusi, C.V., Gray, J.A., and Schmajuk, N.A. (1998). Perplexing effects of hippocampal lesions on latent inhibition: a neural network solution. Behav Neurosci *112*, 316-351.

Burmeister, M., McInnis, M.G., and Zollner, S. (2008). Psychiatric genetics: progress amid controversy. Nat Rev Genet *9*, 527-540.

Burrone, J., O'Byrne, M., and Murthy, V.N. (2002). Multiple forms of synaptic plasticity triggered by selective suppression of activity in individual neurons. Nature *420*, 414-418.

Burwell, R.D., and Amaral, D.G. (1998). Cortical afferents of the perirhinal, postrhinal, and entorhinal cortices of the rat. J Comp Neurol *398*, 179-205.

Buzsaki, G. (1996). The hippocampo-neocortical dialogue. Cereb Cortex *6*, 81-92.

Buzsaki, G. (2002). Theta oscillations in the hippocampus. Neuron *33*, 325-340.

Buzsaki, G., and Draguhn, A. (2004). Neuronal oscillations in cortical networks. Science *304*, 1926-1929.

Cajal, S.R.Y. (1911). Histologie du Systeme nerveux de l'hommes et des vertebres, Vol II (Paris: Maloine).

Canto, C.B., Wouterlood, F.G., and Witter, M.P. (2008). What does the anatomical organization of the entorhinal cortex tell us? Neural Plast *2008*, 381243.

Castle, M., Comoli, E., and Loewy, A.D. (2005). Autonomic brainstem nuclei are linked to the hippocampus. Neuroscience *134*, 657-669.

Chen, Z., Ito, K., Fujii, S., Miura, M., Furuse, H., Sasaki, H., Kaneko, K., Kato, H., and Miyakawa, H. (1996). Roles of dopamine receptors in long-term depression: enhancement via D1 receptors and inhibition via D2 receptors. Receptors Channels *4*, 1-8.

Cheney, D.L., Seyfarth, R.M. (1992). How Monkeys See the World: Inside the Mind of Another Species (Chicago, Illinois: University Of Chicago Press).

Chrobak, J.J., Lorincz, A., and Buzsaki, G. (2000). Physiological patterns in the hippocampo-entorhinal cortex system. Hippocampus *10*, 457-465.

Clark, R.E., and Martin, S.J. (2005). Interrogating rodents regarding their object and spatial memory. Curr Opin Neurobiol *15*, 593-598.

Cohen, B.J. (2003). Theory and practice of psychiatry (Oxford, UK: Oxford University Press).

Cohen, N.J., and Squire, L.R. (1980). Preserved learning and retention of pattern-analyzing skill in amnesia: dissociation of knowing how and knowing that. Science *210*, 207-210.

Cole, A.J., Saffen, D.W., Baraban, J.M., and Worley, P.F. (1989). Rapid increase of an immediate early gene messenger RNA in hippocampal neurons by synaptic NMDA receptor activation. Nature *340*, 474-476.

Colgin, L.L., Moser, E.I., and Moser, M.B. (2008). Understanding memory through hippocampal remapping. Trends Neurosci *31*, 469-477.

Comoli, E., Coizet, V., Boyes, J., Bolam, J.P., Canteras, N.S., Quirk, R.H., Overton, P.G., and Redgrave, P. (2003). A direct projection from superior colliculus to substantia nigra for detecting salient visual events. Nat Neurosci *6*, 974-980.

Correll, R.E., and Scoville, W.B. (1967). Significance of delay in the performance of monkeys with medial temporal lobe resections. Exp Brain Res *4*, 85-96.

Cotter, D., Wilson, S., Roberts, E., Kerwin, R., and Everall, I.P. (2000). Increased dendritic MAP2 expression in the hippocampus in schizophrenia. Schizophr Res *41*, 313-323.

Creese, I., Burt, D.R., and Snyder, S.H. (1976). Dopamine receptor binding predicts clinical and pharmacological potencies of antischizophrenic drugs. Science *192*, 481-483.

Dahl, D., and Sarvey, J.M. (1989). Norepinephrine induces pathway-specific long-lasting potentiation and depression in the hippocampal dentate gyrus. Proc Natl Acad Sci U S A *86*, 4776-4780.

Daitz, H.M., and Powell, T.P. (1954). Studies of the connexions of the fornix system. J Neurol Neurosurg Psychiatry *17*, 75-82.

Danion, J.M., Rizzo, L., and Bruant, A. (1999). Functional mechanisms underlying impaired recognition memory and conscious awareness in patients with schizophrenia. Arch Gen Psychiatry *56*, 639-644.

Davidsson, P., Gottfries, J., Bogdanovic, N., Ekman, R., Karlsson, I., Gottfries, C.G., and Blennow, K.

(1999). The synaptic-vesicle-specific proteins rab3a and synaptophysin are reduced in thalamus and related cortical brain regions in schizophrenic brains. Schizophr Res *40*, 23-29.

Davis, J.O., Phelps, J.A., and Bracha, H.S. (1995). Prenatal development of monozygotic twins and concordance for schizophrenia. Schizophr Bull *21*, 357-366.

Davis, K.L., Kahn, R.S., Ko, G., and Davidson, M. (1991). Dopamine in schizophrenia: a review and reconceptualization. Am J Psychiatry *148*, 1474-1486.

Deller, T., Adelmann, G., Nitsch, R., and Frotscher, M. (1996). The alvear pathway of the rat hippocampus. Cell Tissue Res *286*, 293-303.

Desmond, N.L., Scott, C.A., Jane, J.A., Jr., and Levy, W.B. (1994). Ultrastructural identification of entorhinal cortical synapses in CA1 stratum lacunosum-moleculare of the rat. Hippocampus *4*, 594-600.

Dobrunz, L.E., and Stevens, C.F. (1997). Heterogeneity of release probability, facilitation, and depletion at central synapses. Neuron *18*, 995-1008.

Dolan, R.J., and Fletcher, P.C. (1997). Dissociating prefrontal and hippocampal function in episodic memory encoding. Nature *388*, 582-585.

Dommett, E., Coizet, V., Blaha, C.D., Martindale, J., Lefebvre, V., Walton, N., Mayhew, J.E., Overton, P.G., and Redgrave, P. (2005). How visual stimuli activate dopaminergic neurons at short latency. Science *307*, 1476-1479.

Doniger, G.M., Foxe, J.J., Murray, M.M., Higgins, B.A., and Javitt, D.C. (2002). Impaired visual object recognition and dorsal/ventral stream interaction in schizophrenia. Arch Gen Psychiatry *59*, 1011-1020.

Dudman, J.T., Tsay, D., and Siegelbaum, S.A. (2007). A role for synaptic inputs at distal dendrites: instructive signals for hippocampal long-term plasticity. Neuron *56*, 866-879.

Dvorak-Carbone, H., and Schuman, E.M. (1999). Long-term depression of temporoammonic-CA1 hippocampal synaptic transmission. J Neurophysiol *81*, 1036-1044.

Dvorak-Carbone, H., and Schuman, E.M. (1999). Patterned activity in stratum lacunosum moleculare inhibits CA1 pyramidal neuron firing. J Neurophysiol *82*, 3213-3222.

Dwork, A.J. (1997). Postmortem studies of the hippocampal formation in schizophrenia. Schizophr Bull *23*, 385-402.

Eastwood, S.L., and Harrison, P.J. (1995). Decreased synaptophysin in the medial temporal lobe in schizophrenia demonstrated using immunoautoradiography. Neuroscience *69*, 339-343.

Eichenbaum, H. (2000). A cortical-hippocampal system for declarative memory. Nat Rev Neurosci *1*,

41-50.

El-Ghundi, M., Fletcher, P.J., Drago, J., Sibley, D.R., O'Dowd, B.F., and George, S.R. (1999). Spatial learning deficit in dopamine D(1) receptor knockout mice. Eur J Pharmacol *383*, 95-106.

Empson, R.M., and Heinemann, U. (1995). The perforant path projection to hippocampal area CA1 in the rat hippocampal-entorhinal cortex combined slice. J Physiol *484 (Pt 3)*, 707-720.

Engel, A.K., Fries, P., and Singer, W. (2001). Dynamic predictions: oscillations and synchrony in top-down processing. Nat Rev Neurosci *2*, 704-716.

Engel, A.K., and Singer, W. (2001). Temporal binding and the neural correlates of sensory awareness. Trends Cogn Sci *5*, 16-25.

Floresco, S.B., West, A.R., Ash, B., Moore, H., and Grace, A.A. (2003). Afferent modulation of dopamine neuron firing differentially regulates tonic and phasic dopamine transmission. Nat Neurosci *6*, 968-973.

Fortin, N.J., Agster, K.L., and Eichenbaum, H.B. (2002). Critical role of the hippocampus in memory for sequences of events. Nat Neurosci *5*, 458-462.

Francis, J.T., Gluckman, B.J., and Schiff, S.J. (2003). Sensitivity of neurons to weak electric fields. J Neurosci *23*, 7255-7261.

Fredens, K., Stengaard-Pedersen, K., and Larsson, L.I. (1984). Localization of enkephalin and cholecystokinin immunoreactivities in the perforant path terminal fields of the rat hippocampal formation. Brain Res *304*, 255-263.

Freund, T.F., and Buzsaki, G. (1996). Interneurons of the hippocampus. Hippocampus *6*, 347-470.

Fyhn, M., Molden, S., Hollup, S., Moser, M.B., and Moser, E. (2002). Hippocampal neurons responding to first-time dislocation of a target object. Neuron *35*, 555-566.

Fyhn, M., Molden, S., Witter, M.P., Moser, E.I., and Moser, M.B. (2004). Spatial representation in the entorhinal cortex. Science *305*, 1258-1264.

Gasbarri, A., Packard, M.G., Campana, E., and Pacitti, C. (1994a). Anterograde and retrograde tracing of projections from the ventral tegmental area to the hippocampal formation in the rat. Brain Res Bull *33*, 445-452.

Gasbarri, A., Packard, M.G., Sulli, A., Pacitti, C., Innocenzi, R., and Perciavalle, V. (1996a). The projections of the retrorubral field A8 to the hippocampal formation in the rat. Exp Brain Res *112*, 244-252.

Gasbarri, A., Sulli, A., Innocenzi, R., Pacitti, C., and Brioni, J.D. (1996b). Spatial memory impairment induced by lesion of the mesohippocampal dopaminergic system in the rat. Neuroscience *74*, 1037-1044.

Gasbarri, A., Sulli, A., and Packard, M.G. (1997). The dopaminergic mesencephalic projections to the hippocampal formation in the rat. Prog Neuropsychopharmacol Biol Psychiatry *21*, 1-22.

Gasbarri, A., Verney, C., Innocenzi, R., Campana, E., and Pacitti, C. (1994b). Mesolimbic dopaminergic neurons innervating the hippocampal formation in the rat: a combined retrograde tracing and immunohistochemical study. Brain Res *668*, 71-79.

Giocomo, L.M., Zilli, E.A., Fransen, E., and Hasselmo, M.E. (2007). Temporal frequency of subthreshold oscillations scales with entorhinal grid cell field spacing. Science *315*, 1719-1722.

Gluck, M.A., Myers, C.E. (2001). Gateway to Memory (Cambridge, Massachusetts: The MIT Press).

Gluckman, B.J., Neel, E.J., Netoff, T.I., Ditto, W.L., Spano, M.L., and Schiff, S.J. (1996). Electric field suppression of epileptiform activity in hippocampal slices. J Neurophysiol *76*, 4202-4205.

Golgi, C. (1886). *sulla fina anatomia degli organi centrali del sistma nervasa* (Milan: Hoepli).

Gottesman, I.I. (1991). Schizophrenia Genesis: The Origins of Madness. (New York, NY: W.H. Freeman & Company).

Grace, A.A. (1991). Phasic versus tonic dopamine release and the modulation of dopamine system responsivity: a hypothesis for the etiology of schizophrenia. Neuroscience *41*, 1-24.

Grace, A.A. (2000). Gating of information flow within the limbic system and the pathophysiology of schizophrenia. Brain Res Brain Res Rev *31*, 330-341.

Gray, C.M., Konig, P., Engel, A.K., and Singer, W. (1989). Oscillatory responses in cat visual cortex exhibit inter-columnar synchronization which reflects global stimulus properties. Nature *338*, 334-337.

Gray, J.A., Moran, P.M., Grigoryan, G., Peters, S.L., Young, A.M., and Joseph, M.H. (1997). Latent inhibition: the nucleus accumbens connection revisited. Behav Brain Res *88*, 27-34.

Greene, A.J. (2007). Human hippocampal-dependent tasks: is awareness necessary or sufficient? Hippocampus *17*, 429-433.

Grunwald, T., Lehnertz, K., Heinze, H.J., Helmstaedter, C., and Elger, C.E. (1998). Verbal novelty detection within the human hippocampus proper. Proc Natl Acad Sci U S A *95*, 3193-3197.

Guzowski, J.F., Knierim, J.J., and Moser, E.I. (2004). Ensemble dynamics of hippocampal regions CA3 and CA1. Neuron *44*, 581-584.

Guzowski, J.F., Timlin, J.A., Roysam, B., McNaughton, B.L., Worley, P.F., and Barnes, C.A. (2005). Mapping behaviorally relevant neural circuits with immediate-early gene expression. Curr Opin Neurobiol

15, 599-606.

Harding, A.J., Halliday, G.M., and Kril, J.J. (1998). Variation in hippocampal neuron number with age and brain volume. Cereb Cortex *8*, 710-718.

Hargreaves, E.L., Rao, G., Lee, I., and Knierim, J.J. (2005). Major dissociation between medial and lateral entorhinal input to dorsal hippocampus. Science *308*, 1792-1794.

Harley, C.W. (2004). Norepinephrine and dopamine as learning signals. Neural Plast *11*, 191-204.

Harrison, P.J. (1999). The neuropathology of schizophrenia. A critical review of the data and their interpretation. Brain *122 (Pt 4)*, 593-624.

Harrison, P.J., and Eastwood, S.L. (2001). Neuropathological studies of synaptic connectivity in the hippocampal formation in schizophrenia. Hippocampus *11*, 508-519.

Hartley, T., Bird, C.M., Chan, D., Cipolotti, L., Husain, M., Vargha-Khadem, F., and Burgess, N. (2007). The hippocampus is required for short-term topographical memory in humans. Hippocampus *17*, 34-48.

Hassabis, D., Kumaran, D., Vann, S.D., and Maguire, E.A. (2007). Patients with hippocampal amnesia cannot imagine new experiences. Proc Natl Acad Sci U S A *104*, 1726-1731.

Hasselmo, M.E. (1995). Neuromodulation and cortical function: modeling the physiological basis of behavior. Behav Brain Res *67*, 1-27.

Hasselmo, M.E., and Schnell, E. (1994). Laminar selectivity of the cholinergic suppression of synaptic transmission in rat hippocampal region CA1: computational modeling and brain slice physiology. J Neurosci *14*, 3898-3914.

Hasselmo, M.E., Wyble, B.P., and Wallenstein, G.V. (1996). Encoding and retrieval of episodic memories: role of cholinergic and GABAergic modulation in the hippocampus. Hippocampus *6*, 693-708.

Heckers, S., and Konradi, C. (2002). Hippocampal neurons in schizophrenia. J Neural Transm *109*, 891-905.

Heine, M., Groc, L., Frischknecht, R., Beique, J.C., Lounis, B., Rumbaugh, G., Huganir, R.L., Cognet, L., and Choquet, D. (2008). Surface mobility of postsynaptic AMPARs tunes synaptic transmission. Science *320*, 201-205.

Henze, D.A., Wittner, L., and Buzsaki, G. (2002). Single granule cells reliably discharge targets in the hippocampal CA3 network in vivo. Nat Neurosci *5*, 790-795.

Hjorth-Simonsen, A. (1973). Some intrinsic connections of the hippocampus in the rat: an experimental analysis. J Comp Neurol *147*, 145-161.

Hoffman, D.A., Magee, J.C., Colbert, C.M., and Johnston, D. (1997). K+ channel regulation of signal propagation in dendrites of hippocampal pyramidal neurons. Nature *387*, 869-875.

Hopf, F.W., Cascini, M.G., Gordon, A.S., Diamond, I., and Bonci, A. (2003). Cooperative activation of dopamine D1 and D2 receptors increases spike firing of nucleus accumbens neurons via G-protein betagamma subunits. J Neurosci *23*, 5079-5087.

Horvitz, J.C. (2000). Mesolimbocortical and nigrostriatal dopamine responses to salient non-reward events. Neuroscience *96*, 651-656.

Howell, G.A., Welch, M.G., and Frederickson, C.J. (1984). Stimulation-induced uptake and release of zinc in hippocampal slices. Nature *308*, 736-738.

Huang, Y.Y., and Kandel, E.R. (1995). D1/D5 receptor agonists induce a protein synthesis-dependent late potentiation in the CA1 region of the hippocampus. Proc Natl Acad Sci U S A *92*, 2446-2450.

Hutcheon, B., and Yarom, Y. (2000). Resonance, oscillation and the intrinsic frequency preferences of neurons. Trends Neurosci *23*, 216-222.

Ihalainen, J.A., Riekkinen, P., Jr., and Feenstra, M.G. (1999). Comparison of dopamine and noradrenaline release in mouse prefrontal cortex, striatum and hippocampus using microdialysis. Neurosci Lett *277*, 71-74.

Ikemoto, S., Glazier, B.S., Murphy, J.M., and McBride, W.J. (1997). Role of dopamine D1 and D2 receptors in the nucleus accumbens in mediating reward. J Neurosci *17*, 8580-8587.

Insausti, R., Herrero, M.T., and Witter, M.P. (1997). Entorhinal cortex of the rat: cytoarchitectonic subdivisions and the origin and distribution of cortical efferents. Hippocampus *7*, 146-183.

Ito, H.T., and Schuman, E.M. (2007). Frequency-dependent gating of synaptic transmission and plasticity by dopamine. Front Neural Circuits *1*, 1.

Ito, H.T., and Schuman, E.M. (2008). Frequency-dependent signal transmission and modulation by neuromodulators. Front Neurosci *2*, 138-144.

Jarsky, T., Roxin, A., Kath, W.L., and Spruston, N. (2005). Conditional dendritic spike propagation following distal synaptic activation of hippocampal CA1 pyramidal neurons. Nat Neurosci *8*, 1667-1676.

Jefferys, J.G., Deans, J., Bikson, M., and Fox, J. (2003). Effects of weak electric fields on the activity of neurons and neuronal networks. Radiat Prot Dosimetry *106*, 321-323.

Jurkowlaniec, E., Tokarski, J., and Trojniar, W. (2003). Effect of unilateral ibotenate lesions of the ventral tegmental area on cortical and hippocampal EEG in freely behaving rats. Acta Neurobiol Exp (Wars) *63*,

369-375.

Katsuki, H., Izumi, Y., and Zorumski, C.F. (1997). Noradrenergic regulation of synaptic plasticity in the hippocampal CA1 region. J Neurophysiol *77*, 3013-3020.

Katz, B., and Miledi, R. (1968). The role of calcium in neuromuscular facilitation. J Physiol *195*, 481-492.

Katz, D.B., Rogers, R.F., and Steinmetz, J.E. (2002). Novel factors contributing to the expression of latent inhibition. Behav Neurosci *116*, 824-836.

Kaye, H., and Pearce, J.M. (1987). Hippocampal lesions attenuate latent inhibition and the decline of the orienting response in rats. Q J Exp Psychol B *39*, 107-125.

Kessels, H.W., Kopec, C.D., Klein, M.E., and Malinow, R. (2009). Roles of stargazin and phosphorylation in the control of AMPA receptor subcellular distribution. Nat Neurosci *12*, 888-896.

Kiss, J., Buzsaki, G., Morrow, J.S., Glantz, S.B., and Leranth, C. (1996). Entorhinal cortical innervation of parvalbumin-containing neurons (Basket and Chandelier cells) in the rat Ammon's horn. Hippocampus *6*, 239-246.

Kitchigina, V., Vankov, A., Harley, C., and Sara, S.J. (1997). Novelty-elicited, noradrenaline-dependent enhancement of excitability in the dentate gyrus. Eur J Neurosci *9*, 41-47.

Knierim, J.J., Lee, I., and Hargreaves, E.L. (2006). Hippocampal place cells: parallel input streams, subregional processing, and implications for episodic memory. Hippocampus *16*, 755-764.

Knight, R. (1996). Contribution of human hippocampal region to novelty detection. Nature *383*, 256-259.

Kodama, T., Honda, Y., Watanabe, M., and Hikosaka, K. (2002). Release of neurotransmitters in the monkey frontal cortex is related to level of attention. Psychiatry Clin Neurosci *56*, 341-342.

Koganezawa, N., Taguchi, A., Tominaga, T., Ohara, S., Tsutsui, K., Witter, M.P., and Iijima, T. (2008). Significance of the deep layers of entorhinal cortex for transfer of both perirhinal and amygdala inputs to the hippocampus. Neurosci Res *61*, 172-181.

Koike-Tani, M., Kanda, T., Saitoh, N., Yamashita, T., and Takahashi, T. (2008). Involvement of AMPA receptor desensitization in short-term synaptic depression at the calyx of Held in developing rats. J Physiol *586*, 2263-2275.

Korngreen, A., and Sakmann, B. (2000). Voltage-gated K+ channels in layer 5 neocortical pyramidal neurones from young rats: subtypes and gradients. J Physiol *525 Pt 3*, 621-639.

Krishnan, G.P., Vohs, J.L., Hetrick, W.P., Carroll, C.A., Shekhar, A., Bockbrader, M.A., and O'Donnell, B.F. (2005). Steady state visual evoked potential abnormalities in schizophrenia. Clin Neurophysiol *116*,

614-624.

Kumaran, D., and Maguire, E.A. (2006). An unexpected sequence of events: mismatch detection in the human hippocampus. PLoS Biol *4*, e424.

Kumaran, D., and Maguire, E.A. (2007). Which computational mechanisms operate in the hippocampus during novelty detection? Hippocampus *17*, 735-748.

Kumaran, D., and Maguire, E.A. (2009). Novelty signals: a window into hippocampal information processing. Trends Cogn Sci *13*, 47-54.

Kwon, J.S., O'Donnell, B.F., Wallenstein, G.V., Greene, R.W., Hirayasu, Y., Nestor, P.G., Hasselmo, M.E., Potts, G.F., Shenton, M.E., and McCarley, R.W. (1999). Gamma frequency-range abnormalities to auditory stimulation in schizophrenia. Arch Gen Psychiatry *56*, 1001-1005.

Lacaille, J.C., and Schwartzkroin, P.A. (1988). Stratum lacunosum-moleculare interneurons of hippocampal CA1 region. II. Intrasomatic and intradendritic recordings of local circuit synaptic interactions. J Neurosci *8*, 1411-1424.

Laurent, G. (2002). Olfactory network dynamics and the coding of multidimensional signals. Nat Rev Neurosci *3*, 884-895.

Laurent, G., and Davidowitz, H. (1994). Encoding of Olfactory Information with Oscillating Neural Assemblies. Science *265*, 1872-1875.

Law, A.J., Weickert, C.S., Hyde, T.M., Kleinman, J.E., and Harrison, P.J. (2004). Reduced spinophilin but not microtubule-associated protein 2 expression in the hippocampal formation in schizophrenia and mood disorders: molecular evidence for a pathology of dendritic spines. Am J Psychiatry *161*, 1848-1855.

Leca, J.B., Nahallage, C.A., Gunst, N., and Huffman, M.A. (2008). Stone-throwing by Japanese macaques: form and functional aspects of a group-specific behavioral tradition. J Hum Evol *55*, 989-998.

Lee, A.C., Bussey, T.J., Murray, E.A., Saksida, L.M., Epstein, R.A., Kapur, N., Hodges, J.R., and Graham, K.S. (2005). Perceptual deficits in amnesia: challenging the medial temporal lobe 'mnemonic' view. Neuropsychologia *43*, 1-11.

Lee, I., Yoganarasimha, D., Rao, G., and Knierim, J.J. (2004). Comparison of population coherence of place cells in hippocampal subfields CA1 and CA3. Nature *430*, 456-459.

Lee, S.P., So, C.H., Rashid, A.J., Varghese, G., Cheng, R., Lanca, A.J., O'Dowd, B.F., and George, S.R. (2004). Dopamine D1 and D2 receptor Co-activation generates a novel phospholipase C-mediated calcium signal. J Biol Chem *279*, 35671-35678.

Leutgeb, J.K., Henriksen, E.J., Leutgeb, S., Witter, M.P., Moser, M.B., and Moser, E. (2008). Hippocampal

rate coding depends on input from the lateral entorhinal cortex In SfN meeting (Washington DC).

Leutgeb, J.K., Leutgeb, S., Moser, M.B., and Moser, E.I. (2007). Pattern separation in the dentate gyrus and CA3 of the hippocampus. Science *315*, 961-966.

Leutgeb, S., Leutgeb, J.K., Treves, A., Moser, M.B., and Moser, E.I. (2004). Distinct ensemble codes in hippocampal areas CA3 and CA1. Science *305*, 1295-1298.

Levy, W.B., Desmond, N.L., and Zhang, D.X. (1998). Perforant path activation modulates the induction of long-term potentiation of the schaffer collateral--hippocampal CA1 response: theoretical and experimental analyses. Learn Mem *4*, 510-518.

Li, S., Cullen, W.K., Anwyl, R., and Rowan, M.J. (2003). Dopamine-dependent facilitation of LTP induction in hippocampal CA1 by exposure to spatial novelty. Nat Neurosci *6*, 526-531.

Li, X.G., Somogyi, P., Ylinen, A., and Buzsaki, G. (1994). The hippocampal CA3 network: an in vivo intracellular labeling study. J Comp Neurol *339*, 181-208.

Lieberman, J.A., Kane, J.M., and Alvir, J. (1987). Provocative tests with psychostimulant drugs in schizophrenia. Psychopharmacology (Berl) *91*, 415-433.

Lipska, B.K., Jaskiw, G.E., and Weinberger, D.R. (1993). Postpubertal emergence of hyperresponsiveness to stress and to amphetamine after neonatal excitotoxic hippocampal damage: a potential animal model of schizophrenia. Neuropsychopharmacology *9*, 67-75.

Lisman, J.E., and Grace, A.A. (2005). The hippocampal-VTA loop: controlling the entry of information into long-term memory. Neuron *46*, 703-713.

Lisman, J.E., and Otmakhova, N.A. (2001). Storage, recall, and novelty detection of sequences by the hippocampus: elaborating on the SOCRATIC model to account for normal and aberrant effects of dopamine. Hippocampus *11*, 551-568.

London, M., and Segev, I. (2001). Synaptic scaling in vitro and in vivo. Nat Neurosci *4*, 853-855.

Lowe, G.C., Luheshi, G.N., and Williams, S. (2008). Maternal infection and fever during late gestation are associated with altered synaptic transmission in the hippocampus of juvenile offspring rats. Am J Physiol Regul Integr Comp Physiol *295*, R1563-1571.

Magee, J.C., and Cook, E.P. (2000). Somatic EPSP amplitude is independent of synapse location in hippocampal pyramidal neurons. Nat Neurosci *3*, 895-903.

Manns, J.R., and Eichenbaum, H. (2006). Evolution of declarative memory. Hippocampus *16*, 795-808.

Markram, H., Gupta, A., Uziel, A., Wang, Y., and Tsodyks, M. (1998). Information processing with

frequency-dependent synaptic connections. Neurobiol Learn Mem *70*, 101-112.

Marr, D. (1971). Simple memory: a theory for archicortex. Philos Trans R Soc Lond B Biol Sci *262*, 23-81.

Matsumoto, M., and Hikosaka, O. (2009). Two types of dopamine neuron distinctly convey positive and negative motivational signals. Nature *459*, 837-841.

Mazur, J.E. (2006). Learning and Behavior (Upper Saddle River, New Jersey: Pearson Prentice Hall).

McClure, S.M., Daw, N.D., and Montague, P.R. (2003). A computational substrate for incentive salience. Trends Neurosci *26*, 423-428.

McLaughlin, S., and Poo, M.M. (1981). The role of electro-osmosis in the electric-field-induced movement of charged macromolecules on the surfaces of cells. Biophys J *34*, 85-93.

Mednick, S.A., Machon, R.A., Huttunen, M.O., and Bonett, D. (1988). Adult schizophrenia following prenatal exposure to an influenza epidemic. Arch Gen Psychiatry *45*, 189-192.

Meffert, M.K., Chang, J.M., Wiltgen, B.J., Fanselow, M.S., and Baltimore, D. (2003). NF-kappa B functions in synaptic signaling and behavior. Nat Neurosci *6*, 1072-1078.

Megias, M., Emri, Z., Freund, T.F., and Gulyas, A.I. (2001). Total number and distribution of inhibitory and excitatory synapses on hippocampal CA1 pyramidal cells. Neuroscience *102*, 527-540.

Meltzer, J.A., and Constable, R.T. (2005). Activation of human hippocampal formation reflects success in both encoding and cued recall of paired associates. Neuroimage *24*, 384-397.

Miller, K.D. (1996). Synaptic economics: competition and cooperation in synaptic plasticity. Neuron *17*, 371-374.

Miller, K.D., and Mackay, D.J.C. (1994). The Role of Constraints in Hebbian Learning. Neural Computation *6*, 100-126.

Missale, C., Nash, S.R., Robinson, S.W., Jaber, M., and Caron, M.G. (1998). Dopamine receptors: from structure to function. Physiol Rev *78*, 189-225.

Montague, P.R., Hyman, S.E., and Cohen, J.D. (2004). Computational roles for dopamine in behavioural control. Nature *431*, 760-767.

Morgan, J.I., and Curran, T. (1991). Stimulus-transcription coupling in the nervous system: involvement of the inducible proto-oncogenes fos and jun. Annu Rev Neurosci *14*, 421-451.

Mori, M., Abegg, M.H., Gahwiler, B.H., and Gerber, U. (2004). A frequency-dependent switch from inhibition to excitation in a hippocampal unitary circuit. Nature *431*, 453-456.

Morris, R. (1984). Developments of a water-maze procedure for studying spatial learning in the rat. J Neurosci Methods *11*, 47-60.

Morris, R.G. (2001). Episodic-like memory in animals: psychological criteria, neural mechanisms and the value of episodic-like tasks to investigate animal models of neurodegenerative disease. Philos Trans R Soc Lond B Biol Sci *356*, 1453-1465.

Murchison, C.F., Zhang, X.Y., Zhang, W.P., Ouyang, M., Lee, A., and Thomas, S.A. (2004). A distinct role for norepinephrine in memory retrieval. Cell *117*, 131-143.

Myers, C.E., and Gluck, M.A. (1994). Context, conditioning, and hippocampal rerepresentation in animal learning. Behav Neurosci *108*, 835-847.

Naber, P.A., Witter, M.P., and Lopez da Silva, F.H. (1999). Perirhinal cortex input to the hippocampus in the rat: evidence for parallel pathways, both direct and indirect. A combined physiological and anatomical study. Eur J Neurosci *11*, 4119-4133.

Nakashiba, T., Young, J.Z., McHugh, T.J., Buhl, D.L., and Tonegawa, S. (2008). Transgenic inhibition of synaptic transmission reveals role of CA3 output in hippocampal learning. Science *319*, 1260-1264.

Nakazawa, K., Quirk, M.C., Chitwood, R.A., Watanabe, M., Yeckel, M.F., Sun, L.D., Kato, A., Carr, C.A., Johnston, D., Wilson, M.A., and Tonegawa, S. (2002). Requirement for hippocampal CA3 NMDA receptors in associative memory recall. Science *297*, 211-218.

Nauta, W.J.H. (1950). Uber die sogenannte terminale Degeneration in der Zentralnervensystem und ihre Darstellung durch Silberimpragnation. Schweizer Archiv fur Neurologie und Psychiatrie *66*, 353-376.

Nelson, M.D., Saykin, A.J., Flashman, L.A., and Riordan, H.J. (1998). Hippocampal volume reduction in schizophrenia as assessed by magnetic resonance imaging: a meta-analytic study. Arch Gen Psychiatry *55*, 433-440.

Nicholson, D.A., Trana, R., Katz, Y., Kath, W.L., Spruston, N., and Geinisman, Y. (2006). Distance-dependent differences in synapse number and AMPA receptor expression in hippocampal CA1 pyramidal neurons. Neuron *50*, 431-442.

O'Keefe, J., and Dostrovsky, J. (1971). The hippocampus as a spatial map. Preliminary evidence from unit activity in the freely-moving rat. Brain Res *34*, 171-175.

Okubo, Y., Suhara, T., Suzuki, K., Kobayashi, K., Inoue, O., Terasaki, O., Someya, Y., Sassa, T., Sudo, Y., Matsushima, E.*, et al.* (1997). Decreased prefrontal dopamine D1 receptors in schizophrenia revealed by PET. Nature *385*, 634-636.

Orida, N., and Poo, M.M. (1978). Electrophoretic movement and localisation of acetylcholine receptors in

the embryonic muscle cell membrane. Nature *275*, 31-35.

Orzel-Gryglewska, J., Jurkowlaniec, E., and Trojniar, W. (2006). Microinjection of procaine and electrolytic lesion in the ventral tegmental area suppresses hippocampal theta rhythm in urethane-anesthetized rats. Brain Res Bull *68*, 295-309.

Osipova, D., Takashima, A., Oostenveld, R., Fernandez, G., Maris, E., and Jensen, O. (2006). Theta and gamma oscillations predict encoding and retrieval of declarative memory. J Neurosci *26*, 7523-7531.

Otmakhova, N.A., Lewey, J., Asrican, B., and Lisman, J.E. (2005). Inhibition of perforant path input to the CA1 region by serotonin and noradrenaline. J Neurophysiol *94*, 1413-1422.

Otmakhova, N.A., and Lisman, J.E. (1996). D1/D5 dopamine receptor activation increases the magnitude of early long-term potentiation at CA1 hippocampal synapses. J Neurosci *16*, 7478-7486.

Otmakhova, N.A., and Lisman, J.E. (1998). D1/D5 dopamine receptors inhibit depotentiation at CA1 synapses via cAMP-dependent mechanism. J Neurosci *18*, 1270-1279.

Otmakhova, N.A., and Lisman, J.E. (1999). Dopamine selectively inhibits the direct cortical pathway to the CA1 hippocampal region. J Neurosci *19*, 1437-1445.

Palva, S., and Palva, J.M. (2007). New vistas for alpha-frequency band oscillations. Trends Neurosci *30*, 150-158.

Papez , J.W. (1937). A proposed mechanism of emotion. Arch Neurol Psychiatry *38*, 725-743.

Parkin, A.J. (1997). Human memory: novelty, association and the brain. Curr Biol *7*, R768-769.

Passingham, R.E., Stephan, K.E., and Kotter, R. (2002). The anatomical basis of functional localization in the cortex. Nat Rev Neurosci *3*, 606-616.

Patel, N., and Poo, M.M. (1982). Orientation of neurite growth by extracellular electric fields. J Neurosci *2*, 483-496.

Patterson, P.H. (2007). Neuroscience. Maternal effects on schizophrenia risk. Science *318*, 576-577.

Patterson, P.H. (2008). Immune involvement in schizophrenia and autism: Etiology, pathology and animal models. Behav Brain Res.

Paulsen, O., and Moser, E.I. (1998). A model of hippocampal memory encoding and retrieval: GABAergic control of synaptic plasticity. Trends Neurosci *21*, 273-278.

Pavlov, I. (1903). The Experimental Psychology and Psychopathology of Animals. In International Medical Congress.

Penner, J.D., and Brown, A.S. (2007). Prenatal infectious and nutritional factors and risk of adult schizophrenia. Expert Rev Neurother *7*, 797-805.

Plaznik, A., Stefanski, R., and Kostowski, W. (1989). Interaction between accumbens D1 and D2 receptors regulating rat locomotor activity. Psychopharmacology (Berl) *99*, 558-562.

Poo, M.M., Poo, W.J., and Lam, J.W. (1978). Lateral electrophoresis and diffusion of Concanavalin A receptors in the membrane of embryonic muscle cell. J Cell Biol *76*, 483-501.

Port, R.L., and Patterson, M.M. (1984). Fimbrial lesions and sensory preconditioning. Behav Neurosci *98*, 584-589.

Pouille, F., and Scanziani, M. (2004). Routing of spike series by dynamic circuits in the hippocampus. Nature *429*, 717-723.

Quirk, G.J., Muller, R.U., Kubie, J.L., and Ranck, J.B., Jr. (1992). The positional firing properties of medial entorhinal neurons: description and comparison with hippocampal place cells. J Neurosci *12*, 1945-1963.

Quiroga, R.Q., Reddy, L., Kreiman, G., Koch, C., and Fried, I. (2005). Invariant visual representation by single neurons in the human brain. Nature *435*, 1102-1107.

Rabinowitch, I., and Segev, I. (2008). Two opposing plasticity mechanisms pulling a single synapse. Trends Neurosci *31*, 377-383.

Ranganath, C., and Rainer, G. (2003). Neural mechanisms for detecting and remembering novel events. Nat Rev Neurosci *4*, 193-202.

Rashid, A.J., So, C.H., Kong, M.M., Furtak, T., El-Ghundi, M., Cheng, R., O'Dowd, B.F., and George, S.R. (2007). D1-D2 dopamine receptor heterooligomers with unique pharmacology are coupled to rapid activation of Gq/11 in the striatum. Proc Natl Acad Sci U S A *104*, 654-659.

Reiss, S., Wagner, A.R. (1972). CS habituation produces a "latent inhibition" effect but no active conditioned inhibition. Learning and Motivation *3*, 237-245.

Remondes, M., and Schuman, E.M. (2002). Direct cortical input modulates plasticity and spiking in CA1 pyramidal neurons. Nature *416*, 736-740.

Remondes, M., and Schuman, E.M. (2004). Role for a cortical input to hippocampal area CA1 in the consolidation of a long-term memory. Nature *431*, 699-703.

Riedel, G., Micheau, J., Lam, A.G., Roloff, E.L., Martin, S.J., Bridge, H., de Hoz, L., Poeschel, B., McCulloch, J., and Morris, R.G. (1999). Reversible neural inactivation reveals hippocampal participation in

several memory processes. Nat Neurosci *2*, 898-905.

Rizley, R.C., and Rescorla, R.A. (1972). Associations in second-order conditioning and sensory preconditioning. J Comp Physiol Psychol *81*, 1-11.

Rizzo, L., Danion, J.M, Van Der Linden, M., Grangé, D., Rohmer, JG. (1996). Impairment of memory for spatial context in schizophrenia. Neuropsychology *Vol 10(3)*, 376-384.

Robbins, T.W. (2005). Chemistry of the mind: neurochemical modulation of prefrontal cortical function. J Comp Neurol *493*, 140-146.

Rudy, J.W., and Sutherland, R.J. (1995). Configural association theory and the hippocampal formation: an appraisal and reconfiguration. Hippocampus *5*, 375-389.

Rutishauser, U., Mamelak, A.N., and Schuman, E.M. (2006). Single-trial learning of novel stimuli by individual neurons of the human hippocampus-amygdala complex. Neuron *49*, 805-813.

Sagar, H.J., Cohen, N.J., Corkin, S., and Growdon, J.H. (1985). Dissociations among processes in remote memory. Ann N Y Acad Sci *444*, 533-535.

Sara, S.J. (2009). The locus coeruleus and noradrenergic modulation of cognition. Nat Rev Neurosci *10*, 211-223.

Sara, S.J., Dyon-Laurent, C., and Herve, A. (1995). Novelty seeking behavior in the rat is dependent upon the integrity of the noradrenergic system. Brain Res Cogn Brain Res *2*, 181-187.

Sato, M.J., Kuwayama, H., van Egmond, W.N., Takayama, A.L., Takagi, H., van Haastert, P.J., Yanagida, T., and Ueda, M. (2009). Switching direction in electric-signal-induced cell migration by cyclic guanosine monophosphate and phosphatidylinositol signaling. Proc Natl Acad Sci U S A *106*, 6667-6672.

Schmidt, H.D., and Pierce, R.C. (2006). Cooperative activation of D1-like and D2-like dopamine receptors in the nucleus accumbens shell is required for the reinstatement of cocaine-seeking behavior in the rat. Neuroscience *142*, 451-461.

Schultz, W. (1998). Predictive reward signal of dopamine neurons. J Neurophysiol *80*, 1-27.

Schultz, W., and Dickinson, A. (2000). Neuronal coding of prediction errors. Annu Rev Neurosci *23*, 473-500.

Scoville, W.B., and Milner, B. (1957). Loss of recent memory after bilateral hippocampal lesions. J Neurochem *20*, 11-21.

Sebestikova, L., Slamova, E., and Sevcikova, H. (2005). Control of wave propagation in a biological excitable medium by an external electric field. Biophys Chem *113*, 269-274.

Shepherd, G.M. (2004). The synaptic organization of the brain (Oxford university press).

Shi, L., Fatemi, S.H., Sidwell, R.W., and Patterson, P.H. (2003). Maternal influenza infection causes marked behavioral and pharmacological changes in the offspring. J Neurosci *23*, 297-302.

Shigemoto, R., Kinoshita, A., Wada, E., Nomura, S., Ohishi, H., Takada, M., Flor, P.J., Neki, A., Abe, T., Nakanishi, S., and Mizuno, N. (1997). Differential presynaptic localization of metabotropic glutamate receptor subtypes in the rat hippocampus. J Neurosci *17*, 7503-7522.

Siapas, A.G., Lubenov, E.V., and Wilson, M.A. (2005). Prefrontal phase locking to hippocampal theta oscillations. Neuron *46*, 141-151.

Siegel, S.J., Agranoff, B.W., Albers, R.W., Fisher, S.K., Uhler, M.D. (1999). Basic Neuochemistry (Lippincott Williams & Wilkins).

Singer, W. (1999). Neuronal synchrony: a versatile code for the definition of relations? Neuron *24*, 49-65, 111-125.

Smialowski, A. (1976). The effect of intrahippocampal administration of dopamine or apomorphine on EEG of limbic structures in the rabbit brain. Pol J Pharmacol Pharm *28*, 579-585.

Smith, D.M., and Mizumori, S.J. (2006). Hippocampal place cells, context, and episodic memory. Hippocampus *16*, 716-729.

Smith, M.A., Ellis-Davies, G.C., and Magee, J.C. (2003). Mechanism of the distance-dependent scaling of Schaffer collateral synapses in rat CA1 pyramidal neurons. J Physiol *548*, 245-258.

Sorra, K.E., and Harris, K.M. (1993). Occurrence and three-dimensional structure of multiple synapses between individual radiatum axons and their target pyramidal cells in hippocampal area CA1. J Neurosci *13*, 3736-3748.

Squire, L.R., Stark, C.E., and Clark, R.E. (2004). The medial temporal lobe. Annu Rev Neurosci *27*, 279-306.

Stahl, S.M. (2008). Stahl's Essential Psychopharmacology (Cambridge: Cambridge University Press).

Steffenach, H.A., Sloviter, R.S., Moser, E.I., and Moser, M.B. (2002). Impaired retention of spatial memory after transection of longitudinally oriented axons of hippocampal CA3 pyramidal cells. Proc Natl Acad Sci U S A *99*, 3194-3198.

Stellwagen, D., and Malenka, R.C. (2006). Synaptic scaling mediated by glial TNF-alpha. Nature *440*, 1054-1059.

Stengaard-Pedersen, K., Fredens, K., and Larsson, L.I. (1981). Enkephalin and zinc in the hippocampal mossy fiber System. Brain Res *212*, 230-233.

Steriade, M. (2001). Impact of network activities on neuronal properties in corticothalamic systems. J Neurophysiol *86*, 1-39.

Stern, C.E., Corkin, S., Gonzalez, R.G., Guimaraes, A.R., Baker, J.R., Jennings, P.J., Carr, C.A., Sugiura, R.M., Vedantham, V., and Rosen, B.R. (1996). The hippocampal formation participates in novel picture encoding: evidence from functional magnetic resonance imaging. Proc Natl Acad Sci U S A *93*, 8660-8665.

Steward, O., and Scoville, S.A. (1976). Cells of origin of entorhinal cortical afferents to the hippocampus and fascia dentata of the rat. J Comp Neurol *169*, 347-370.

Storm-Mathisen, J. (1978). Localization of putative transmitters in the hippocampal formation. In Functions of the septo-hippocampal system (Amsterdam: Elsevier-Excerpta Medica).

Straughan, D.W. (1975). Neurotransmitters and the hippocampus. In The hippocampus (New York: Plenum Press).

Sutton, M.A., Ito, H.T., Cressy, P., Kempf, C., Woo, J.C., and Schuman, E.M. (2006). Miniature neurotransmission stabilizes synaptic function via tonic suppression of local dendritic protein synthesis. Cell *125*, 785-799.

Sutton, M.A., and Schuman, E.M. (2006). Dendritic protein synthesis, synaptic plasticity, and memory. Cell *127*, 49-58.

Swanson, L. (1987). The limbic region I. The septohippocampal system. In Handbook of Chemical neuroanatomy (Amsterdam: Elsevier), pp. 125-227.

Swanson, L.W. (1982). The projections of the ventral tegmental area and adjacent regions: a combined fluorescent retrograde tracer and immunofluorescence study in the rat. Brain Res Bull *9*, 321-353.

Takakusaki, K., Saitoh, K., Miyokawa, N., and Koyama, Y. (2006). Neurobiological basis of state-dependent control of motor behaviors. Sleep and Biological Rhythms *4*, 87-104.

Tamamaki, N., and Nojyo, Y. (1995). Preservation of topography in the connections between the subiculum, field CA1, and the entorhinal cortex in rats. J Comp Neurol *353*, 379-390.

Taussig, R., Iniguez-Lluhi, J.A., and Gilman, A.G. (1993). Inhibition of adenylyl cyclase by Gi alpha. Science *261*, 218-221.

Thompson, S. (1982). Aminopyridine block of transient potassium current. J Gen Physiol *80*, 1-18.

Thorndike, E.L. (1898). Animal intelligence: An experimental study of the associative processes in animals. Psychological Review Monograph Supplement *2*, 8.

Toda, M., and Abi-Dargham, A. (2007). Dopamine hypothesis of schizophrenia: making sense of it all. Curr Psychiatry Rep *9*, 329-336.

Tolman, E.C., Honzik, C.H. (1930). Introduction and removal of reward, and maze performance in rats. University of California Publications in Psychology *4*, 257-275.

Treves, A., and Rolls, E.T. (1994). Computational analysis of the role of the hippocampus in memory. Hippocampus *4*, 374-391.

Tucek, S., Michal, P., and Vlachova, V. (2002). Modelling the consequences of receptor-G-protein promiscuity. Trends Pharmacol Sci *23*, 171-176.

Tulving, E. (1972). Episodic and semantic memory. In Organization and memory, E. Tulving, and E. Donaldson, eds. (San Diego: Academic Press).

Turrigiano, G.G. (2008). The self-tuning neuron: synaptic scaling of excitatory synapses. Cell *135*, 422-435.

Turrigiano, G.G., Leslie, K.R., Desai, N.S., Rutherford, L.C., and Nelson, S.B. (1998). Activity-dependent scaling of quantal amplitude in neocortical neurons. Nature *391*, 892-896.

Uhlhaas, P.J., Linden, D.E., Singer, W., Haenschel, C., Lindner, M., Maurer, K., and Rodriguez, E. (2006). Dysfunctional long-range coordination of neural activity during Gestalt perception in schizophrenia. J Neurosci *26*, 8168-8175.

Uhlhaas, P.J., and Singer, W. (2006). Neural synchrony in brain disorders: relevance for cognitive dysfunctions and pathophysiology. Neuron *52*, 155-168.

Ungerleider, L.G., and Haxby, J.V. (1994). 'What' and 'where' in the human brain. Curr Opin Neurobiol *4*, 157-165.

van Groen, T., Miettinen, P., and Kadish, I. (2003). The entorhinal cortex of the mouse: organization of the projection to the hippocampal formation. Hippocampus *13*, 133-149.

Vankov, A., Herve-Minvielle, A., and Sara, S.J. (1995). Response to novelty and its rapid habituation in locus coeruleus neurons of the freely exploring rat. Eur J Neurosci *7*, 1180-1187.

Varela, F., Lachaux, J.P., Rodriguez, E., and Martinerie, J. (2001). The brainweb: phase synchronization and large-scale integration. Nat Rev Neurosci *2*, 229-239.

Vazdarjanova, A., and Guzowski, J.F. (2004). Differences in hippocampal neuronal population responses to

modifications of an environmental context: evidence for distinct, yet complementary, functions of CA3 and CA1 ensembles. J Neurosci *24*, 6489-6496.

Venton, B.J., Zhang, H., Garris, P.A., Phillips, P.E., Sulzer, D., and Wightman, R.M. (2003). Real-time decoding of dopamine concentration changes in the caudate-putamen during tonic and phasic firing. J Neurochem *87*, 1284-1295.

Vinogradova, O.S. (2001). Hippocampus as comparator: role of the two input and two output systems of the hippocampus in selection and registration of information. Hippocampus *11*, 578-598.

von Frisch, K., Seeley ,T.D. (1993). The Dance Language and Orientation of Bees (Cambridge, Massachusetts: The Belknap Press of Harvard University Press).

Walker, J.A., and Olton, D.S. (1979). Spatial memory deficit following fimbria-fornix lesions: independent of time for stimulus processing. Physiol Behav *23*, 11-15.

Weinberger, D., Laruelle, M. (2001). Neurochemical and neuropharmacological imaging in schizophrenia. In Neuropsychopharmacology (Philadelphia: Lippincott Williams & Wilkins).

Wheeler, D.B., Randall, A., and Tsien, R.W. (1996). Changes in action potential duration alter reliance of excitatory synaptic transmission on multiple types of Ca2+ channels in rat hippocampus. J Neurosci *16*, 2226-2237.

Williams, S.R., and Stuart, G.J. (2002). Dependence of EPSP efficacy on synapse location in neocortical pyramidal neurons. Science *295*, 1907-1910.

Winograd, T. (1975). Frame representations and the declarative / procedural controversy. In Representation and understanding, D.G. Bobrow, and A. Collins, eds. (San Diego: Academic Press).

Witter, M.P., Amaral, D.G. (2004). Hippocampal Formation. In The Rat Nervous System, G. Paxinos, ed. (Amsterdam: Elsevier academic press).

Witter, M.P., and Moser, E.I. (2006). Spatial representation and the architecture of the entorhinal cortex. Trends Neurosci *29*, 671-678.

Wittmann, B.C., Schott, B.H., Guderian, S., Frey, J.U., Heinze, H.J., and Duzel, E. (2005). Reward-related FMRI activation of dopaminergic midbrain is associated with enhanced hippocampus-dependent long-term memory formation. Neuron *45*, 459-467.

Wu, J., and Hablitz, J.J. (2005). Cooperative activation of D1 and D2 dopamine receptors enhances a hyperpolarization-activated inward current in layer I interneurons. J Neurosci *25*, 6322-6328.

Wynn, J.K., Green, M.F., Engel, S., Korb, A., Lee, J., Glahn, D., Nuechterlein, K.H., and Cohen, M.S. (2008). Increased extent of object-selective cortex in schizophrenia. Psychiatry Res *164*, 97-105.

Yoshida, M., Hayashi, H., Tateno, K., and Ishizuka, S. (2002). Stochastic resonance in the hippocampal CA3-CA1 model: a possible memory recall mechanism. Neural Netw *15*, 1171-1183.

Young, C.E., Arima, K., Xie, J., Hu, L., Beach, T.G., Falkai, P., and Honer, W.G. (1998). SNAP-25 deficit and hippocampal connectivity in schizophrenia. Cereb Cortex *8*, 261-268.

Young, S.H., and Poo, M.M. (1983). Topographical rearrangement of acetylcholine receptors alters channel kinetics. Nature *304*, 161-163.

Zhao, M., Pu, J., Forrester, J.V., and McCaig, C.D. (2002). Membrane lipids, EGF receptors, and intracellular signals colocalize and are polarized in epithelial cells moving directionally in a physiological electric field. FASEB J *16*, 857-859.

Zhao, M., Song, B., Pu, J., Wada, T., Reid, B., Tai, G., Wang, F., Guo, A., Walczysko, P., Gu, Y*., et al.* (2006). Electrical signals control wound healing through phosphatidylinositol-3-OH kinase-gamma and PTEN. Nature *442*, 457-460.

Zola-Morgan, S., and Squire, L.R. (1986). Memory impairment in monkeys following lesions limited to the hippocampus. Behav Neurosci *100*, 155-160.

Zoli, M., Torri, C., Ferrari, R., Jansson, A., Zini, I., Fuxe, K., and Agnati, L.F. (1998). The emergence of the volume transmission concept. Brain Res Brain Res Rev *26*, 136-147.

Zucker, R.S. (1973). Changes in the statistics of transmitter release during facilitation. J Physiol *229*, 787-810.

Zucker, R.S., and Regehr, W.G. (2002). Short-term synaptic plasticity. Annu Rev Physiol *64*, 355-405.